UMTRI-2025-01 JANUARY 2025

EVALUATING WHEELCHAIRS FOR POTENTIAL USE AS AIRCRAFT SEATING: DYNAMIC VERTICAL AND STATIC TEST CONDITIONS (SECOND INTERIM PROJECT REPORT)

KATHLEEN D. KLINICH, NICHOLE R. ORTON, TYLER VALLIER, CARL MILLER, BRIAN EBY, JENNIFER BISHOP, GARY WEISSEL, KYLE BOYLE, MIRIAM A. MANARY

UMTRI TRANSPORTATION RESEARCH INSTITUTE UNIVERSITY OF MICHIGAN

DISCLAIMER

This research was sponsored by the National Institute on Disability, Independent Living, and Rehabilitation Research (NIDILRR). The opinions, findings, and conclusions expressed in this publication are those of the authors and not necessarily those of NIDILRR, the Department of Transportation (DOT), or the Federal Aviation Administration (FAA). If trade or manufacturers' names or products are mentioned, it is because they are considered essential to the object of the publication and should not be construed as an endorsement.

ACKNOWLEDGEMENTS

We would like to thank the following individuals for their expertise and guidance on this project.

Brian Bard, NIDILRR

Anjali Forber-Pratt, NIDILRR

Kelly Buckland, DOT

Jeff Gardin, FAA

Paul Jaramillo, FAA

David Moorcroft, FAA

Joseph Pelletiere, FAA

Stacey Zinke, FAA

We would also like the FAA for loaning us a FAA Hybrid III anthropomorphic test device (ATD) for testing.

Technical Report Documentation Page

1. Report No.	2. Government Accession No.	3. Recipient's Catalog No.
UMTRI-2025-01		

4. Title and Subtitle	5. Report Date
Evaluating Wheelchairs for Potential Use as Aircraft Seating: Dynamic Vertical and Static Test Conditions (Second Interim Project Report)	January 2025
	6. Performing Organization Code

7. Author(s	8. Performing Organization Report No.
Kathleen D. Klinich, Nichole R. Orton, Tyler Vallier, Carl Miller, Brian Eby, Jennifer Bishop, Kyle J. Boyle, Gary Weissel, Miriam A. Manary	UMTRI-2025-01

9. Performing Organization Name and Address	10. Work Unit No. (TRAIS)
University of Michigan Transportation Research Institute 2901 Baxter Rd. Ann Arbor, MI 48109	11. Contract or Grant No. 90IFRE0072-01-00

12. Sponsoring Agency Name	13. Type of Report and Period Covered
National Institute on Disability, Independent Living, and Rehabilitation Research (NIDILRR)	Interim 9-23 to 12-24
	14. Sponsoring Agency Code

15. Supplementary Notes

16. Abstract

For this project, we hypothesized that wheelchairs meeting the voluntary standards for vehicle crashworthiness (RESNA WC19) would be able to pass the FAA crashworthiness standards for aircraft seating. This report covers initial results from dynamic tests of WC19 wheelchairs under the FAA vertical dynamic testing conditions, as well as additional static testing results using an adapted version of the FAA static test procedures. Six WC19 wheelchairs were selected for dynamic testing using a fixture that rotates the mounting platform by 60 degrees to simulate loading that might happen during a plane crash. Wheelchairs were secured using 4-point strap tiedowns in the geometry specified by WC19, and the ATD was restrained by both the WC-mounted lap belt and a vehicle-mounted lap belt. No catastrophic failures occurred, although a footrest partially detached from one manual wheelchair and a drive motor partially detached from a power wheelchair. ATD lumbar loads measured in the power wheelchairs exceeded FAA limits. For the static testing, we adapted the FAA procedures to split the load for rear and frontal tests, and for wheelchairs >50 kg in lateral and upward tests. Loading based on occupant mass was applied through the body block, while loading based on wheelchair mass was applied through wheelchair securement points. Wheelchairs were secured using 4-point strap tiedowns in the geometry specified by WC19, and the body block was restrained by both the WC-mounted lap belt and a vehicle-mounted lap belt. No excessive damage occurred, with most measured deformations < 25 mm. These results support future use of personal wheelchairs on aircraft if they use WC19 wheelchairs secured to the aircraft with 4-point strap tiedown systems, supplemented by an occupant lap belt anchored to the aircraft.

17. Key Words	18. Distribution Statement
Wheelchairs, aircraft, static, vertical, FAA, WC19	

19 Security Classif. (of this report)	20. Security Classif. (of this page)	21 No. of Pages	22. Price
Unclassified	Unclassified	86	

Contents

List of Figures ___ ***vi***

List of Tables ___ ***ix***

Introduction ___ ***1***

Project Objective ___ ***1***

Dynamic Vertical Testing ___ ***2***

Methods ___ **2**

Results ___ **10**

Static testing ___ ***25***

Methods ___ **25**

Results ___ **32**

Discussion ___ ***38***

Summary and Conclusions ___ ***40***

Ongoing Work ___ ***41***

Bibliography ___ ***41***

Appendix A. Draft Vertical Dynamic Test Procedure for Wheelchairs Used as Aircraft Seating ___ ***42***

Introduction ___ **43**

Wheelchair Test Methods ___ **43**

Wheelchair Performance Criteria ___ **45**

Appendix B. Additional Dynamic Testing Results ___ ***46***

Appendix C. Draft Static Test Procedures for Wheelchairs Used as Aircraft Seating ___ ***49***

Objectives ___ **50**

Test Methods ___ **50**

Wheelchair Performance Criteria ___ **58**

Appendix D. Detailed Static Testing Results ___ ***59***

Appendix Key ___ **60**

Frontal Static Pull ___ **61**

Rearward Static Pull ___ **65**

Lateral Static Pull 71
Upward Static Pull 76
Downward Static Compression 80

List of Figures

Figure 1. Comparison of ideal and UMTRI versions of the FAA vertical pulse. 3

Figure 2. Comparison of kinematics between the UMTRI and triangular versions of the FAA vertical pulse. 4

Figure 3. Comparison of head and pelvis excursions for UMTRI (red) and triangular (blue) versions of the FAA vertical pulse. 4

Figure 4. Comparison of resultant head, chest and pelvis accelerations (top row) and ATD-to-seat force, WC-to-floor-force, and seatbelt-to-ATD contact force between UMTRI (red) and triangular (blue) vertical FAA pulse conditions. 5

Figure 5. Comparison of lumbar axial force for UMTRI (red) and triangular (blue) versions of the FAA vertical pulse. 5

Figure 6. Drawings of fixture to conduct FAA vertical loading tests on the UMTRI sled fixture. 7

Figure 7. Illustration of configuration used for securing wheelchairs with 4-point strap tiedowns. 7

Figure 8. Illustration of rear SWTORS and extra vehicle-mounted lap belt secured to the test fixture. 8

Figure 9. Wheelchair and ATD in horizontal position (upper left), rotating platform to 60 degrees (upper right), measuring ATD in rotated position (lower left), and adjusting ATD with foam inserts to match horizontal position (lower right). 9

Figure 10. CS18 footrests with straps, plus detached right footrest post-test. 10

Figure 11. Detached drive motor from test WA2404. 11

Figure 12. Average sled accelerations from all vertical tests. 11

Figure 13. Sled change in velocity from all vertical tests. 12

Figure 14. Lap belt loads from all vertical tests (WA=wheelchair-anchored, VA=vehicle-anchored) 13

Figure 15. Rear tiedown loads from all vertical tests (LR=left rear, RR=right rear). 14

Figure 16. Head resultant acceleration from all vertical tests. 14

Figure 17. Lumbar axial force from all vertical tests 15

Figure 18. ATD head path relative to the wheelchair seat junction from all vertical tests. 16

Figure 19. Path of the hip during vertical tests. 17

Figure 20. Manual wheelchair tests at time zero and at time of peak dynamic displacement, annotated with lines showing original and deformed seatpan and seatback relative to fixture reference. 18

Figure 21. Power wheelchair tests at time zero and at time of peak dynamic displacement, annotated with lines showing original and deformed seatpan and seatback relative to fixture reference. 19

Figure 22. Side and front views of initial and post-test shape of PDG Stellar GL. 20

Figure 23. Side and front views of initial and post-test shape of Sunrise Quickie 2. 20

Figure 24. Side and front views of initial and post-test shape of Convaid SFT18. 21

Figure 25. Side and front views of initial and post-test shape of Quantum Q6 Edge 2. 21

Figure 26. Side and front views of initial and post-test shape of Quantum 4Front 2. 22

Figure 27. Side and front views of initial and post-test shape of MC Rovi. 22

Figure 28. Pre-test photos, overlaid with plots of FARO arm data pre-and post indicating residual deformation of wheel axles and top of seatback. (Data missing for test 5, so pre-and post pictures overlaid.) 23

Figure 29. Post-test photo of a manual wheelchair following vertical impact 25

Figure 30. Examples of wheelchairs that would not allow a direct vertical loading path through the securement points. 26

Figure 31. Pretest photo of downward static test, showing carpeted platform, floor pulleys, and loading plate. 27

Figure 32. Test platform showing carpeting, anchor brackets, and holes to allow appropriate lateral spacing of pulleys. 28

Figure 33. Static test setup in all conditions for the Edge 2: upward through body block, upward through frame, downward, lateral, rear, frontal. 29

Figure 34. Winch controller software interface that provides control and live feedback of peak loads, loading rate and video. 30

Figure 35. Example illustration of points used to calculate wheelchair deformation during static testing. 31

Figure 36. Example controller output showing ability to accommodate for drops in load from shifting of body block. 32

Figure 37. Indirect lateral loading to securement points for 4Front. 35

Figure 38. Chest resultant acceleration from all vertical tests. 47

Figure 39. Pelvis resultant acceleration from all vertical tests. 47

Figure 40. Upper neck axial force from all vertical tests. 48

Figure 41. Loading history for Rovi frontal static test. 61

Figure 42. Rovi X3 frontal static test: initial test setup vs. peak from video. 61

Figure 43. Loading history for Edge2 frontal static test. 63
Figure 44. Edge2 frontal static test: initial test setup vs. peak from video 63
Figure 45. Loading history for 4Front frontal static test. 64
Figure 46. 4Front frontal static test: initial test setup vs. peak from video 64
Figure 47. Loading history for Rovi rear static test. 65
Figure 48. Rovi X3 rear static test: initial test setup vs. peak from video 65
Figure 49. Loading history for Edge2 rear static test 66
Figure 50. Edge2 rear static test: initial test setup vs. peak from video 66
Figure 51. Loading history for 4Front rear static test. 67
Figure 52. 4Front rear static test: initial test setup vs. peak from video 67
Figure 53. Loading history for Quickie 2 rear static test. 69
Figure 54. Quickie2 rear static test: initial test setup vs. peak from video 69
Figure 55. Loading history for Rovi lateral static test. 71
Figure 56. Rovi X3 lateral static test: initial test setup vs. peak from video 71
Figure 57. Loading history for Edge2 lateral static test. 72
Figure 58. Edge2 lateral static test: initial test setup vs. peak from video 72
Figure 59. Loading history for 4Front lateral static test. 73
Figure 60. 4Front lateral static test: initial test setup vs. peak from video 74
Figure 61. Loading history for Quickie 2 lateral static test. 75
Figure 62. Quickie2 lateral static test: initial test setup vs. peak from video 75
Figure 63. Loading history for Rovi upward static test. 76
Figure 64. Rovi X3 upward static tests: initial test setup vs. peak from video, with separate tests loading through body block (top) and frame (bottom). 76
Figure 65. Loading history for Edge 2 upward static test. 77
Figure 66. Edge2 upward static test: initial test setup vs. peak from video, with separate tests loading through body block (top) and frame (bottom). 77
Figure 67. Loading history for Quickie 2 upward static test. 78
Figure 68. Quickie2 lateral upward test: initial test setup vs. peak from video 78
Figure 69. Loading history for Rovi downward static test. 80
Figure 70. Rovi X3 Downward lateral static test: initial test setup vs. peak from video 80

Figure 71. Loading history for Edge 2 downward static test. 82
Figure 72. Edge2 upward static test: initial test setup vs. peak from video 82
Figure 73. Loading history for 4Front downward static test. 84
Figure 74. 4Front downward static test: initial test setup vs. peak from video 84
Figure 75. Loading history for Quickie 2 downward static test. 86
Figure 76. Quickie2 downward static test: initial test setup vs. peak from video 86

List of Tables

Table 1. Summary of wheelchairs acquired for vertical and static testing. 6
Table 2. Summary of vertical test conditions and outcomes. 10
Table 3. Summary of residual deformation measured from different methods. 24
Table 4. Summary of static test conditions and outcomes 33
Table 5. Summary of resultant residual deformations from first and last completed test on each wheelchair. 36
Table 6. Front and back seatpan coordinates pre- and post test, plus angle calculations. 37
Table 7. Rovi X3 deformation analysis from frontal pre- and post-test scan data. 62
Table 8. 4Front deformation analysis from rear static pre- and post-tests 68
Table 9. Quickie 2 deformation analysis, pre and post rear static test 70
Table 10. Quickie2 deformation analysis from upwards pre- and post test measurements 79
Table 11. Rovi deformation analysis before and after downward static loading 81
Table 12. Edge2 deformation from downward static testing 83
Table 13. 4Front deformation from downward static testing 85

Introduction

The Rehabilitation Engineering Society of North America (RESNA) has developed standards that establish ways to measure, define, and test wheelchairs and wheelchair components. The RESNA voluntary standards are recognized by the American National Standards Institute (ANSI) and include Section 19 Wheelchairs used as Seats in Motor Vehicles (WC19)[1]. For this project, we hypothesized that wheelchairs meeting the WC19 voluntary standards for vehicle crashworthiness would be able to pass the FAA crashworthiness standards for aircraft seating. Additional background information relevant to the project is provided in our first interim report [2].

The first interim report describes initial results of dynamic frontal testing and static testing. Initially in all tests, wheelchairs were secured using surrogate 4-point strap tiedowns in the anchoring geometry specified by WC19. Seven wheelchairs representing a range of wheelchair design styles were tested. For the static tests, two manual wheelchairs met requirements, but applying the entire load through the seat caused damage to the power wheelchairs. Discussion with FAA experts suggested an alternative interpretation of the standard to allow splitting the load between the seat and base for future static trials.

For the dynamic frontal testing, modeling was used to demonstrate the suitability of using the trapezoidal pulse achieved with the University of Michigan Transportation Research Institute (UMTRI) sled rather than the typical triangular shaped FAA pulse, as well as the minimal effect of simulating pitch and roll with the test fixture because of the non-rigid 4-point strap tiedowns. In the first two dynamic frontal tests, the left front caster wheel broke. Subsequent tests of five wheelchair models using an additional aircraft-mounted lap belt to restrain the occupant (suggested by FAA experts) were successful.

Based on the results documented in the first interim project report, it may be feasible for people to use their own wheelchairs on aircraft if they use WC19 wheelchairs secured to the aircraft with 4-point strap tiedown systems, supplemented by an occupant lap belt anchored to the aircraft. The current document shares results from initial dynamic vertical testing of six wheelchairs, as well as additional static test results using an adapted version of the FAA static test procedure.

Project Objective

We hypothesize that wheelchairs meeting voluntary crashworthiness standards for use as seating in motor vehicles would meet current FAA standards for aircraft seats. During this three-year project, we will be testing this hypothesis. One task involves constructing test fixtures that will allow testing of wheelchairs to the FAA requirements for aircraft seats under the frontal impact condition, and testing different commercial wheelchairs that meet current WC19 requirements. A second task involves construction of a fixture that allows testing of wheelchairs to the vertical loading requirements of FAA aircraft seating, followed by testing different commercial wheelchairs to these requirements. The third task involves testing commercial wheelchairs to the static testing requirements using a fixture designed to accommodate wheelchairs. Should our

hypothesis be incorrect, we will develop and test solutions that might improve the performance of commercial wheelchairs relative to FAA seating requirements. With either hypothesis outcome, we will draft test procedures based on the initial tasks and work with a standards committee to include them as an annex to current crashworthiness standards to allow development of wheelchairs suitable for use as aircraft seating. We will also document results in reports that could be used to support requests to the FAA to move forward with allowing people to travel in their own wheelchairs on aircraft.

This second interim report documents progress on the following tasks:

- Developing methods for conducting vertical dynamic aircraft seating tests of wheelchairs, including modeling to support methods development
- Conducting vertical aircraft seating tests on six commercial wheelchair models
- Developing adapted methods for performing static aircraft seating tests on power wheelchairs
- Conducting static aircraft seating tests on four commercial wheelchairs

Dynamic Vertical Testing

Methods

ATD Selection

The original ATD used for testing aircraft seats is the Hybrid II midsized male (Part 572:B). When the Hybrid III ATD was introduced as a more biofidelic ATD for assessing occupant safety in motor vehicles, it was not accepted as equivalent to the Hybrid II for evaluating aircraft seats [3]. The primary reason was a difference in response during the vertical testing condition, where a requirement is a compressive axial force less than 6500 N. Differences in the pelvis design may also contribute to this difference in response.

A project was undertaken to make a kit for the Hybrid III ATD that made it respond more closely to the Hybrid II in areas most important for aircraft seat assessment. Changes involved:

1. Using an 1891 Hybrid II lumbar load cell and pelvic adaptor block.
2. Using a Hybrid II lumbar column.
3. Using a different upper-lumbar-thorax adaptor.
4. Using a Hybrid II abdominal insert.
5. Using Hybrid II upper leg elements.
6. Using a Hybrid II chest flesh, with a notch cut in the chest flesh.

While we used the recommended FAA Hybrid III ATD for our frontal testing, we note the differences here, as our simulations to investigate how different factors might affect testing choices used the standard Hybrid III computational model we have available.

Sled Pulse

14 CFR Part 25 specifies that the vertical dynamic test pulse have a minimum delta V of 38 kph and a peak acceleration of 14 *g* achieved within 80 ms, but no minimum rise time is specified.

The Federal regulation does not prescribe the shape, but AS8049 describes the ideal shape as triangular.

Figure 1 compares the ideal FAA vertical pulse with a trapezoidal pulse produced by the UMTRI sled that meets the specifications but not the ideal shape. The sharper rise time of the UMTRI pulse likely produces more severe loading than required. We performed simulations with the surrogate wheelchair base (SWCB) and a standard Hybrid III midsize male ATD to evaluate the potential effect of the different pulse shapes.

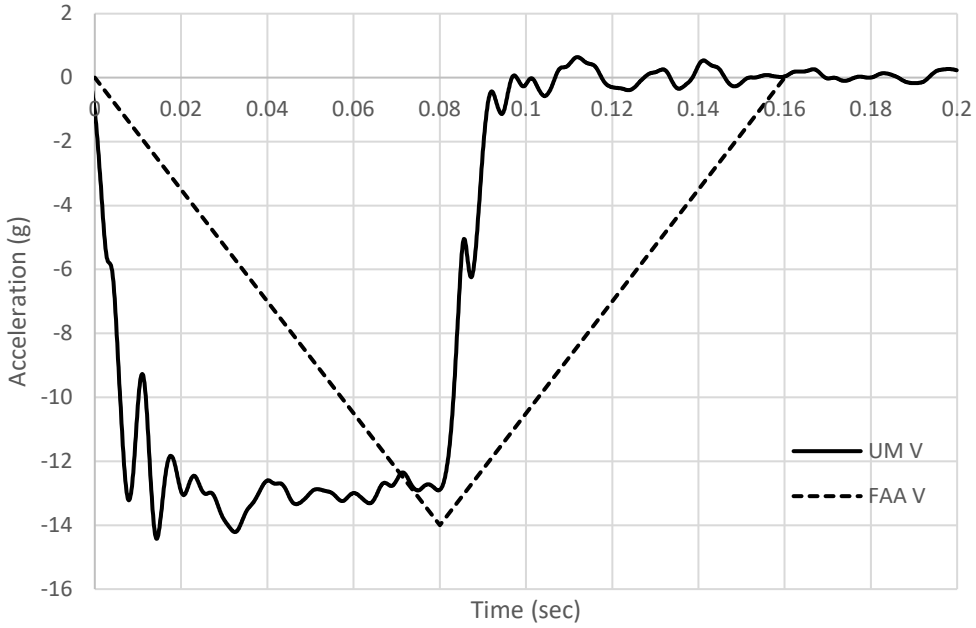

Figure 1. Comparison of ideal and UMTRI versions of the FAA vertical pulse.

A comparison of the kinematic differences arising from the pulse characteristics is shown in Figure 2. The UMTRI pulse is the shown by the red line while the FAA triangular pulse is shown by the blue line. The UMTRI pulse causes the ATD to begin moving sooner, but the ATD position at peak acceleration is similar for both pulses. Plots of the head and pelvis x and z excursions shown in Figure 3 confirm this observation. Both pulses produce maximum x displacements near 600 m and maximum z displacements around -600 mm, but the peaks occur about 40 ms later with the triangular pulse. The pelvis x excursion is slightly higher with the UMTRI pulse, and the difference in peak timing is also about 50 ms. However, the pulses produce similar head trajectories for the head as indicated in the right column of Figure 3, while the UMTRI pulse produces greater pelvis motion. This result is consistent with an earlier FAA evaluation of triangular vs. trapezoidal pulses [4]

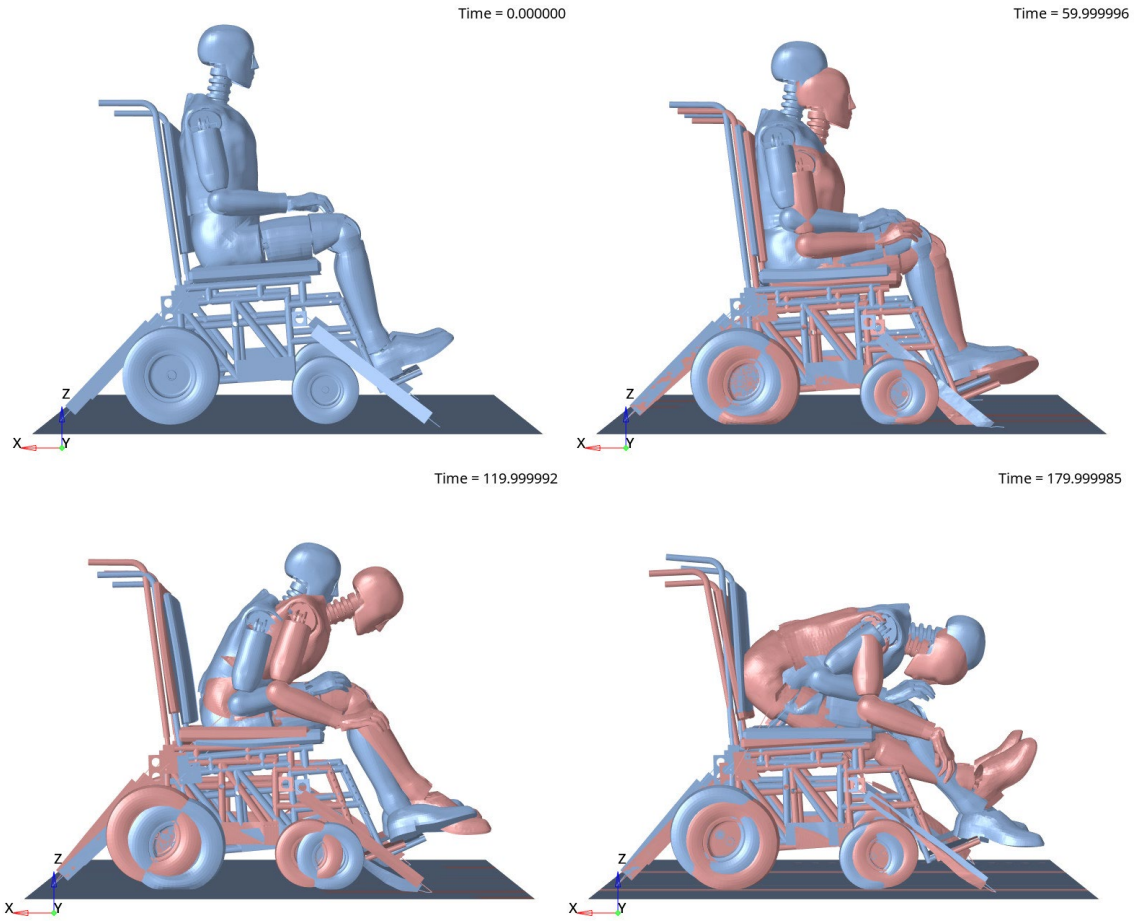

Figure 2. Comparison of kinematics between the UMTRI and triangular versions of the FAA vertical pulse.

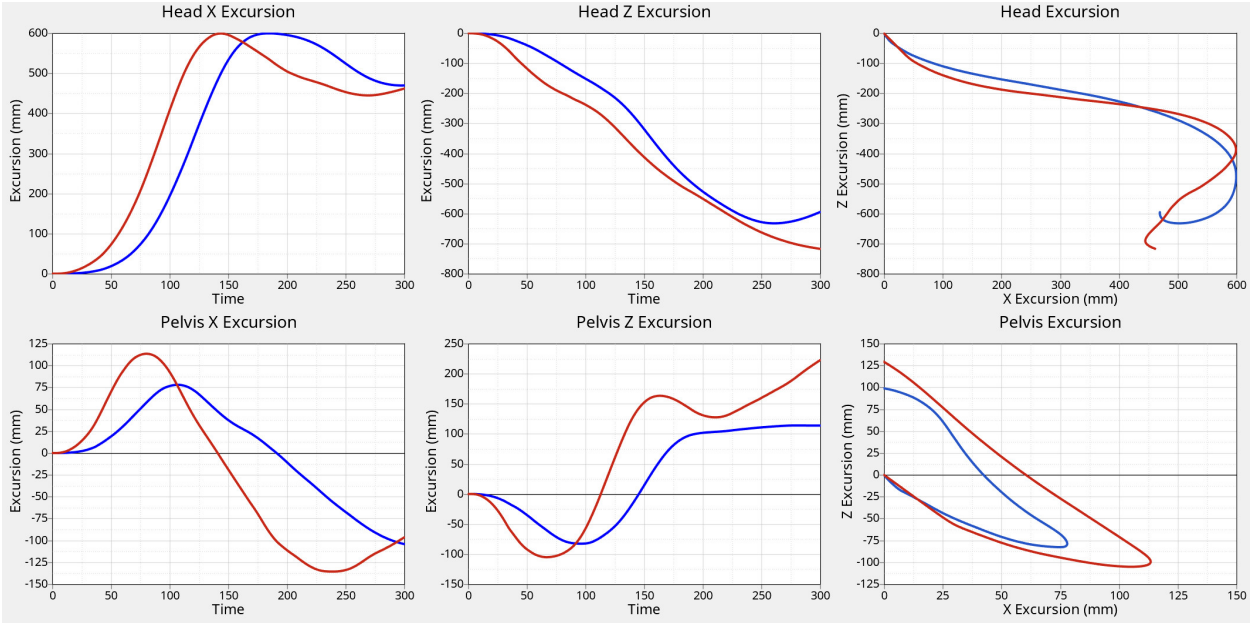

Figure 3. Comparison of head and pelvis excursions for UMTRI (red) and triangular (blue) versions of the FAA vertical pulse.

Differences in simulated ATD signals are shown in Figure 4 and Figure 5. Results include resultant head, chest, and pelvis acceleration, ATD-to-seat force, WC-to-floor force, seatbelt-to-ATD contact force, and lumbar axial force. For each comparison, the peak values occur about 20 to 50 ms earlier with the UMTRI pulse and are 25 to 50% higher, with the largest variation seen in the chest acceleration.

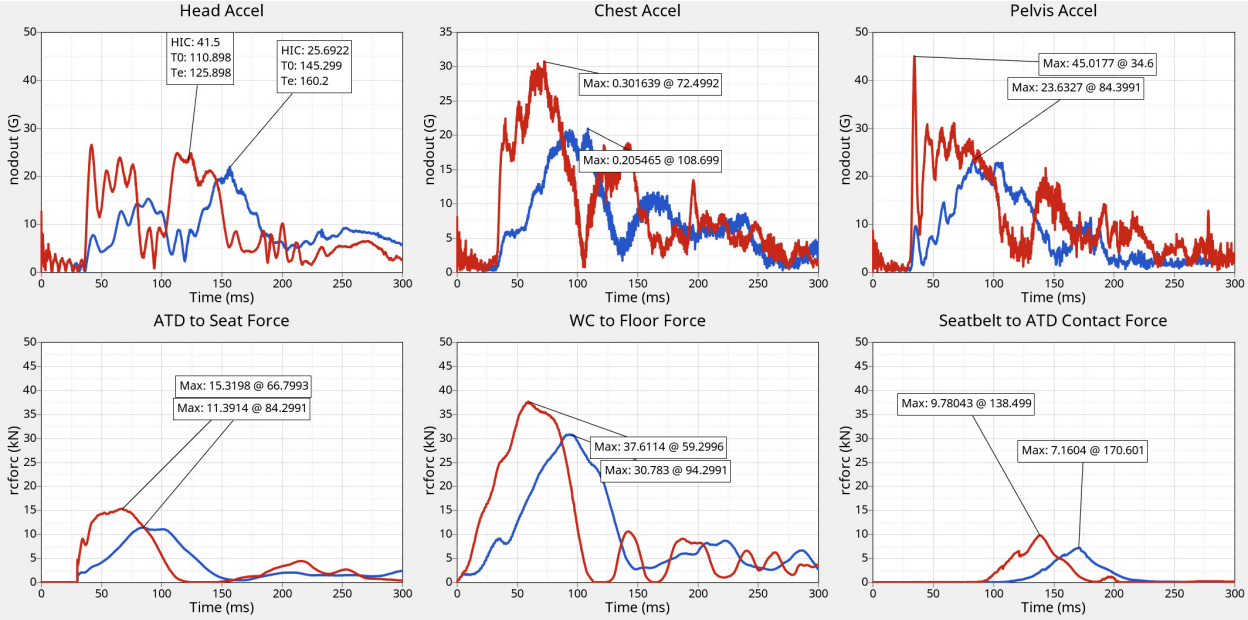

Figure 4. Comparison of resultant head, chest and pelvis accelerations (top row) and ATD-to-seat force, WC-to-floor-force, and seatbelt-to-ATD contact force between UMTRI (red) and triangular (blue) vertical FAA pulse conditions.

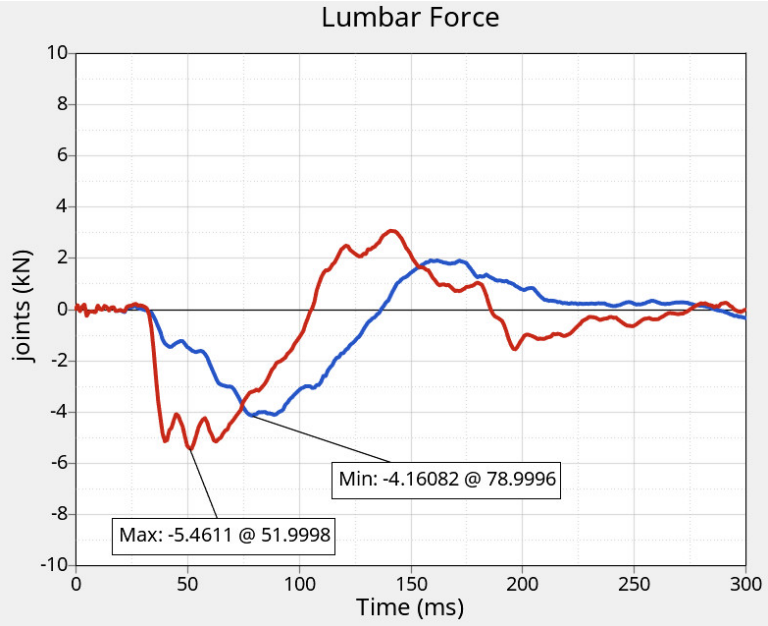

Figure 5. Comparison of lumbar axial force for UMTRI (red) and triangular (blue) versions of the FAA vertical pulse.

These simulations show that peak head excursions are similar but the UMTRI pulse results in higher pelvis displacements. The UMTRI pulse provides loading conditions that meet or exceed ideal pulse loading, so wheelchairs that pass vertical requirements using our pulse should also meet requirements using a more triangular pulse.

Wheelchair selection

Based on the level of wheelchair damage observed in our initial static and frontal testing, we conducted the vertical dynamic testing prior to the static testing. **Error! Reference source not found.** lists the commercial wheelchair models obtained for both types of testing that were selected to span a range of wheelchair design characteristics. All wheelchairs tested were selected from our list of products meeting WC19 requirements and came with a wheelchair-anchored crashworthy lap belt. To redirect project budget towards additional needed static methods development, two wheelchairs without visible damage previously tested under nearside lateral loading conditions in another project were used for testing. The abbreviations for these two tests have an "NS" suffix to indicate the nearside prior testing.

Table 1. Summary of wheelchairs acquired for vertical and static testing.

Wheelchair Model	Abbrev.	WC Mass (kg)	WC Mass (lb)	Type
PDG Stellar GL	PSG	34	74	Manual, rigid
Sunrise Quickie 2	SQ2_NS	20	45	Manual, folds laterally
Convaid SFT 18	CS18	22	49	Manual, folds laterally and fore-aft
Quantum Q6 Edge 2	QE2_NS	163	360	Power base with suspension
Quantum 4Front 2	Q4F	173	382	Power front wheel drive
MC Rovi X3	MCR	161	355	Midwheel drive with suspension

Vertical Test Fixture

Figure 6 shows the drawings of the fixture built to provide vertical loading to the wheelchair. The FAA test procedures specify a floor platform rotated to 60 degrees, to simulate both frontal and upward loading of seats that might occur during a crash. The wheelchair and ATD are first placed and measured in a horizontal position. The platform is then rotated upward and a bracing structure is positioned underneath. While in the rotated configuration, the ATD posture and position is measured again. If rotation has altered the ATD relative to the horizontal position, foam supports are used to shift the ATD head and torso into the original position within a tolerance of 25 mm. For some of the cases where the wheelchair seatback deformed relative to the horizontal position, we maintained the same position of the ATD relative to the seatback in the rotated position for two reasons. One is that the seatback would be expected to deform in a similar manner in a crash. The other is that there is not a viable method to shift the deformed seatback to match its original horizontal position.

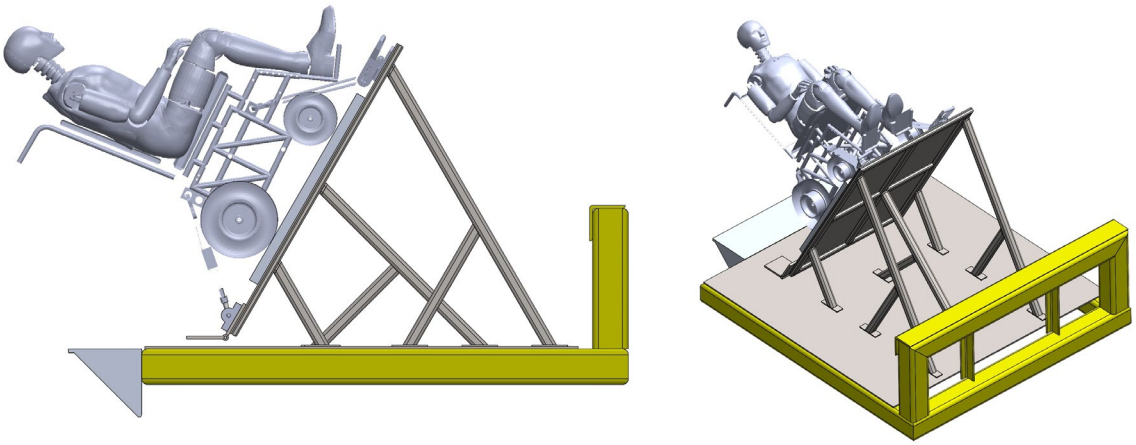

Figure 6. Drawings of fixture to conduct FAA vertical loading tests on the UMTRI sled fixture.

Protocol

For the dynamic testing, the FAA loaned UMTRI one of their FAA-Hybrid III ATDs. It was instrumented with triaxial accelerometers in the head, chest, and pelvis, as well as load cells in the upper and lower neck and lumbar spine, and triaxial angular velocity sensors in the head. Additional measured signals were tiedown and belt loads. All signal data were gathered and filtered using SAE J211 protocols.

Video data were used to record four views that include overhead, right side, right side rear (to capture rebound), and oblique rear left. The video data were used to assess overall kinematic response of the wheelchair and ATD, including the head trajectory.

The wheelchair was placed and secured using the procedures in RESNA WC19, illustrated in Figure 7 and described in Appendix A. The angle of the rear tiedown straps should be 45 degrees with respect to horizontal and extend straight back from the securement brackets, parallel to the wheelchair centerline. The front straps should be anchored forward and spaced slightly wider than the wheelchair for increased stability. A front strap angle between 30 and 70 degrees with respect to horizontal is typical.

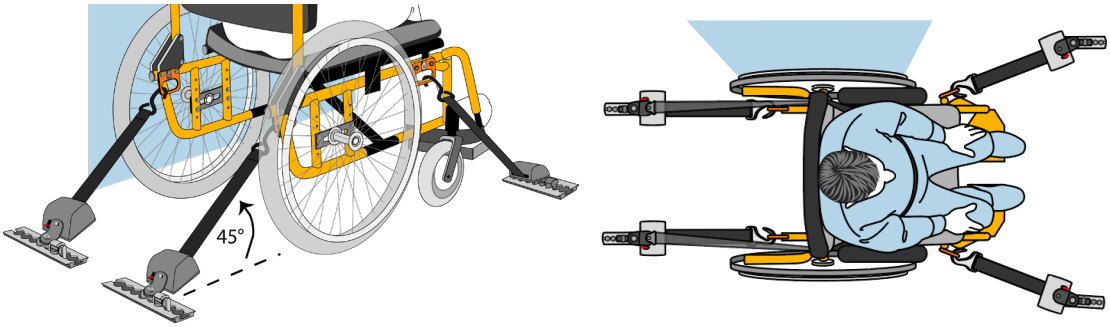

Figure 7. Illustration of configuration used for securing wheelchairs with 4-point strap tiedowns.

Once the wheelchair was mounted to the fixture, we applied targets to key landmarks. We then scanned the empty wheelchair in the horizontal position using a 3D Sense scanner, including a reference to allow alignment with post-test scans. The ATD was also placed in the wheelchair using the methods prescribed by WC19; no modifications to the seating procedure were required

with the FAA version of the H3 ATD. The leg strap required by the WC19 test protocol to prevent unrealistic lower extremity kinematics was not used for this test series. The ATD was restrained by both a wheelchair-mounted lap belt and a vehicle-mounted lap belt, based on conditions that led to successful frontal dynamic test performance in our previous work. Figure 8 shows the rear tiedowns and vehicle-anchored lap belt secured to the test fixture. The vehicle-anchored lap belt used standard automotive seatbelt webbing.

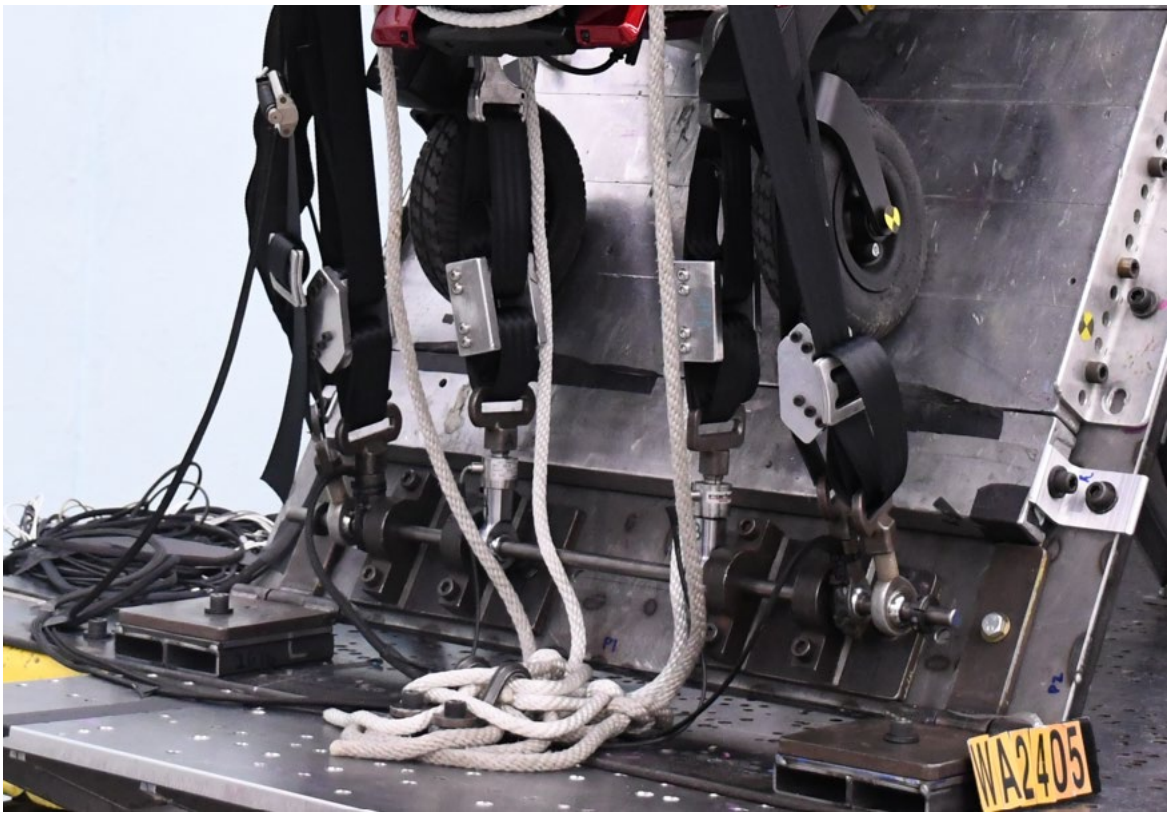

Figure 8. Illustration of rear SWTORS and extra vehicle-mounted lap belt secured to the test fixture.

A FARO Arm 3D coordinate measurement device was used to record landmarks on both the wheelchair and ATD, with the reference landmarks placed on the platform that rotates to allow comparison of initial horizontal and rotated position of the ATD. As shown in Figure 9, the platform was then rotated into position, and the ATD position recorded with the FARO Arm. When necessary, foam inserts were used to shift the ATD so it had the same location relative to the wheelchair seatback within a 25 mm tolerance.



Figure 9. Wheelchair and ATD in horizontal position (upper left), rotating platform to 60 degrees (upper right), measuring ATD in rotated position (lower left), and adjusting ATD with foam inserts to match horizontal position (lower right).

After testing and before removing the tiedowns, we remeasured the wheelchair landmarks with the FARO arm in the rotated position to record deformation. We also scanned the empty wheelchair in the horizontal position as an additional means to identify permanent deformation, including a reference to facilitate alignment with pre-test scans. Post-test observations and measurements recorded the physical damage and deformation of the wheelchair. Any detached hardware was noted and described.

Appendix A contains a draft test procedure for evaluating wheelchairs under vertical aircraft seating conditions. The tasks are modified versions of WC19 procedures, revised to accommodate FAA vertical seating procedure requirements.

Results

Damage Overview

Table 2 summarizes the test conditions and outcomes. In all tests, the ATD was restrained by both the wheelchair-anchored lap belt and a vehicle-anchored lap belt.

Table 2. Summary of vertical test conditions and outcomes.

ID	Wheelchair	Prior test	Abbreviation	Outcome
WA2401	PDG Stellar GL	None	PSG	No damage
WA2402	Sunrise Quickie 2	Nearside	SQ2_NS	No damage
WA2403	Convaid SFT 18	None	CS18	Front footrest broke
WA2404	Quantum Q6 Edge 2	Nearside	QE2_NS	Drive motor detached
WA2405	Quantum 4Front 2	None	Q4F	No damage
WA2406	MC Rovi	None	MCR	No damage

For test WA2403, one of the footrests broke off, but this wheelchair also incorporates straps for the occupant's feet, so it did not fully detach and become a projectile. Damage is shown in Figure 10. Because it created a sharp edge, it would not have met WC19 specifications for allowable damage.

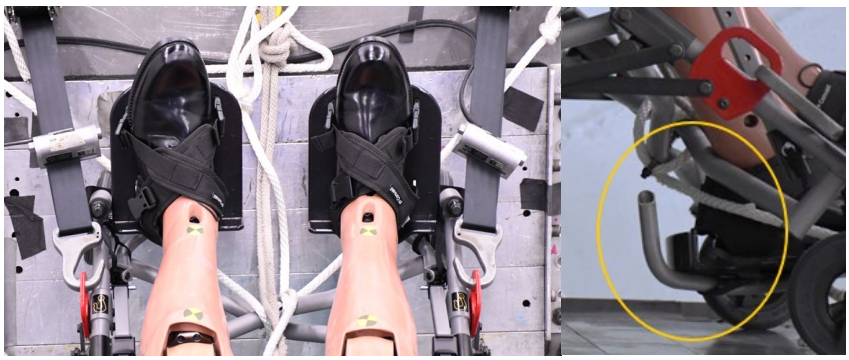

Figure 10. CS18 footrests with straps, plus detached right footrest post-test.

For test WA2404, the drive motor broke off during the test, but it was tethered to the wheelchair by the cable as shown in Figure 11, so it would have passed WC19 requirements.



Figure 11. Detached drive motor from test WA2404.

Sled, Belt, and Tiedown Responses

Figure 12 shows an overlap plot of the sled acceleration, while Figure 13 shows the integrated sled velocity. All tests achieved the targeted minimum change in velocity of 38 km/hr, and the peak deceleration ranged from 13.6 to 15.7 *g*. As noted previously, our rise time of approximately 10 ms is steeper than the maximum allowed time to peak of 80 ms.

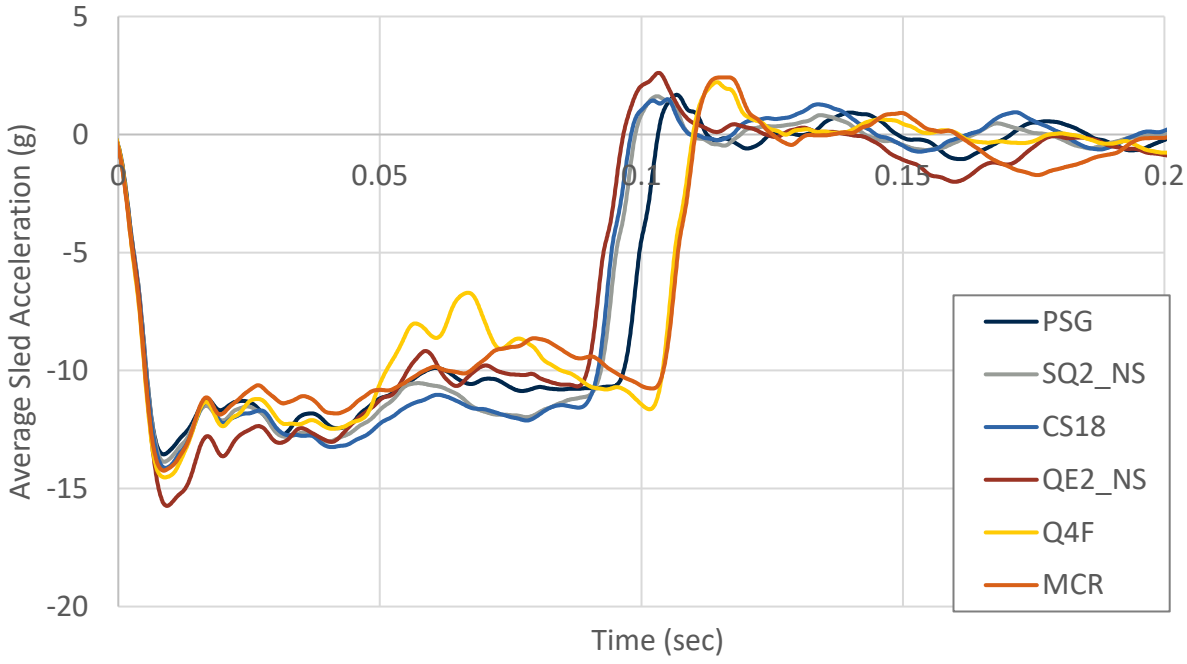

Figure 12. Average sled accelerations from all vertical tests.

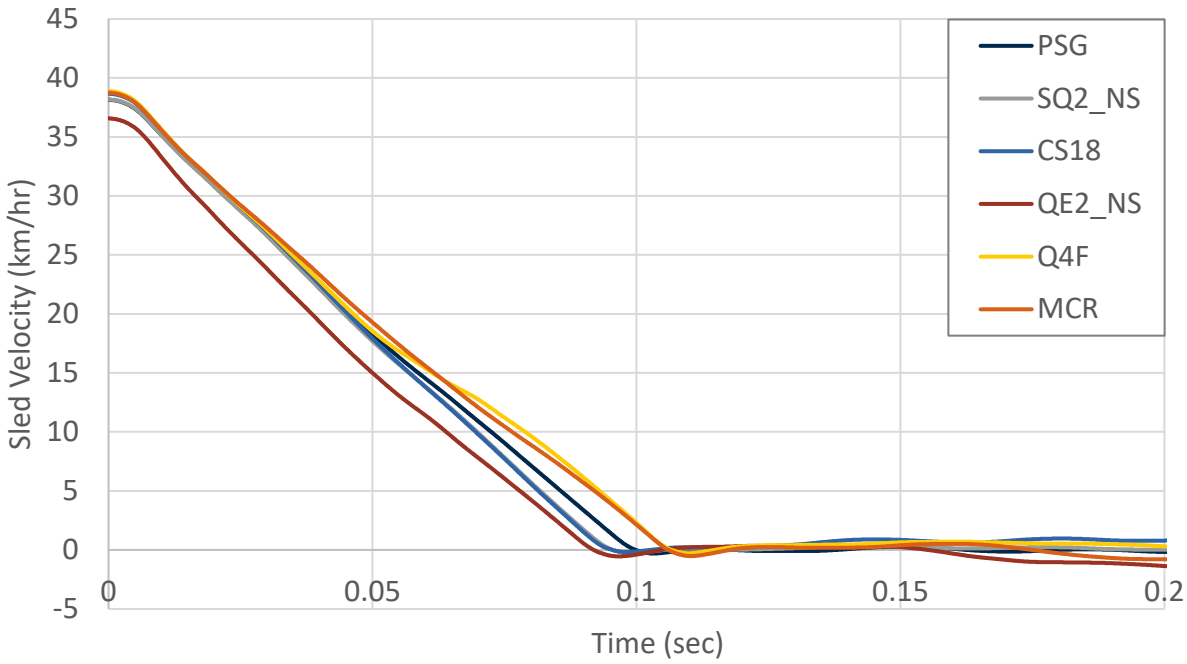

Figure 13. Sled change in velocity from all vertical tests.

Figure 14 shows the lap belt loads from the vertical dynamic tests. In Figure 14, the solid lines show the load from the wheelchair-attached lap belt, while the dashed lines show the loads from the vehicle-mounted lap belt. For the vertical loading condition, the loads in the vehicle-attached belt were minimal compared to those in the wheelchair-attached lap belt. Review of the videos indicates that the vehicle-attached lap belt appears visibly slack for much of the test, consistent with the low values. The wheelchair-attached lap belt load for test CS18 is substantially lower than the rest of the tests, likely because this wheelchair also has a robust postural belt.

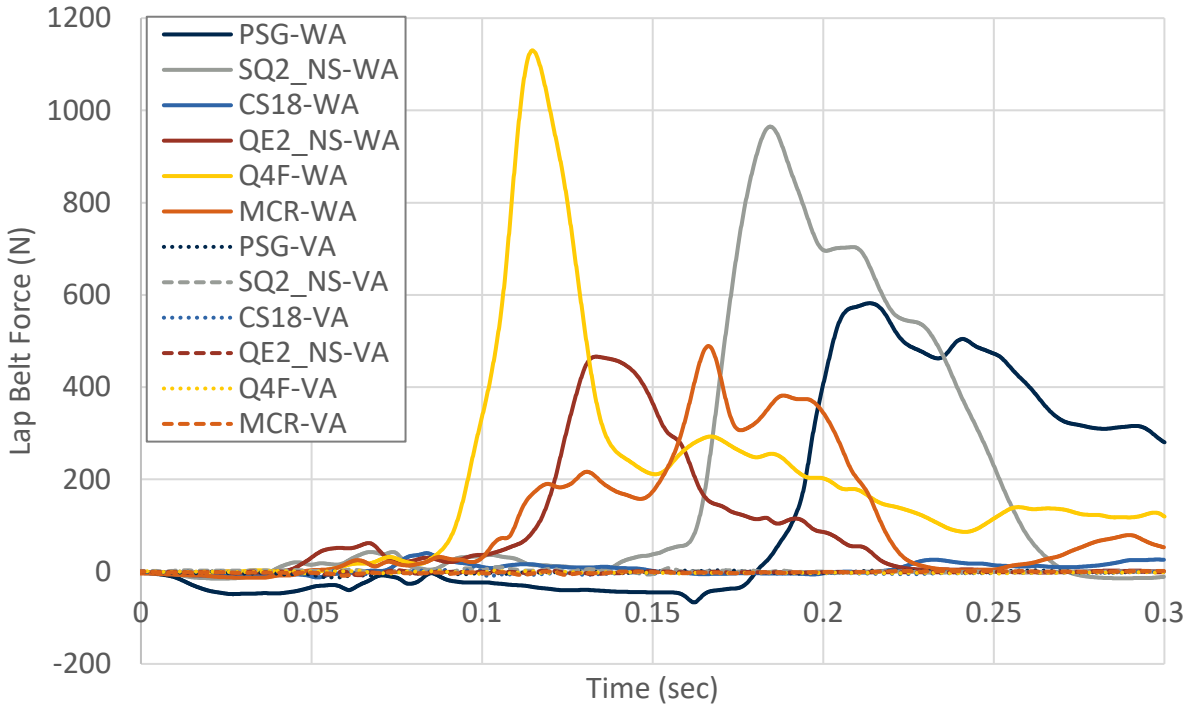

Figure 14. Lap belt loads from all vertical tests (WA=wheelchair-anchored, VA=vehicle-anchored).

Figure 15 shows the rear tiedown loads; front tiedown loads were measured but negligible. On this plot, solid lines are the left rear tiedown and dashed lines are the right rear tiedown. The tiedown loads under vertical aircraft testing are similar in magnitude to the range seen in WC19 testing.

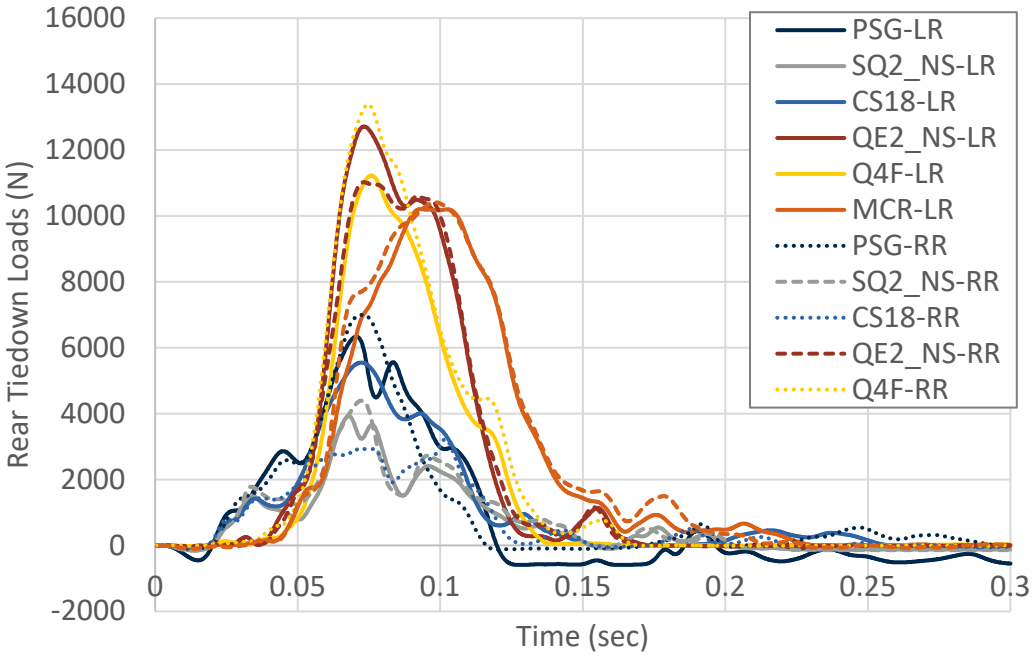

Figure 15. Rear tiedown loads from all vertical tests (LR=left rear, RR=right rear).

ATD Responses

Figure 16 shows the head resultant acceleration from the dynamic vertical tests. No head contact occurred with the ATD lower extremity during vertical testing.

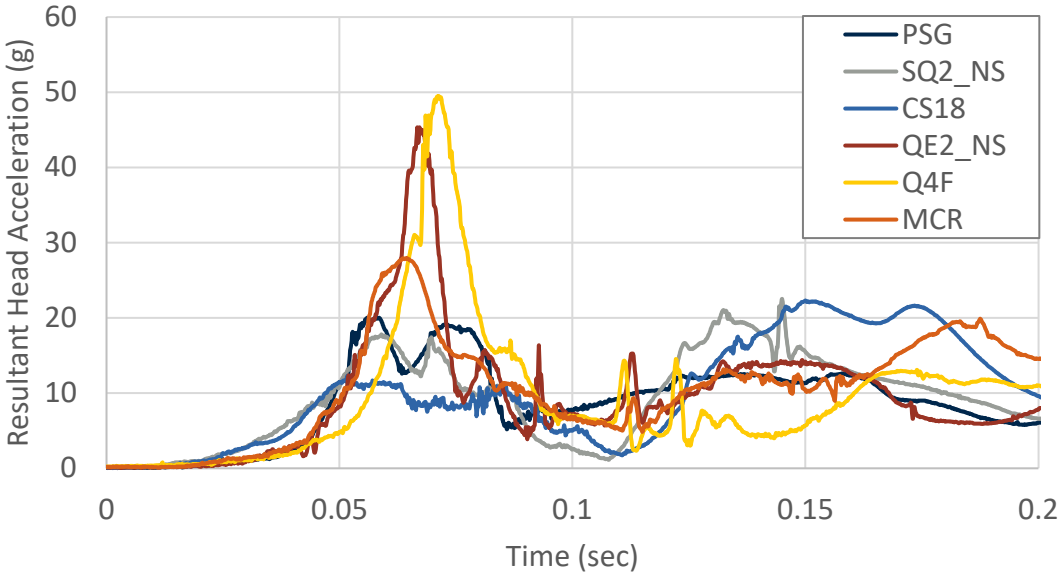

Figure 16. Head resultant acceleration from all vertical tests.

The axial lumbar forces from the dynamic frontal tests are shown in Figure 17, together with the FAA threshold of -6500 N. The three manual wheelchairs met the lumbar compression requirement, but the three power wheelchairs did not.

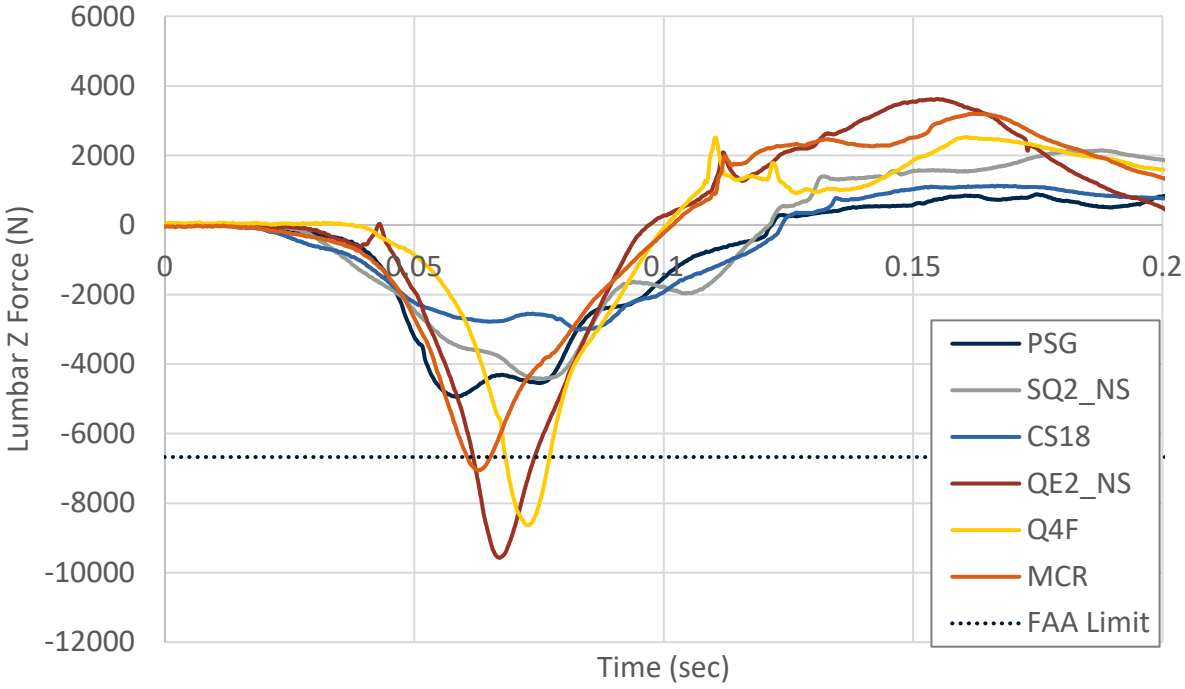

Figure 17. Lumbar axial force from all vertical tests.

FAA assessment measures are limited to maximum compressive lumbar force, along with strap loads, femur force, and HIC when there is a forward bulkhead representation. However, we collected additional data on the chest, pelvis, and neck response that are included in Appendix B.

Head trajectories digitized from the head CG target in each test are shown in Figure 18, with the origin at the WC seat/seatback junction. Overall, trajectories of the manual and power wheelchairs did not have substantial differences, with the manual rigid-style wheelchair having the lowest amount of head excursion. Trajectories of the P-point, an approximation of the hip joint, are shown in Figure 19. The stroller-style wheelchair experienced the largest vertical displacement during tests.

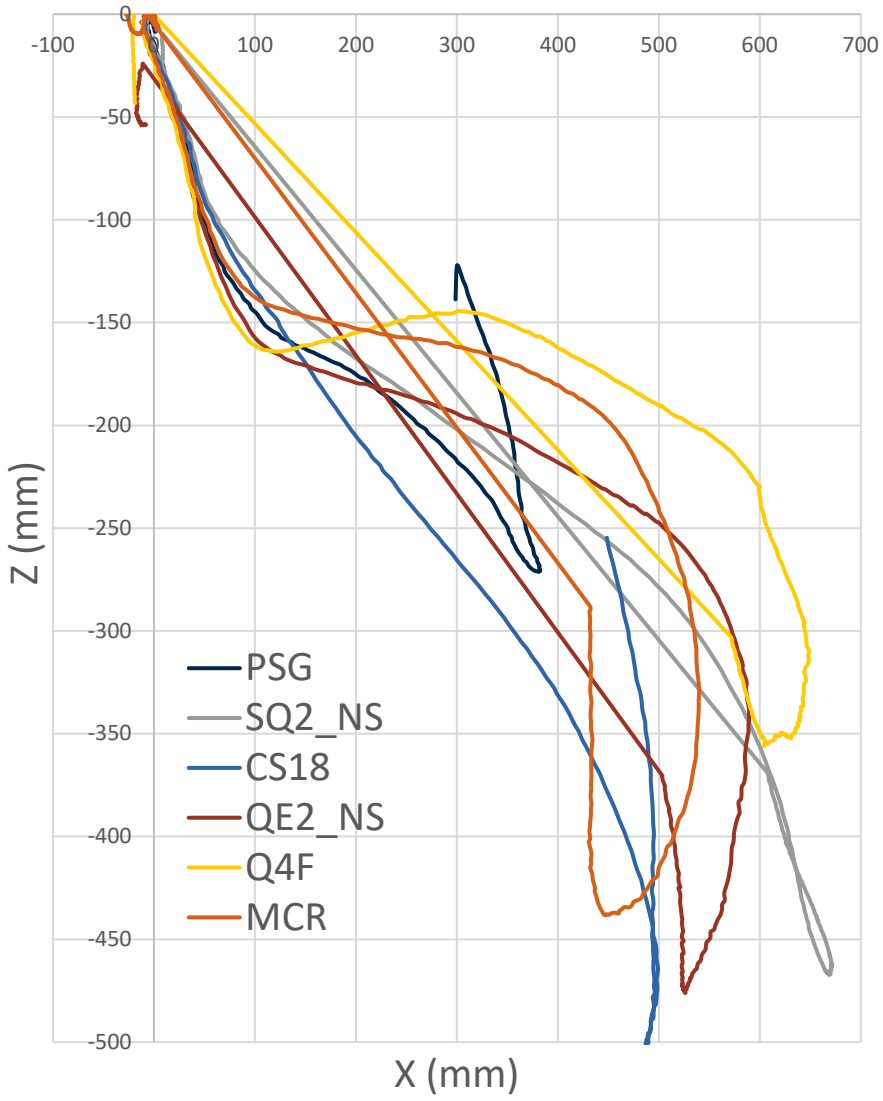

Figure 18. ATD head path relative to the wheelchair seat junction from all vertical tests.

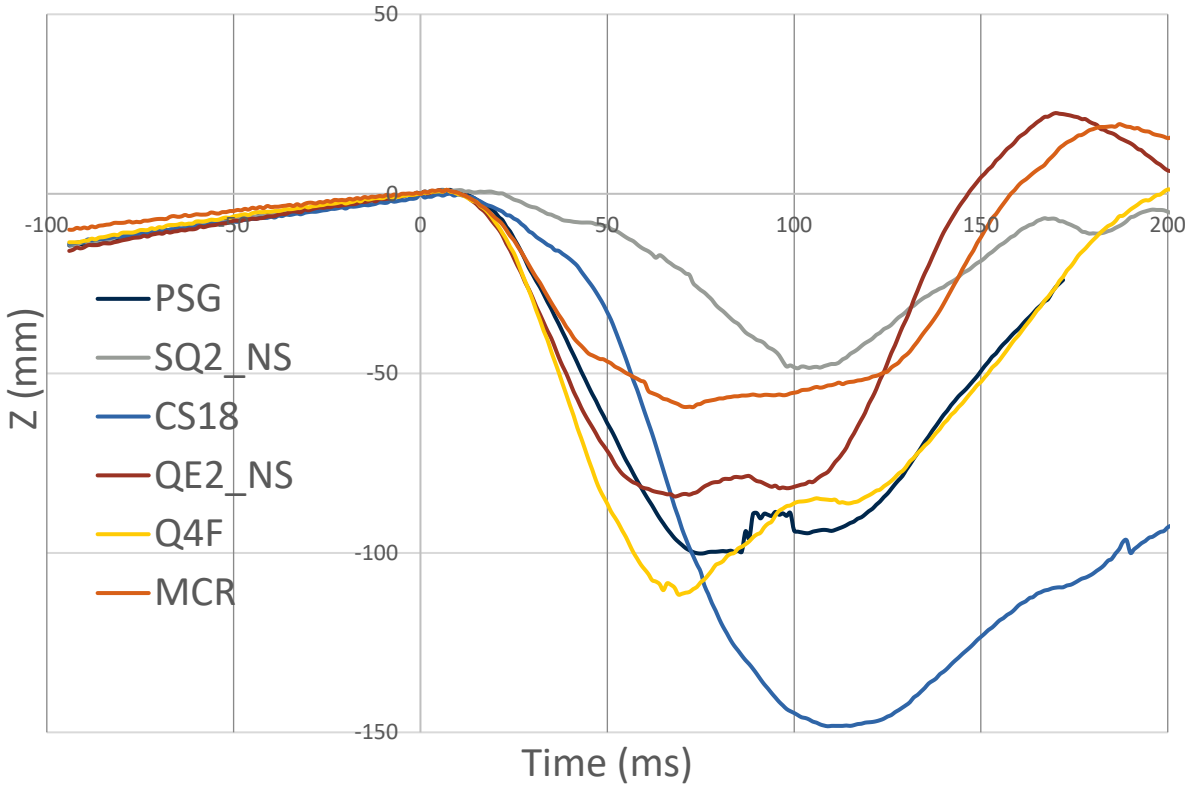

Figure 19. Path of the hip during vertical tests.

Deformation

Figure 20 shows sideview shots of the manual wheelchairs at time zero and at the time of maximum downward seat deformation, while Figure 21 shows the same photos for power wheelchairs. A thick yellow line shows the original orientation of the seatpan and seatback targets on each pair of photos, while the lighter yellow line shows the deformed shape. For reference, an orange triangle shows the position of the seatpan/seatback junction height relative to a sled fixture floor reference; the shifted triangle at peak deformation allows visual estimates of horizontal and vertical displacement. Across these wheelchair models, the amount of forward and vertical deformation, as well as how the seatback and seatpan deflected, varied considerably.

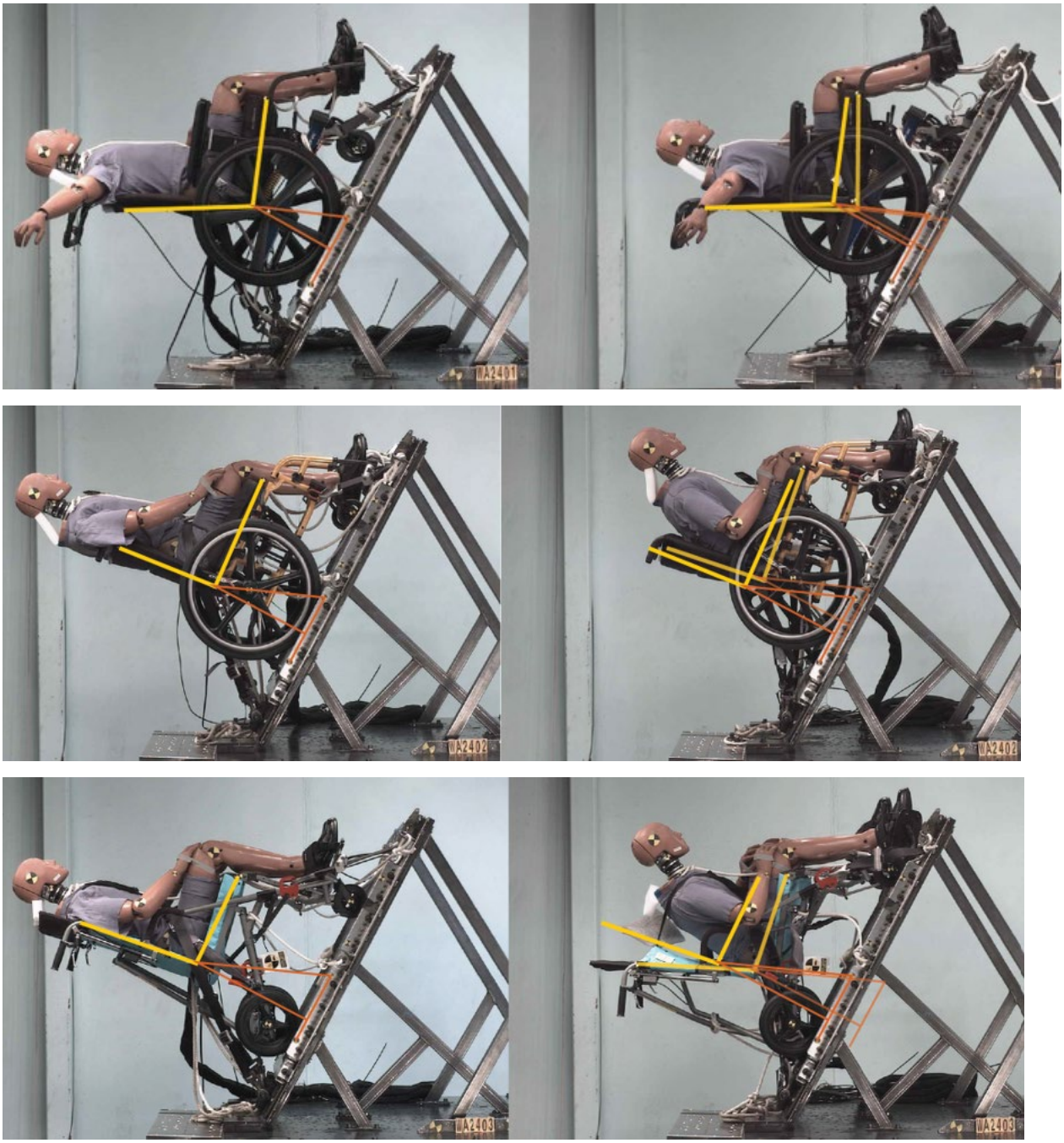

Figure 20. Manual wheelchair tests at time zero and at time of peak dynamic displacement, annotated with lines showing original and deformed seatpan and seatback relative to fixture reference.

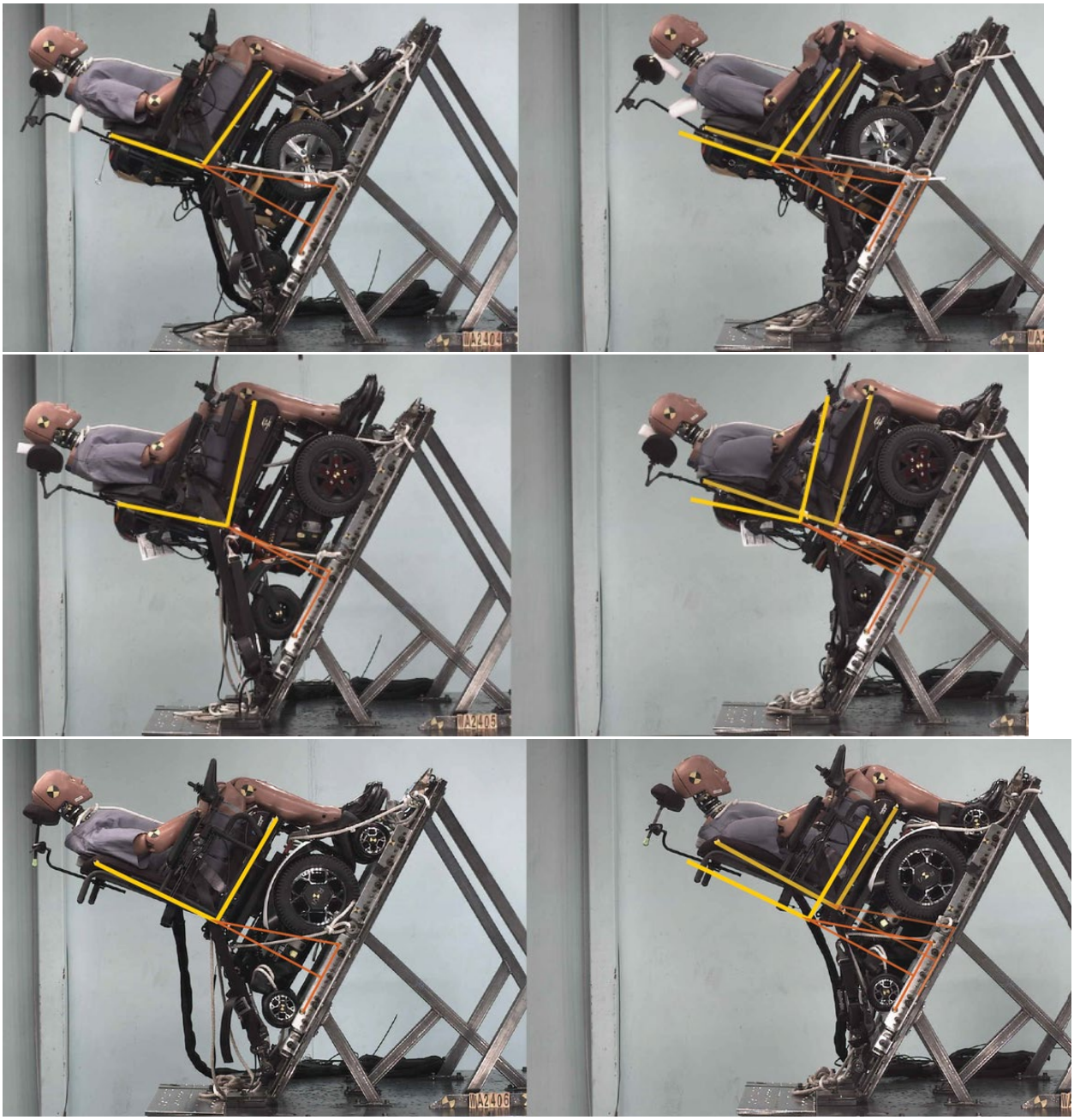

Figure 21. Power wheelchair tests at time zero and at time of peak dynamic displacement, annotated with lines showing original and deformed seatpan and seatback relative to fixture reference.

Two different strategies were used to evaluate residual deformation. Figure 22 through Figure 27 show overlays of the 3D scans of the empty wheelchairs before and after each test, positioned on a horizontal flat surface. We also collected 3-dimensional coordinates of key landmarks before and after testing, with the wheelchairs in the rotated configuration. Figure 28 shows pretest photos overlaid with plots of pre- and post-measurements of wheel axles and the top of the seatback. Pretest data are missing for test WA2405, so post-test data are overlaid to provide a visual.

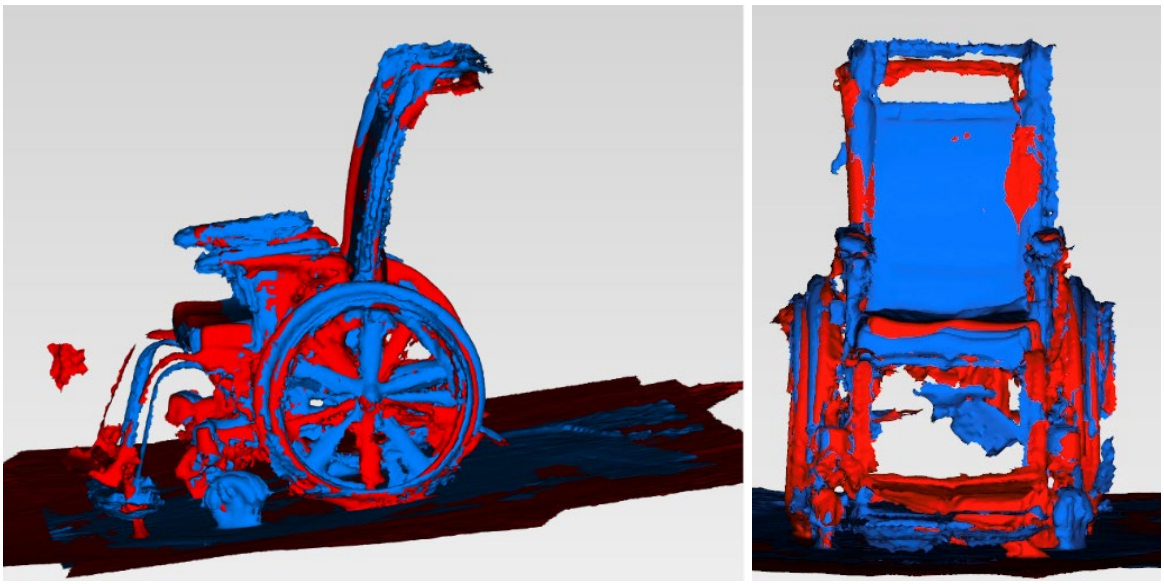

Figure 22. Side and front views of initial and post-test shape of PDG Stellar GL.

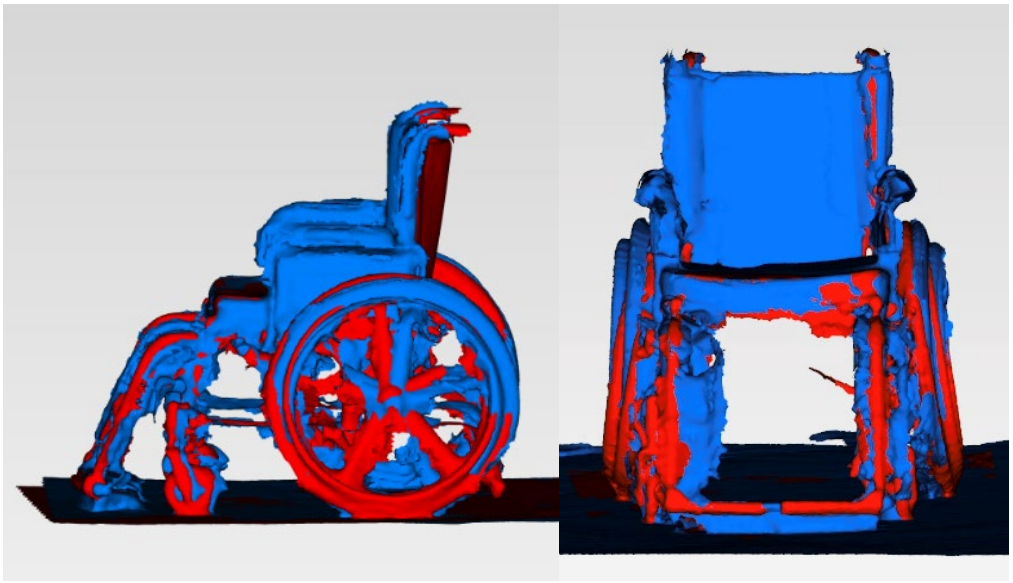

Figure 23. Side and front views of initial and post-test shape of Sunrise Quickie 2.

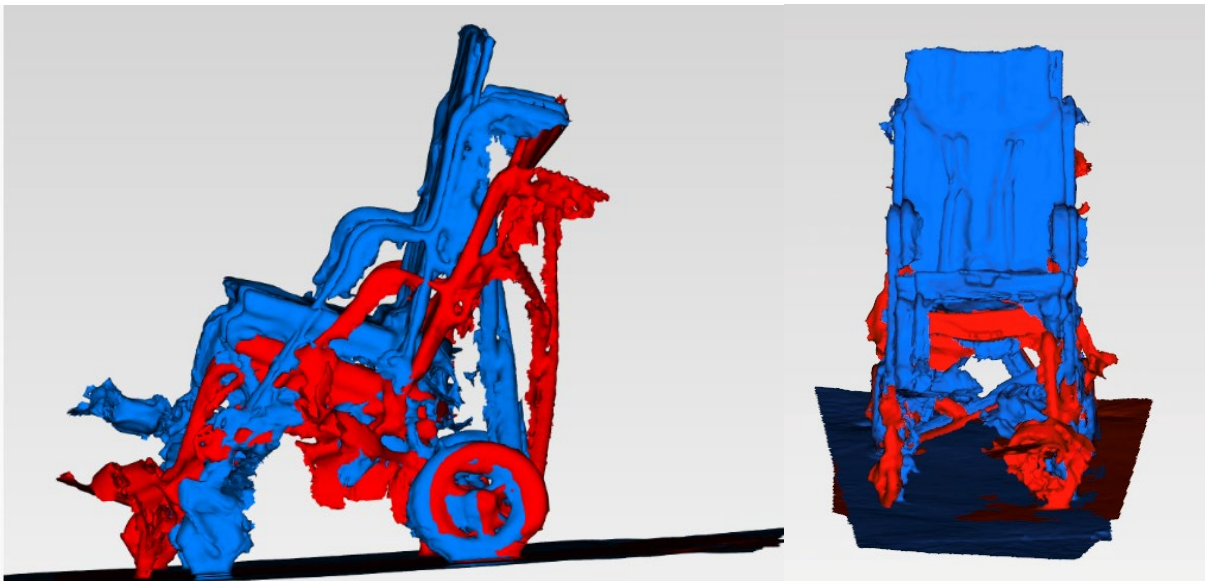

Figure 24. Side and front views of initial and post-test shape of Convaid SFT18.

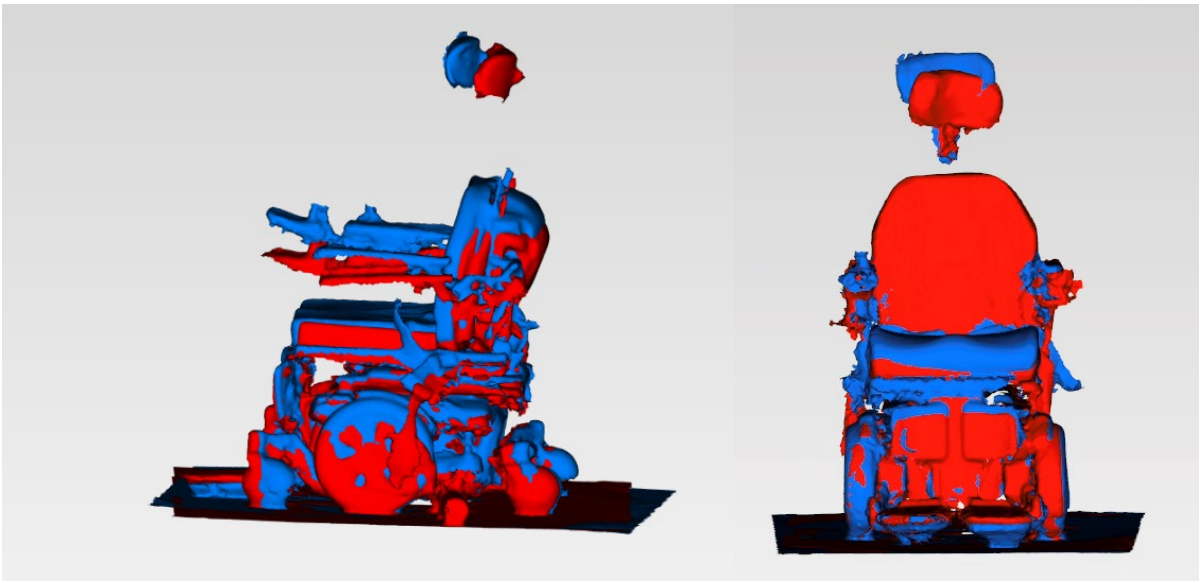

Figure 25. Side and front views of initial and post-test shape of Quantum Q6 Edge 2.

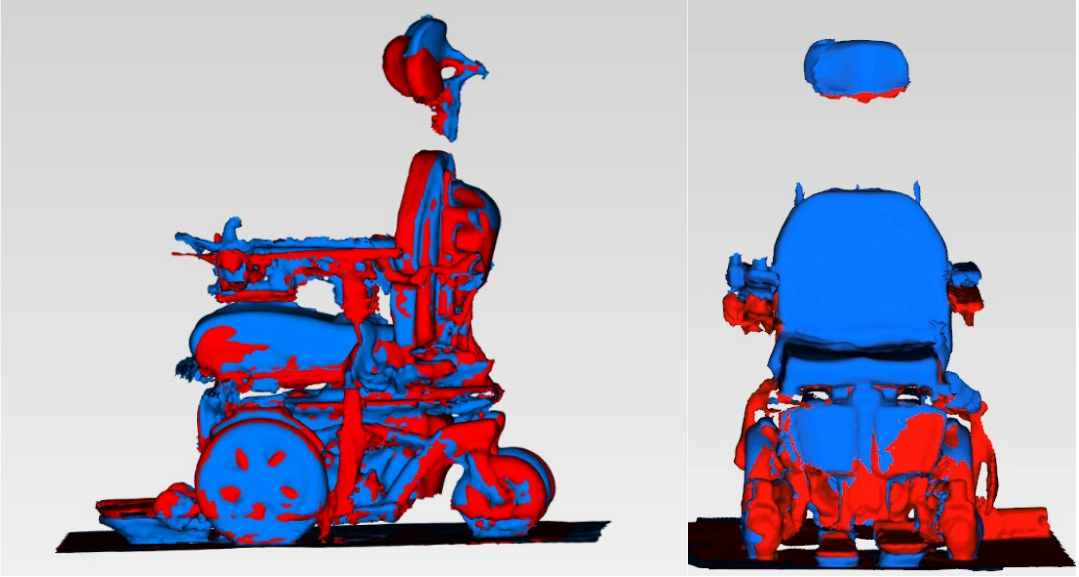

Figure 26. Side and front views of initial and post-test shape of Quantum 4Front 2.

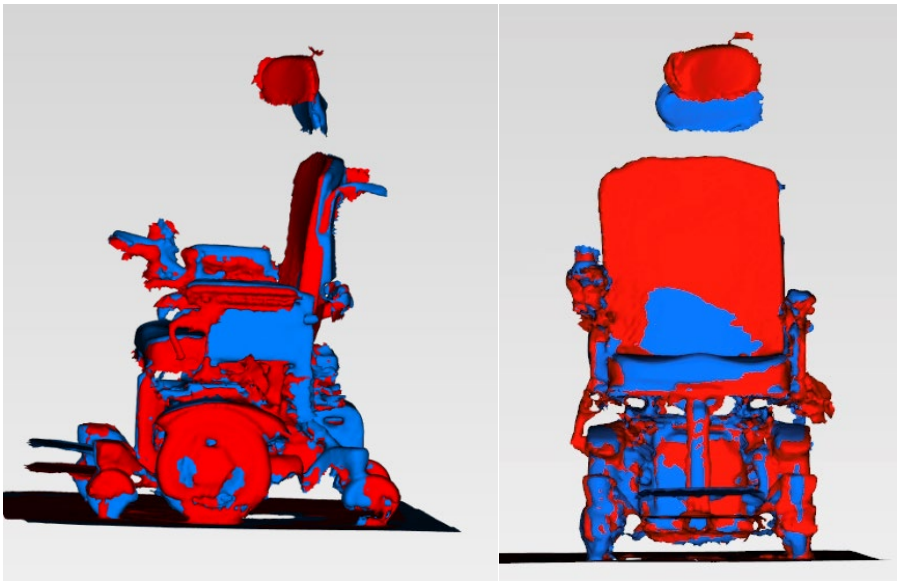

Figure 27. Side and front views of initial and post-test shape of MC Rovi.

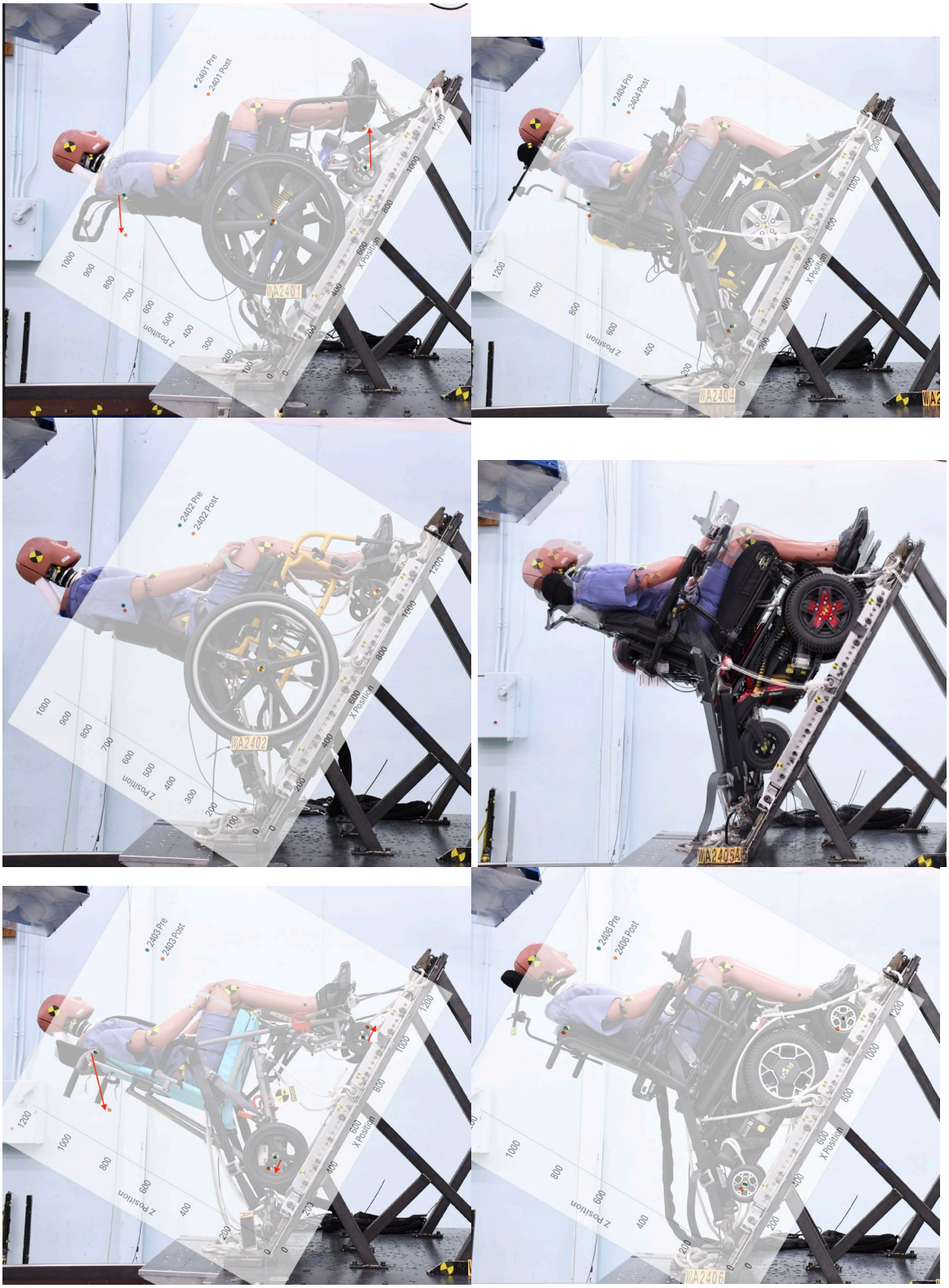

Figure 28. Pre-test photos, overlaid with plots of FARO arm data pre-and post indicating residual deformation of wheel axles and top of seatback. (Data missing for test 5, so pre-and post pictures overlaid.)

Table 3 shows residual deformations of key landmarks using both FARO arm and Sense scan data. The FARO arm measurements were taken with the occupied wheelchair strapped onto the platform in the angled configuration post vertical test, so often caster wheels were not touching the ground and the ATD was loading the seatback as shown below in Figure 29. The Sense scans were completed while the wheelchair was unloaded and sitting flat on the ground.

Table 3. Summary of residual deformation measured from different methods.

Measure (mm)	Method	Axis	WA2401	WA2402	WA2403	WA2404	WA2405	WA2406
Right Front axle	F	X	-134	0	-46	-7	n/a	48
Right Front axle	S	X	-25	-38	-45	-26	-1	14
Right Front axle	S	Y	0	-4	116	-22	12	0
Right Front axle	F	Z	-91	-1	-6	-4	n/a	-3
Right Front axle	S	Z	7	-3	31	-8	15	-4
Right front seatpan	S	X	-27	6	-11	19	-10	11
Right front seatpan	S	Y	6	-8	-45	-12	-24	4
Right front seatpan	S	Z	-25	1	88	-5	7	12
Right Rear Axle	F	X	-13	6	55	23	n/a	25
Right Rear Axle	S	X	-18	-7	20	-4	1	8
Right Rear Axle	S	Y	1	-7	-9	3	-5	6
Right Rear Axle	F	Z	-2	0	0	1	n/a	2
Right Rear Axle	S	Z	3	-9	3	-2	-5	-3
Right seatpan/seatback	S	X	16	-5	4	32	3	0
Right seatpan/seatback	S	Y	-42	9	-52	-27	11	-7
Right seatpan/seatback	S	Z	40	12	83	10	1	-19
Right top seatback	F	X	136	14	182	45	n/a	19
Right top seatback	S	X	11	8	55	21	-6	27
Right top seatback	S	Y	-9	-23	-213	-11	11	22
Right top seatback	F	Z	96	17	178	29	n/a	1
Right top seatback	S	Z	48	-1	232	15	-4	8



Figure 29. Post-test photo of a manual wheelchair following vertical impact

Static testing

Methods

For static testing, we adapted the test procedures found in SAE Aerospace Standard AS8049, revised in November 2020. We used the procedures associated with seat type A-T (transport airplane) specified in 14 CFR Part 25. We focused on the static tests and did not consider flammability requirements. When aircraft seating manufacturers are certifying seats, they first create a test plan indicating how they are interpreting requirements for their products and how they intend to demonstrate compliance with the requirements through testing and/or analysis. They submit this plan for approval by the FAA before testing.

For this task, we hypothesize that wheelchairs meeting RESNA WC19 frontal crashworthiness standards should be able to meet FAA 25.561 static tests requirements for aircraft seats when secured by a 4-point strap tiedown system. The static tests involve loading in upward, forward, lateral, downward, and rearward directions, with the required force level varying for each direction. Appendix C contains draft procedures for static testing of wheelchairs used as aircraft seating.

The standard specifies use of a body block to transmit load to the seat. We purchased a body block fixture meeting the specifications (Schap, Inc.). The fixture contains a loading hook positioned 270 mm above the base and 215 mm forward of the back such that load applied through the hook meets the load application specifications. Prior to testing with commercial products, we evaluated each condition with the SWCB. This fixture was used rather than the surrogate wheelchair (SWC), because the width of the body block would not fit between the fixed armrests on the SWC.

For the adapted static test procedures, we considered the load management approach behind WC18 and WC19 requirements, where the tiedowns secure the wheelchair and the seatbelt restrains the occupant, and developed procedures to divide the applied static loads accordingly. We constructed a dedicated laboratory space for conducting static wheelchair testing that allowed us to split the load between the body block and the tiedown securement points on the wheelchair. For each static test, our initial plan was to load the body block with a target load of 77.1 kg representing occupant mass multiplied by a safety factor of 1.33 (except lateral, following FAA procedures), multiplied by the appropriate load factor for each test direction. During this event we applied a load based on the mass of the wheelchair (without the 1.33 scaling factor) and the appropriate load factor for each test direction through the tiedowns.

This plan required modifications for several reasons. For the upward and downward directions, there are some wheelchairs where it would not be possible to route loading cables in a straight path to the securement points, as shown in Figure 30. To address this issue, our FAA advisors suggested that for the upward tests, we first run one test applying load representing the occupant through the body block, and then conduct a second test applying load representing the wheelchair mass through the securement points, removing the seat and body block if needed to facilitate loading through the securement points. While we initially intended to do this for all wheelchairs, for lighter weight wheelchairs, the mass of the wheelchair is small compared to the mass of the occupant. This led us to adjust our upward testing protocol depending on the mass of the wheelchair. For those weighing less than 50 kg (most manual wheelchairs), we load upward through the body block only using a load of (wheelchair mass + 77.1*1.33) multiplied by the load factor of 3. For those heavier than 50 kg, separate tests loading through the body block (occupant mass) and frame (wheelchair mass).



Figure 30. Examples of wheelchairs that would not allow a direct vertical loading path through the securement points.

For some of the lateral tests of manual wheelchairs, we could not achieve the target loads through the body block and securement points simultaneously because of shifting of the body

block and wheelchair relative to the available winch stroke. This also led us to use the 50 kg threshold for lateral tests, where we would split the load for heavier wheelchairs but apply combined load only through the body block for lighter wheelchairs. This protocol adjustment eliminated the problem.

For the downward tests, we loaded all wheelchairs through the loading plate without the body block. The applied load is (77.1*1.33+wheelchair mass) times the downward scale factor of 6 *g*.

For test setup conditions, the frictional characteristics of the floor may have an effect, particularly in the lateral direction. We purchased aircraft carpet and glued it to the plywood test platform to provide a realistic condition as shown in Figure 31. The wheelchairs were all secured to the test platform using the SWTORS and geometry specified by WC19. When used, the body block was restrained by the wheelchair-anchored lap belt and the additional vehicle-anchored lap belt required to pass the dynamic frontal test. For lateral static testing, the vehicle-anchored lap belt needs to be routed outboard of the wheelchair wheels.

Pulleys secured to the floor are required to conduct the downward test using an overhead winch. Figure 32 shows the fixture constructed to allow variations in lateral placement of the pulleys based on the wheelchair width.



Figure 31. Pretest photo of downward static test, showing carpeted platform, floor pulleys, and loading plate.



Figure 32. Test platform showing carpeting, anchor brackets, and holes to allow appropriate lateral spacing of pulleys.

In our proposed test procedure in Appendix C, we indicate that tests should be conducted with armrests shifted out of the way or removed. One reason is for consistency, as some wheelchairs do not have armrests, and others are designed to easily rotate out of position to facilitate transfers to and from the wheelchair. The second reason is that the body block representing a midsize male does not always fit between the armrests in their use position.

Figure 33 shows all static testing configurations for one wheelchair. The first two photos show the upward tests with the body block and through the frame, where we use cables and an overhead jig to apply load over the four securement brackets. The third photo shows use of the downward loading plate and pulleys. The lateral pull test is in the fourth photo, showing two separate winches on the left side of the wheelchair pulling on the body block and the frame (through the two left securement points) simultaneously. The left armrest was pivoted upward and out of the way of the body block pull assembly path. Photo five shows the rearward pull by two separate winches pulling on the body block and the wheelchair frame (through the two rear securement points) simultaneously. The upper winch pulls on a length of webbing wrapped around the outside of the back canes and through the loop on the body block. Photo six shows the forward pull by two separate winches pulling simultaneously on the body block and the frame (through the two front securement points).



Figure 33. Static test setup in all conditions for the Edge 2: upward through body block, upward through frame, downward, lateral, rear, frontal.

The winches, one mounted to a horizontal beam over the wheelchair station with a pulley, and two mounted to a vertical beam beside the station, had capacities of 22kN (5000 lb). A load cell was used to record the force applied through each winch. A winch controller and software were designed to help monitor the load rates and peak loads. Figure 34 shows the user interface, which includes locations to enter the load and loading rate, as well as a live plot of the data and a way to record video of the test. Once activated, the controller adjusts the winches until they all reach the target load and hold for 3 seconds.

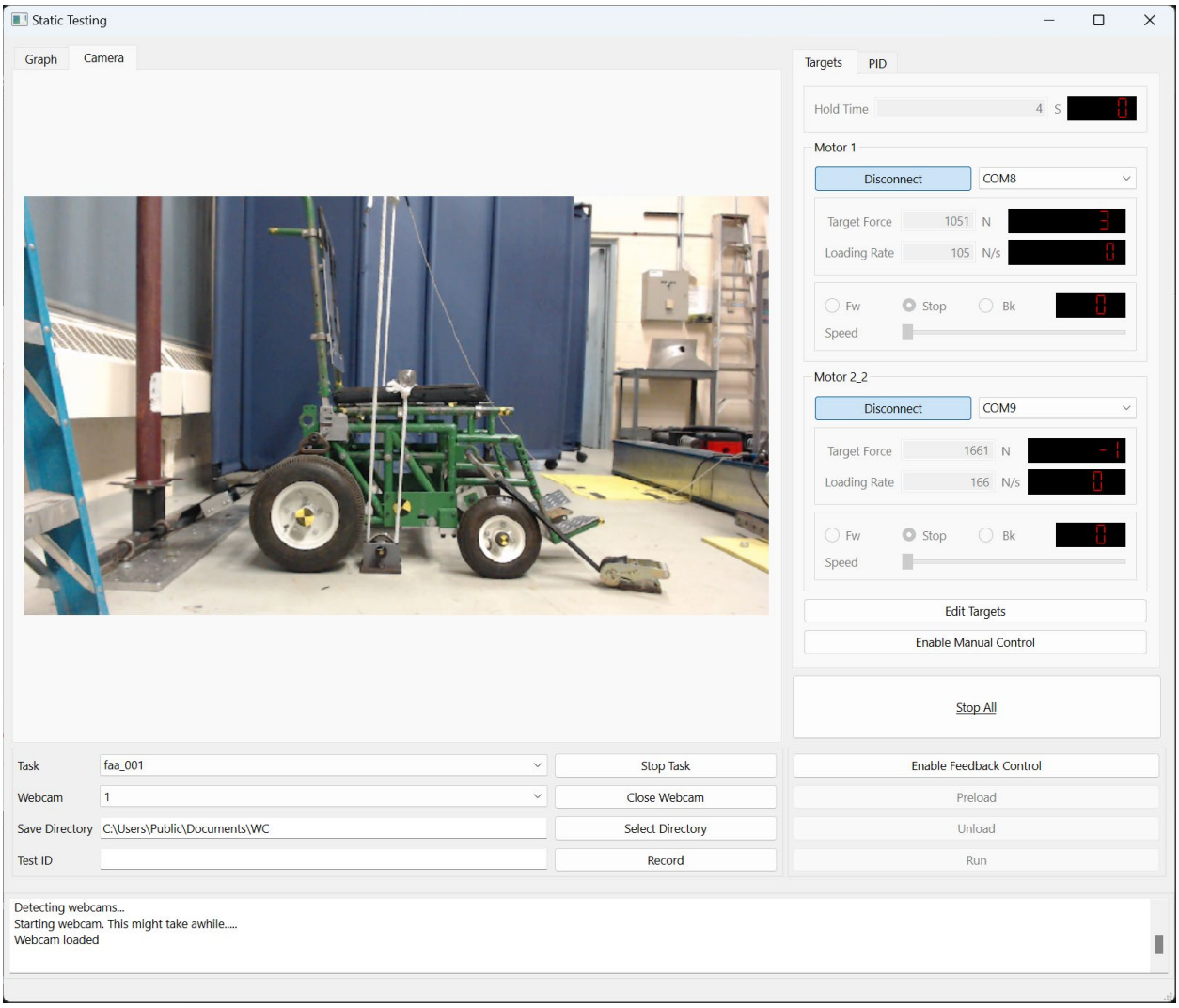

Figure 34. Winch controller software interface that provides control and live feedback of peak loads, loading rate and video.

Pictures of the test setup were taken before and after each test. In addition, we used a portable Sense 3D scanner to capture the geometry of wheelchairs before and after each test. To facilitate consistent alignment of pre- and post-test scans, we conducted them with the wheelchair secured by the tiedowns. We used MeshScape software to calculate the amount of residual deformation from the static tests. Figure 35 illustrates the points digitized to calculate deformation.

The FAA has a requirement that the seatpan cannot pitch upward more than 35 degrees or downward more than 20 degrees. To calculate the seatpan angle before and after each test, we averaged the left and right front and back corners of the seatpan, and calculated seatpan angle from these points.

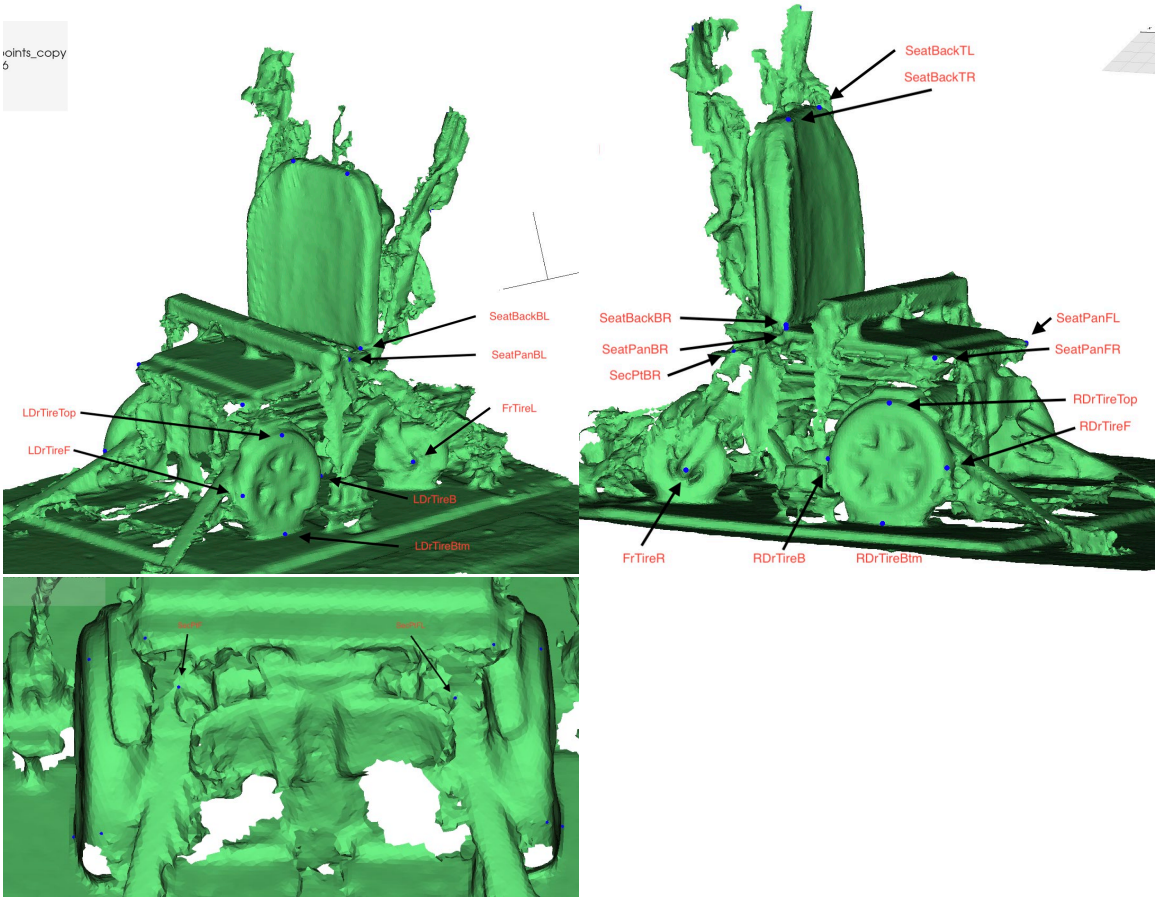

Figure 35. Example illustration of points used to calculate wheelchair deformation during static testing.

Results

Overview

Appendix D contains summary data for each static test, including initial and peak displacement screenshots from videos, controller output, deformation photos (when calculated), and any issues with the test. An example of controller output for one test is shown in Figure 36. The maroon shaded zone is the target load through the frame, while the blue shaded zone is the target for the body block. The green shaded vertical zone shows that the minimum target load was held for 3 sec. This example shows how the controller was able to compensate for a dip in body block load from shifting of the body block. For some tests (such as the example in Figure 36), achieving both loads for the minimum 3 sec required one load to be held for substantially longer.

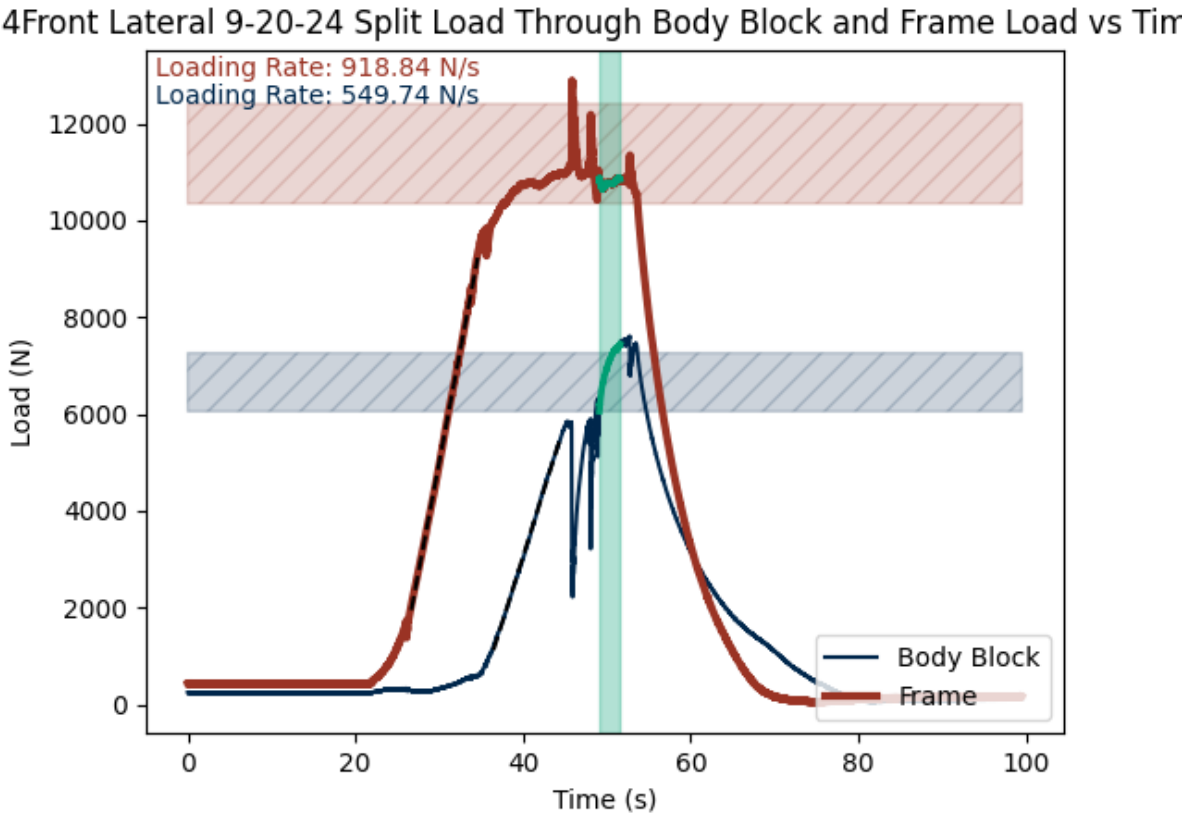

Figure 36. Example controller output showing ability to accommodate for drops in load from shifting of body block.

Table 4 records a matrix of all tests. While we had previously run pilot tests in each direction using the SWCB, testing with commercial wheelchairs identified other issues that needed to be addressed. Changes included adding an additional pulley to the overhead winch, switching to combined loading for lighter weight wheelchairs, and redesigning the downward loading distribution plate. We list all tests conducted, both successful and unsuccessful, because incomplete tests still have the potential to weaken the wheelchair structure and affect outcome of subsequent tests.

Table 4. Summary of static test conditions and outcomes

Test #	Date	Time	WC	Direction	WC Mass (kg)	Prior static	Target Load (N) WC	Target Load (N) BB	Outcome	Notes
AS06	9/19/2024	11:30 AM	**4Front**	Rear	176	N	2590	1513	ok	
AS11	9/20/2024	1:00 PM	4Front	Lateral	176	R	10342	6051	ok	6 g vs. 4 g
AS19	9/23/2024	3:00 PM	4Front	Front	176	R L	15539	9076	ok	
AS20	9/24/2024	9:30 AM	4Front	Down	176	R L F	15645		Incomplete	Target load not achieved
AS24	9/24/2024	2:00 PM	4Front	Down	176	R L F D	15645		ok	Added pulley
AS04	9/18/2024	4:00 PM	**Edge2**	Down	163	N	16410		Incomplete	Application hooks broke
AS07	9/19/2024	12:00 PM	Edge2	Down	163	D	16410		Incomplete	Target load not achieved
AS08	9/19/2024	2:00 PM	Edge2	Rear	163	D D	2399	1513	ok	
AS09	9/20/2024	10:00 AM	Edge2	Lateral	163	D D R L	9593	6051	ok	6 g vs. 4 g
AS16	9/23/2024	1:30 PM	Edge2	Up-BB	163	D D R L		3025	ok	
AS17	9/23/2024	2:00 PM	Edge2	Up-WC	163	D D R L u	4797		ok	
AS18	9/23/2024	2:20 PM	Edge2	Front	163	D D R L u U	14391	9076	ok	
AS23	9/24/2024	2:00 PM	Edge2	Down	163	D D R L u U F	16410		ok	
AS01	9/18/2024	11:00 AM	**Quickie2**	Up-All	18	N		3555	Incomplete	Data issue
AS02	9/18/2024	1:30 PM	**Quickie2**	Up-All	18	U		3555	ok	
AS03	9/18/2024	2:00 PM	Quickie2	Down	18	U U	7110		ok	
AS05	9/19/2024	10:30 AM	Quickie2	Rear	18	U D	706	1513	ok	
AS10	9/20/2024	11:30 AM	Quickie2	Lateral	18	U D R	1042	6051	Incomplete	6 g vs. 4 g, target load not achieved
AS13	9/23/2024	11:00 AM	**Rovi X3**	Front	160	N	14126	9076	ok	
AS21	9/24/2024	10:30 AM	Rovi X3	Up-BB	160	F		3025	ok	
AS22	9/24/2024	10:50 AM	Rovi X3	Up-WC	160	F u	4709		ok	
AS28	9/24/2024	3:00 PM	Rovi X3	Lateral	160	F u U	6278	4042	ok	
AS29	9/24/2024	3:30 PM	Rovi X3	Rear	160	F u U L	2354	1513	ok	

Test #	Date	Time	WC	Direction	WC Mass (kg)	Prior static	Target Load (N) WC	Target Load (N) BB	Outcome	Notes
AS31	9/24/2024	11:30 PM	Rovi X3	Down	160	F u U L R	15468		ok	
AS12	9/23/2024	9:30 AM	**Stellar GL**	Lateral	33	N	2004	6051	Incomplete	6g vs. 4g, damage, target load not achieved
AS14	9/23/2024	11:30 AM	Stellar GL	Front	33	*L*	3002	9076	Incomplete	Target load not achieved
AS15	9/23/2024	11:45 AM	Stellar GL	Front	33	*L F*	3002	9076	deformed caster wheels and securement points	
AS25	9/24/2024	2:30 PM	Stellar GL	Down	33	*L F F*	8052		ok	
AS26	9/24/2024	2:30 PM	Stellar GL	Up-All	33	*L F F D*		4026	Incomplete	Target load not achieved
AS27	9/24/2024	2:30 PM	Stellar GL	Up-All	33	*L F F D U*		4026	ok	
AS30	9/24/2024	4:00 PM	Stellar GL	Rear	33	*L F F D U U*	500	1513	ok	

Bold: no prior static tests Italic: visible damage prior to testing, Underline: incorrect scale factor used

U: upward testing through frame u: upward testing through body block

Ok: test ran to target loads, held for 3 s, no visible damage

Upward Downward Rear Lateral Frontal

As shown in Figure 37, for one lateral test, the wheel did not allow a direct horizontal path between the winch and the securement bracket. To compensate, we routed the cable over a splash guard on the wheelchair, and this approach worked to apply the load.

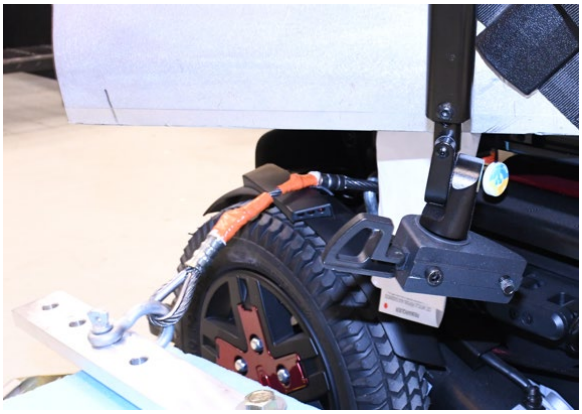

Figure 37. Indirect lateral loading to securement points for 4Front.

We did not conduct tests on the Convaid SFT 18 wheelchair, as it sustained the greatest amount of permanent deformation during the vertical tests. For the Stellar wheelchair, in the first lateral test, we broke the nearside wheel because of routing of vehicle-anchored lap belt inboard, as well as inadvertently setting the target load too high (6 *g* vs. 4 *g* scale factor). This test led to our procedural requirement to route the belt outboard of the propel wheel. The armrest was also damaged, and one securement bracket deformed. We did conduct tests in other directions, but are not including the test data in the report because of the compromised structure from the first static test. No additional damage was observed after the down, rear, and upward tests. After the frontal tests, the front casters and securement points were deformed but still attached.

Deformation Analysis

A summary of resultant residual deformations for selected tests is shown in 0. Detailed deformations in each axis are included in Appendix D. Deformations were calculated for the first and last static test conducted to completion on each wheelchair. While we attempted to compare the total deformation that occurred between each vertical and last static test, the pretest scan prior to the first test was at a different orientation from the posttest scan of the last test, so it was not possible to align the scans with enough confidence to calculate the total deformation that occurred over all tests. The majority of residual deformations were less than 25 mm. For the few larger than this, they occurred at locations within the baseline footprint of the wheelchair, so would not block egress after a crash.

Table 5. Summary of resultant residual deformations from first and last completed test on each wheelchair.

Wheelchair	**4Front**	**4Front**	**Edge2**	**Rovi**	**Rovi**	**Quickie2**	**Quickie2**
Direction	Rear	Down	Down	Front	Down	Up	Rear
Prior Tests	V	V R L F D	V D D R L u U F	V	V F u U L R	V	V U D
Seat Pan Front Right	13	0	11	12	11	20	12
Seat Pan Front Left	14	10	11	7	25	11	0
Seat Pan Rear Left	10	0	11	5	16	12	26
Seat Pan Rear Right	8	10	6	18	15	22	12
Seat Back Top Right	4	12	7	30	27	7	9
Seat Back Top Left	14	21	9	22	26	12	27
Seat Back Bottom Left	19	25	16	8	12	7	10
Seat Back Bottom Right	9	14	17	22	18	12	8
Right Drive Tire Top	6	0	9	6	17	15	6
Right Drive Tire Bottom	10	0	5	5	17	19	4
Right Drive Tire Front	22	8	10	21	17	20	10
Right Drive Tire Back	12	0	6	22	22	14	19
Left Drive Tire Top	15	0	9	7	29	10	20
Left Drive Tire Bottom	0	0	0	10	17	10	15
Left Drive Tire Front	16	8	5	6	24	12	0
Left Drive Tire Back	23	16	19	10	25	7	15
Front Tire Right	10	7	6	46	13	0	5
Front Tire Left	4	5	11	35	24	0	4
Securement Point Front Right	13	6	5	15	0	24	7
Securement Point Front Left	19	23	4	8	17	7	7
Securement Point Back Left	4	0	8	29	13	19	10
Securement Point Back Right	6	0	21	63	17	6	11

Table 6 summarizes data used to calculate residual change in seatpan angle. The greatest change in angle was 2.5 degrees, with the other five calculations less than one degree.

Table 6. Front and back seatpan coordinates pre- and post test, plus angle calculations.

Test ID	**AS02**	**AS05**	**AS13**	**AS23**	**AS24**	**AS31**
Wheelchair	Quickie	Quickie	Rovi	Edge2	4Front	Rovi
Direction	Up	Rear	Front	Down	Down	Down
Front Pre X	54	-143	56	-231	-32	101
Front Pre Z	484	480	438	462	445	455
Rear Pre X	-37	-207	-134	-566	-371	-233
Rear Pre Z	474	473	434	458	458	473
Front Post X	38	-148	46	-235	-29	105
Front Post Z	486	474	439	460	439	433
Rear Post X	-19	-212	-155	-569	-374	-246
Rear Post Z	480	468	433	458	456	468
Pre Angle	5.9	6.3	1.1	0.7	-2.3	-3.1
Pre Angle	6.1	5.7	1.7	0.3	-2.7	-5.6
Delta Angle	**0.2**	**-0.6**	**0.6**	**-0.4**	**-0.4**	**-2.5**

Discussion

In all of our tests adapting FAA aircraft seating procedures to evaluate wheelchairs, we secured the wheelchairs using surrogate, 4-point, strap tiedowns using the geometry specified for testing in WC19, which also matches best practice recommendations for securing wheelchairs in vehicles. We chose this tiedown configuration because it would load the wheelchair's securement brackets in a similar manner for which it was designed, and it is compatible with wheelchair spaces that comply with the ADA specifications. This securement geometry aims to have the rear tiedown strap angle oriented between 45 - 30 degrees, with the rear tiedowns placed straight back from the securement points (parallel to the wheelchair centerline) and the front tiedowns placed forward and outboard of the front securement points for increased lateral stability. In practice, implementation of the recommended tiedown geometry varies; drivers will adjust tiedown anchor locations using adjustable tracks similar to those used on aircraft to secure wheelchairs, while in some vehicles, a platform with fixed anchor geometry can reasonably accommodate many wheelchairs (Q'Straint One). Since the ADA requires a minimum wheelchair station footprint of 762 mm (30 in) wide by 1219 mm (48 in) long on vehicles, most wheelchairs and tiedown systems are designed to work within this space.

Should WC19 wheelchairs be allowed for use as seating on aircraft, we would recommend a similar configuration of anchor hardware for wheelchair stations on aircraft, to avoid needing to conduct additional testing using alternative tiedown anchor geometry. While the recommended configuration could have potential to impede egress for any passengers located outboard of the wheelchair station, this tiedown configuration is recommended and regularly used on public and school buses. Strategies from these configurations could provide insight on how to implement wheelchair stations with similar geometry on aircraft. In addition, simulations conducted with the recommended anchor geometry compared to a system that anchors directly below the securement points shows that increased head excursion and floor loads would occur with more compact tiedown geometries. With regard to the size of wheelchair stations on aircraft, a longer length of 1524 mm (60 in), based on the ADA requirement for alcove dimensions in buildings, would allow sufficient room for most wheelchairs to maneuver into position.

Our method of documenting 3-dimensional deformation before and after each static test using a Sense scanner was successful, as we conducted scans with the wheelchair secured by the tiedown straps which allowed us to align them sufficiently to allow calculations of deformation. For the vertical tests, the use of the FARO 3-dimensional tool with the wheelchairs in the rotated position did not necessarily capture residual deformation, as the gravitational loading of the ATD sometimes lifted the front wheels off the platform, or shifted the non-rigid seatback; these displacements would likely not occur with a rigid aircraft seat bolted to the floor. The Sense scans, performed without the ATD and wheelchairs on the floor, provide a better measure of permanent residual deformation from the vertical testing.

A limitation of this study is that the UMTRI sled pulse is trapezoidal, and cannot be used to generate the ideal triangular-shaped pulse. While our vertical pulse meets all the legal requirements of 14 CFR 25 in terms of achieving the peak acceleration and change in velocity within 80 ms, it achieves them sooner than is required. Thus, the UMTRI version of the FAA pulse is somewhat more severe than is needed. Simulations estimated that ATD kinematics

would be similar in magnitude but happen earlier. Peak ATD measures and forces between the wheelchair, ATD, and floor are 19-50% higher with the UMTRI FAA pulse compared to the triangular FAA pulse. This means that wheelchairs passing dynamic FAA requirements at UMTRI will likely have no issues passing dynamic tests using the triangular FAA pulse. In the first two tests, the peak deceleration was within 0.5 *g* of the minimum 14 *g* requirement. Given the higher loading provided by the trapezoidal UMTRI pulse, we would expect these wheelchairs to pass under the minimum 14 *g* loading.

For the dynamic frontal testing reported previously, wheelchairs were able to pass when the ATD was restrained by an additional vehicle-anchored lap belt, in addition to the wheelchair-anchored lap belt available on WC19 products. Consequently, all of the vertical and static tests also used a vehicle-anchored lap belt. The loads in the vehicle-mounted lap belt under vertical testing were negligible compared to those measured in the wheelchair-anchored lap belt. Use of the vehicle-anchored lap belt contributed to the power wheelchairs passing the static requirements.

The adapted static test procedure included in this report, developed through discussion with FAA advisors, showed acceptable results for the wheelchairs tested. Our interpretation of the FAA standards to apply occupant load through the body block and wheelchair load through the securement brackets follows the intentions of WC19. Testing with the aircraft-mounted lap belt also contributed to better performance compared to our initial results using a strict interpretation of the static testing requirements. Minimal residual deformations resulted from each test condition, and no catastrophic failures occurred. Given that all wheelchairs had previously been dynamically tested vertically, and multiple static tests were conducted on each wheelchair, WC19 wheelchairs are unlikely to deform in a crash such that they would block passenger egress.

All wheelchairs tested in this study meet WC19 test requirements, including a wheelchair-attached crashworthy lap belt. However, these findings do not directly apply to wheelchairs that meet ISO 7176-19 standards. A key difference between the standards is that the ISO standard does not require testing with a wheelchair-mounted crashworthy lap belt. As a result, WC19 wheelchairs experience more load during WC19 frontal impact testing than ISO-compliant wheelchairs. Many wheelchair models that pass ISO 7176-19 do not pass when tested to WC19. More simply, the WC19 wheelchairs are tested under higher loading. In the vertical tests, most of the occupant load was routed through the wheelchair-mounted lap belt and loads through the vehicle-mounted lap belts were negligible. Additional testing of more ISO 7176-19 products would be needed to confirm whether the vehicle-mounted belt alone would produce acceptable results under vertical loading.

The SWCB was developed to take the place of commercial wheelchair frames when assessing different seating systems. We primarily chose to use it during development of FAA static testing procedures, rather than the SWC, because the static body block would not fit in between the fixed armrest of the SWC. All tests were first conducted using the SWCB to identify procedural issues before conducting tests on commercial products. However, additional modifications were needed to the procedure to appropriately complete the static test procedures.

This study evaluated wheelchairs meeting WC19 requirements for ground vehicles, to determine if they might be appropriate for use as seats on aircraft. While preliminary results support this hypothesis, a challenge is that most people currently do not use WC19 wheelchairs. In an ongoing study of wheelchair geometry being performed by the UMTRI team, only two of 99 volunteers were using WC19 wheelchairs. Wheelchairs are regulated as medical devices by the Food and Drug Administration (FDA), which does not require wheelchairs to be crashworthy for use as vehicle seating. The National Highway Traffic Safety Administration (NHTSA) does not address wheelchairs used as vehicle seats. While the cost of adding WC19 hardware is an added $200 to $500 on wheelchairs with a typical total cost $1500 to $20,000, the cost is not currently covered by most insurers, with the exception of the Veterans Administration. As a result of this and also concerns about product liability, most wheelchair manufacturers do not promote the availability of the WC19 option. It may be possible to retrofit some wheelchair models with hardware, but most insurers cover wheelchair replacement every five years, and many users would not be able to cover the out-of-pocket costs to add the WC19 option themselves.

Summary and Conclusions

This report describes the response of WC19-compliant wheelchairs tested under the dynamic vertical tests required for aircraft seating, as well as using an adapted version of the FAA static tests. Observations to date include:

- Computer simulations showed that the UMTRI version of the FAA vertical pulse provides similar kinematic response to the triangular pulse.
- Two manual wheelchairs passed the vertical dynamic testing requirements within the allowable deformation requirements. For a third, one of the footrests fractured, causing a sharp edge, but remained in place because it was strapped to the ATD foot, as would be recommended with this wheelchair when used.
- Three power wheelchairs passed the vertical dynamic testing requirements within the allowable deformation requirements, but exceeded the allowable lumbar force. For one wheelchair, a motor detached but was retained by its cable, so it would not become a projectile and thus would still meet WC19 requirements.
- An adapted version of the FAA static test procedures that splits the loading through the body block and wheelchair securement points under some conditions was developed. This procedure would be used for wheelchairs with masses greater than 50 kg when conducting frontal, upward, rearward, and lateral static testing. For wheelchairs <50 kg, a combined load through the body block representing occupant and wheelchair mass would be used for lateral, upward, and downward testing, while the load would be split for frontal and rearward testing.
- Despite previous testing under vertical conditions, static testing of multiple wheelchairs under multiple static loading conditions resulted in good performance and minimal permanent deformations, with most measures less than 25 mm and a maximum deformation across all tests of 63 mm.

Ongoing Work

Continuing work in the current project to evaluate wheelchairs as potential aircraft seating will include the following tasks:

- Test additional wheelchairs using updated static testing procedures.
- Test additional wheelchairs under frontal dynamic loading conditions.
- Test additional wheelchairs under vertical dynamic loading conditions.
- Publish a final report on the entire project.

Bibliography

[1] RESNA, *Wheelchairs Used as Seats in Motor Vehicles*. 2017, pp. 1–105.

[2] K. D. Klinich *et al.*, "Evaluating Wheelchairs for Potential Use as Aircraft Seating: Static and Dynamic Frontal Test Conditions (Interim Project Report)," University of Michigan Transportation Research Institute, 2024. doi: 10.7302/22383.

[3] V. Gowdy *et al.*, "A lumbar spine modification to the hybrid III ATD for aircraft seat tests," in *SAE Technical Papers*, SAE International, 1999. doi: 10.4271/1999-01-1609.

[4] Philippens Mat MGM, Forbes Patrick A, Wismans Jac SHM, DeWeese Rick, and Moorcroft David, "Neck Injury Criteria for Side-Facing Aircraft Seats," 2011.

Appendix A. Draft Vertical Dynamic Test Procedure for Wheelchairs Used as Aircraft Seating

Introduction

These procedures were developed to evaluate how to test wheelchairs according to FAA requirements for aircraft seating. The FAA requirements have been adapted for wheelchair testing using methods and requirements from RESNA WC-4:2017.

Wheelchair Test Methods

Equipment

The equipment needed to conduct this testing includes:

- A complete commercial wheelchair that complies with ANSI/RESNA WC19 with the crashworthy commercial wheelchair-anchored lap belt required by WC19.
- A dynamic sled capable of producing the 14-*g*, 38 km/hr test specified in 14 CFR 25
- A rotating fixture that allows securement and measurement of the wheelchair in a horizontal configuration, which can then be rotated upward 60 degrees and braced to provide a loading condition that simulates frontal and upward loading of the seat that might occur in a plane crash.
- Calibrated instrumentation to verify the tested pulse with a data collection system that complies with SAE J211.
- A midsized male FAA Hybrid III ATD.
- A surrogate WTORS meeting the description of Annex D of ANSI/RESNA WC19.
- Four high speed digital video cameras capable of recording images at 1000 fps, placed right side perpendicular to sled travel, right side perpendicular to sled travel towards the rear to capture rebound, overall left side perpendicular to the WPS, and overhead.

Prior to conducting the test, make sure the sled instrumentation has been calibrated per the manufacturer in the previous 12 months. Inspect the ATD for damage and adjust the joints to a resistance of 1 *g*. Clothe the ATD in snug fitting cotton clothing as specified in federal crash testing standards. Verify that the wheelchair is in good working order and the tires are inflated per manufacturer's specifications.

Test Procedures

1. Define a wheelchair station on the sled platform that is at least 76 cm (30 in) wide and 123 (48 in) long.
2. Orient the centerline of the wheelchair station so that in the plan (overhead) view, the centerline of the station aligns with the primary direction of sled travel.
3. The wheelchair should be adjusted to fit the ATD per the manufacturer's instructions and all adjustment mechanisms should be tightened per the user manual.
4. Adjustable elements of the seat (such as tilt and recline) should be in a middle position rather than at the end of adjustment travel.
5. The seat back support angle should be between 5 and 30 degrees from vertical when measured unloaded at the seatback centerline.
6. The seat pan angle should be between 5 and 30 degrees from horizontal when measured unloaded at the seat centerline.
7. Install the SWTORS so that the anchor points are:

a. Symmetrically located with respect to the wheelchair center line (aka the wheelchair reference place).
b. At least 48 inches apart from front to rear of the wheelchair.
c. Installed so that the rear anchorages are directly behind the wheelchair securement points and the rear tiedown straps are parallel to the wheelchair centerline when viewed from overhead.
d. Installed so that the front tiedown points are outboard of the front wheelchair securement points, but not further apart than 76 cm (30 in).

8. Secure the wheelchair with the SWTORS.
    a. While maintaining the wheelchair reference plane within 3° of the centerline of the wheelchair station, adjust the fore/aft position of the wheelchair while tensioning the tiedown straps to between 100 N and 200 N (about 22 lbf and 44 lbf), to achieve a side-view projected angle of the rear tiedown straps of 45° ± 3° to the horizontal.
    b. If a rear tiedown-strap angle in this range cannot be achieved with a tiedown-strap length of at least 495 mm (19.5 in.), adjust the length of the rear tiedown strap assemblies to between 495 mm and 508 mm (19.5 in. and 20 in.), and measure the resulting side-view projected angle of the rear tiedown straps.
9. Place targets on the wheelchair landmarks listed below. (Optional: scan the empty wheelchair with a 3D surface measurement sensor.)
    a. Top of seatback
    b. Front of seatpan
    c. Seatback/seatpan junction
    d. Each end of each wheel axle
10. Place the ATD into the wheelchair making sure the ATD is seated symmetrically with the torso upright and the back and legs pushed into and in contact with the wheelchair back support and seat.
11. Position the wheelchair-anchored seat belt on the ATD with the lap belt routed at the junction of the pelvis/thigh.
12. Position a second vehicle-mounted lap belt using the rear tiedown anchors as securement points and tighten until snug.
13. Measure the location of wheelchair and ATD landmarks, using a reference point on the platform that will rotate.
14. Measure and record the SWTORS anchorage locations, tiedown strap angles, seat belt angles, the wheelchair width at the seat rails, the ATD H-point height, wheelchair back support angle, and wheelchair seat pan angle.
15. Rotate the platform to 60 degrees and install the bracing structure.
16. Measure the location of the ATD head, neck, and thorax landmarks. They should be within 25 mm of the location relative to the wheelchair seatback in the horizontal position. If necessary, shift the ATD torso using foam inserts to achieve the same position relative to the seatback (within 25 mm) as recorded in the horizontal position.
17. Conduct the sled test.

18. Measure and record the same landmarks measured in steps 14 and 16 after the test is complete. (Optional: scan the empty wheelchair with a 3D surface measurement sensor to record permanent deformation.)

Wheelchair Performance Criteria

When tested according to the procedures in this document, the wheelchair should meet the following requirements:

1. The wheelchair securement point structural components shall not fail completely.
2. The wheelchair securement points shall not deform such that the hooks of the four-point, strap-type surrogate tiedown system cannot be disengaged and removed.
3. The wheelchair should be in an upright position at the end of the test.
4. The ATD should be in a seated posture in the wheelchair at the end of the test, with the ATD torso leaning less than 45° from a vertical axis rotated 60° relative to the sled travel direction when viewed from all directions.
5. No rigid components, parts, equipment, or accessories with a mass greater than 150 grams (5.3 oz) should detach from the wheelchair during the test.
6. Wheelchair components that could contact the occupant seated in a wheelchair or nearby occupants should not break or separate in a manner that produces sharp edges with a radius of less than 2 mm (0.08 in.).
7. Locking mechanisms of tilt seating systems shall not have structural components that completely fail during the test. Shifting of seating-system orientation from release or slipping of a friction clamp are allowed if the sideview angle of the seating surface does not rotate below horizontal.
8. At the end of the test, the average height of the left and right ATD H-points relative to the wheelchair ground plane shall not have decreased by more than 20% from the pre-test average height.
9. At the end of the test, the average wheelchair width, measured at the seat rails shall not have decreased by more than 20% from the pre-test width.
10. Seats and back supports shall not separate or detach from the wheelchair or wheelchair frame unless there is a backup at the same point that remains functional.
11. No webbing of the surrogate wheelchair tiedown and occupant restraint system (SWTORS) or commercial WTORS shall completely fail due to interaction with the wheelchair or its components during a test.
12. All securement hooks of the SWTORS or commercial tiedown shall remain attached to the wheelchair securement points throughout the test.
13. Wheelchair-anchored belt restraints shall not become detached at anchorages, disconnected at buckles, or show complete webbing failure.
14. Batteries of power wheelchairs or their surrogate replacement parts shall:
    i) not move completely outside the wheelchair footprint,
    ii) remain attached or tethered to the battery compartment throughout the test, and
    iii) shall not contact the ATD

Appendix B. Additional Dynamic Testing Results

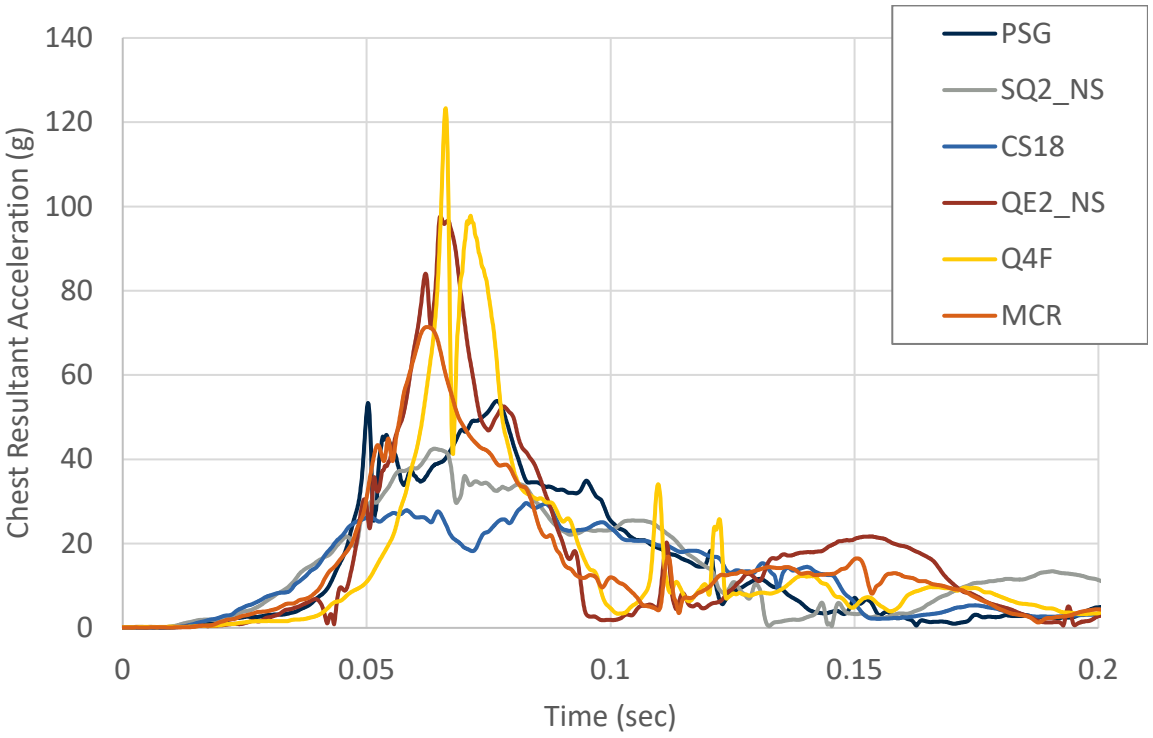

Figure 38. Chest resultant acceleration from all vertical tests.

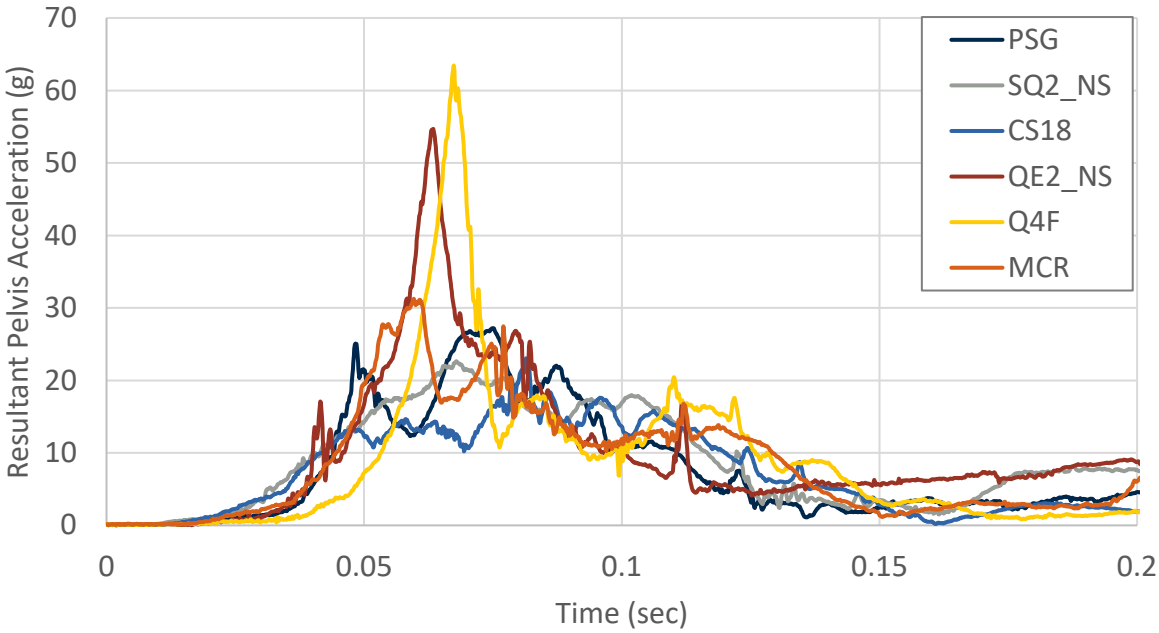

Figure 39. Pelvis resultant acceleration from all vertical tests.

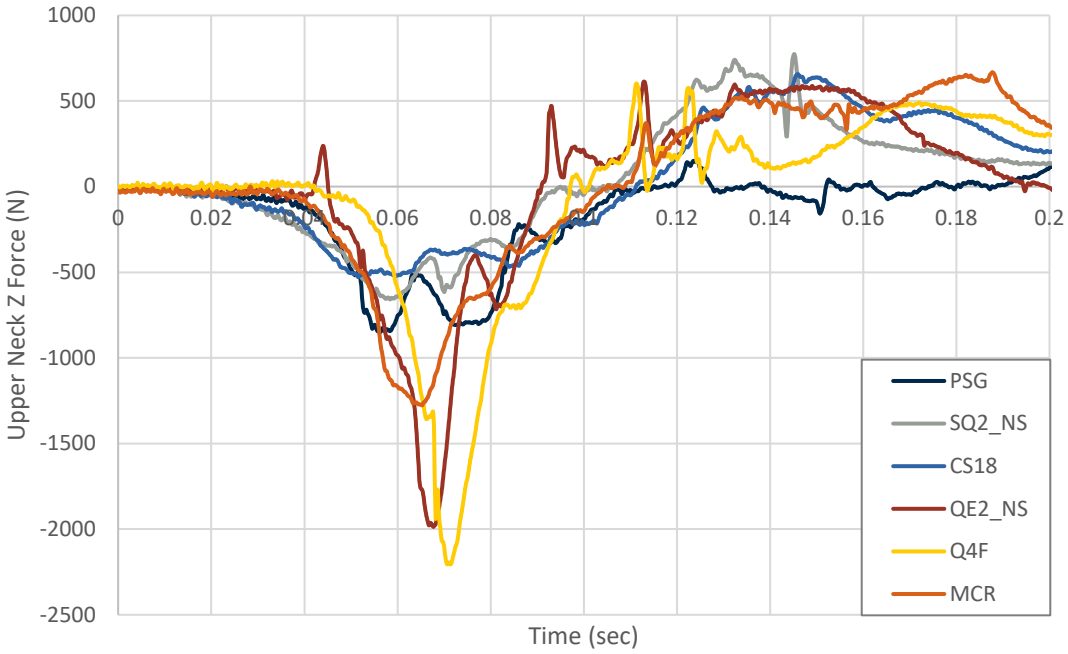

Figure 40. Upper neck axial force from all vertical tests.

Appendix C. Draft Static Test Procedures for Wheelchairs Used as Aircraft Seating

Objectives

This procedure describes a method for adapting the FAA static pull tests specified by FAA 25.561 and SAE Aerospace Standard AS8049 for aircraft seating to wheelchairs used as seats in aircraft cabins.

Test Methods

Equipment

The equipment needed to conduct this testing includes:

1. A test platform that can accommodate mounting of the surrogate wheelchair tiedown and occupant restraint system (SWTORS) defined in WC19 Annex D and is strong enough to serve as a rigid, immobile platform for all the pull testing conditions.
2. A complete commercial wheelchair that complies with ANSI/RESNA WC19 with the crashworthy commercial wheelchair-anchored lap belt required by WC19.
3. A rigid body block specified in SAE Aerospace Standard AS8049.
4. The SWTORS system defined in WC19 Annex D, including:
    a. at least two rear tiedown assemblies with split-drum mechanisms for securing and adjusting the length of rear tiedown straps,
    b. two front tiedown assemblies with pivoting ratchet mechanisms for adjusting tiedown strap tensions, and
    c. a surrogate vehicle-anchored lap belt with appropriate floor anchorage hardware and a means to remove slack from the belt.
5. Low pile carpeting meeting the FAA specification FAR 25.853.
6. At least two winches capable of generating a peak force as high as 22,000 N at a rate of 2200 N/s and as low as 85 N at a rate of 8 N/s per second. The winch mounting must be adjustable, so that the line of pull application can be tuned for each wheelchair model.
7. An external structure and means to mount the winches relative to the test platform to achieve the desired orthogonal pull direction.
8. Instrumentation to measure the inline tension loads generated by each winch.
9. Digital video camera to capture pull event kinematics. The camera should be capable of capturing the wheelchair, floor surface, test ID markers and any reference targets needed for post-test processing.
10. Still camera to document the pre-test set up and post-test response after loading.
11. Method to capture and compare deformation of the wheelchair frame before and after the test, such as 3-D surface scanning.
12. High contrast targets for marking key wheelchair landmarks.

Prior to conducting the test make sure all instrumentation has been calibrated per the manufacturer in the past 12 months.

Test Procedures

1. Define a wheelchair station on the static pull platform that is at least 30 inches wide and 48 inches long, and preferably 36 inches wide and 60 inches long.

2. Apply the carpeting to the floor surface so that the wheelchair wheels will interact with the carpeted surface for the duration of the pull test to create typical floor friction characteristics. When applying the carpet, take care that the carpeting does not interfere with the WTORS fixturing and do not allow the carpeting to slide during the test.
3. Orient the centerline of the wheelchair station so that in the plan (overhead) view, the centerline of the station and the wheelchair are aligned.
4. Adjustable elements of the seat (such as tilt and recline adjustment) should be in a middle position rather than at the end of adjustment travel.
5. The seat back support angle should be between 5 and 30 degrees from vertical when measured unloaded at the back support centerline.
6. The seat pan angle should be between 5 and 30 degrees from horizontal when measured unloaded at the seat centerline.
7. The wheelchair caster wheels should be in the trailing position, which is the orientation that is achieved when the wheelchair is moving forward in a straight line.
8. Install the SWTORS so that the anchor points are:
    a. Symmetrically located with respect to the wheelchair center line (aka the wheelchair reference plane),
    b. At least 48 inches apart from front to rear of the wheelchair,
    c. Installed so that the rear anchorages are directly behind the wheelchair securement points and the rear tiedown straps are parallel to the wheelchair centerline when viewed from overhead, and
    d. Installed so that the front tiedown points are outboard of the front wheelchair securement points, but not further apart than 30 inches.
9. Secure the wheelchair with the SWTORS.
    a. While maintaining the wheelchair reference plane within 3° of the centerline of the wheelchair station, adjust the fore/aft position of the wheelchair while tensioning the tiedown straps to between 100 N and 200 N (about 22 lbf and 44 lbf), to achieve a side-view projected angle of the rear tiedown straps of 45° ± 3° to the horizontal.
    b. If a rear tiedown-strap angle in this range cannot be achieved with a tiedown-strap length of at least 495 mm (19.5 in.), adjust the length of the rear tiedown strap assemblies to between 495 mm and 508 mm (19.5 in. and 20 in.), and measure the resulting side-view projected angle of the rear tiedown straps.

Note 1: The length of a rear tiedown-strap assembly is defined as the straight-line distance from the point of intersection of the surrogate tiedown hook with the wheelchair securement point, to the center of the rod supporting the rod-end bearing of the surrogate tiedown rear anchorage.

Note 2: If using a wheelchair with more than two rear securement points, follow instructions provided by the wheelchair manufacturer for adjusting the length and/or angle of rear straps. If no specific instruction is provided, adjust two of the rear straps according to 9b and adjust additional straps so that slack is removed when the system is tensioned.

10. Remove the wheelchair armrests or move them to a position where they will not interfere with the winch cable or movement of the body block.

11. Place the body block into the wheelchair with the centerline of the body block aligned with the centerline of the wheelchair seat if use of the body block is indicated in Table 1.
12. Position the wheelchair-anchored and vehicle-anchored seat belts on the body block with the lap belt routed at the junction of the pelvis/thigh. Snug both belts to between 2-4 N tension.
13. Apply high contrast targets to the wheelchair so that they can be seen in the camera view. Apply targets to the top of the back support, near the back support-to-seat junction, the front of the seat and near the CG of the wheelchair frame (usually just forward and above the rear axle).
14. Adjust the location of the winches to achieve a straight line pull in the desired orthogonal direction. For the forward, rearward, and lateral pulls, make sure the direction of the applied force is parallel to the ground within +/- 5 degrees. For the upward and downward pulls, make sure the direction of the pull is perpendicular to the ground +/- 5 degrees.
15. Attach either one or two winches. Check Table 1 and Figures 1 to 7 to verify the appropriate test configuration.
    a. A winch pulling on the body block attaches to the ring feature on the front of the block.
    b. A winch pulling forward, laterally, or rearward on the wheelchair frame is attached so load is evenly distributed between the two wheelchair securement points on the side of the wheelchair adjacent to load application (the two front securement points for forward pull, the two side securement points for lateral pull, or the two rear securement points for rearward pull).
    c. A winch applying an upward or downward load splits that load evenly among the 4 wheelchair securement points.
16. Document the shape of the wheelchair before loading (i.e., use a 3D scanner).
17. Calculate the desired peak load(s) and loading rate(s), where:
    a. The peak body block load (N) = 77.1 kg * (*g*-level from Table 1) * (fitting factor multiplier from Table 1) *9.81 m/s^2
    b. The rate of loading for the body block = (peak body block load)/10
    c. The frame load (N) = (WC mass in kg) * (*g* -level from Table 1) * 9.81 m/s^2
    d. The rate of loading for the frame = (peak frame load)/10
18. Apply a preload ~5% of the target load to the winch to remove slack from the system.
19. Take pre-test photos of the setup.
20. Conduct the pull test in the desired direction, with the parameters and configurations described below.

Table 1. Summary of Static Pull Conditions

Pull Direction	One winch or two winches?	*g*-level multiplier	Use 1.33 fitting factor multiplier on body block load?	Body Block present for pull?	Illustration
Frontal	2	9	Yes	Yes	Figure 1
Lateral WC < 50kg	1	4	No	Yes	Figure 2
Lateral WC >= 50kg	2	4	No	Yes	Figure 3
Rearward	2	1.5	Yes	Yes	Figure 4
Downward	1	6	Yes	No	Figure 5
Upward WC < 50kg	1	3	Yes	Yes	Figure 6
Upward WC >= 50kg	1st Test – 1 for body block load	3	Yes	Yes	Figure 7a
Upward WC >= 50kg	2nd Test – 1 for frame load	3	NA	No	Figure 7b

Illustrations of Pull Configurations

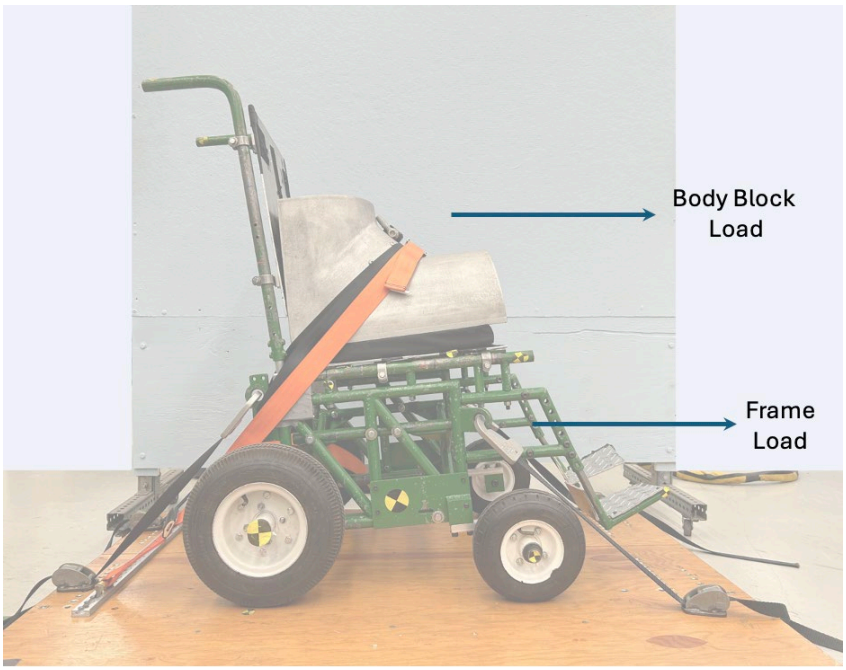

Figure 1. Frontal Pull Set Up for All Wheelchairs



Figure 2. Lateral Pull Set Up for Wheelchairs < 50 kg

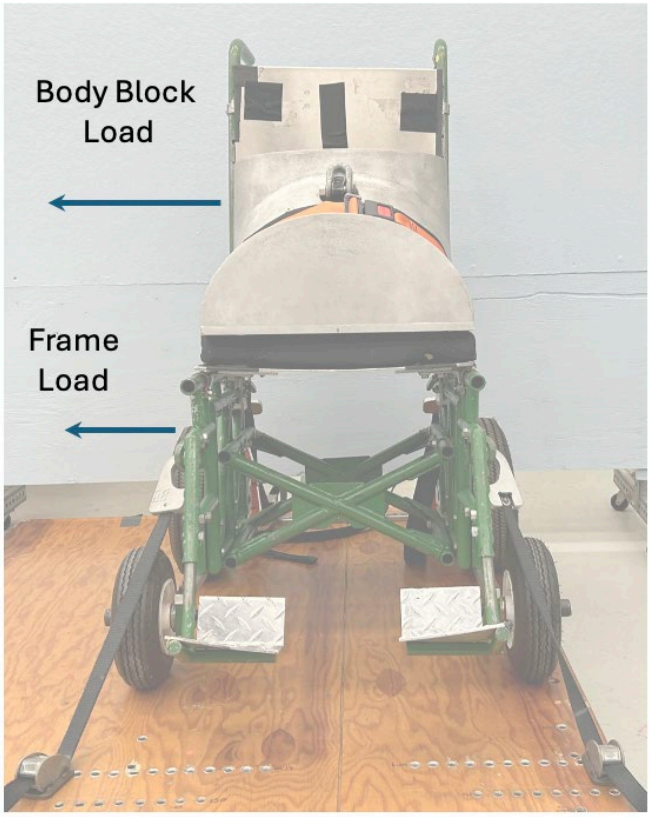

Figure 3. Lateral Pull Set Up for Wheelchairs > 50 kg

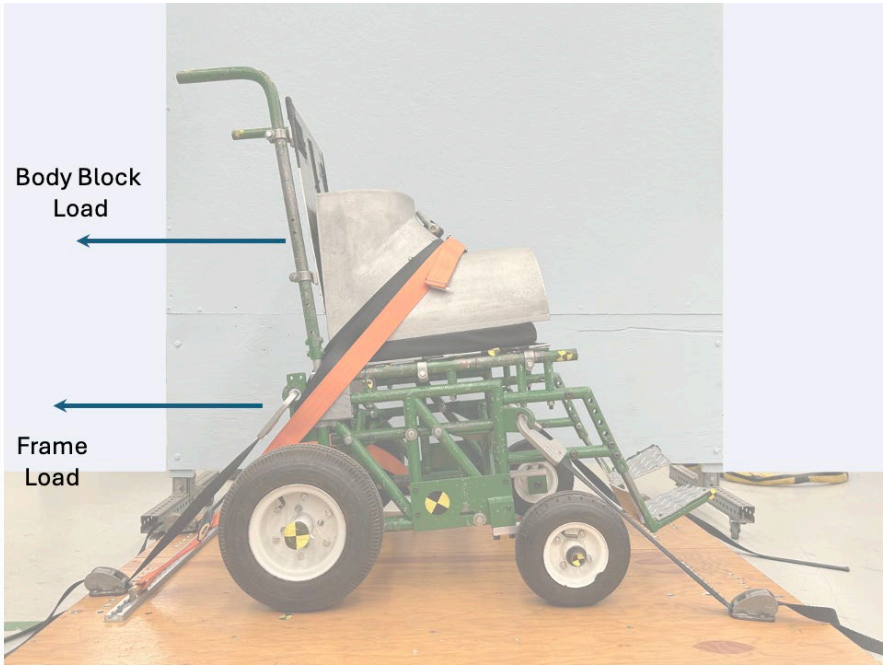

Figure 4. Rearward Pull Set Up for All Wheelchairs



Figure 5. Downward Loading for All Wheelchairs

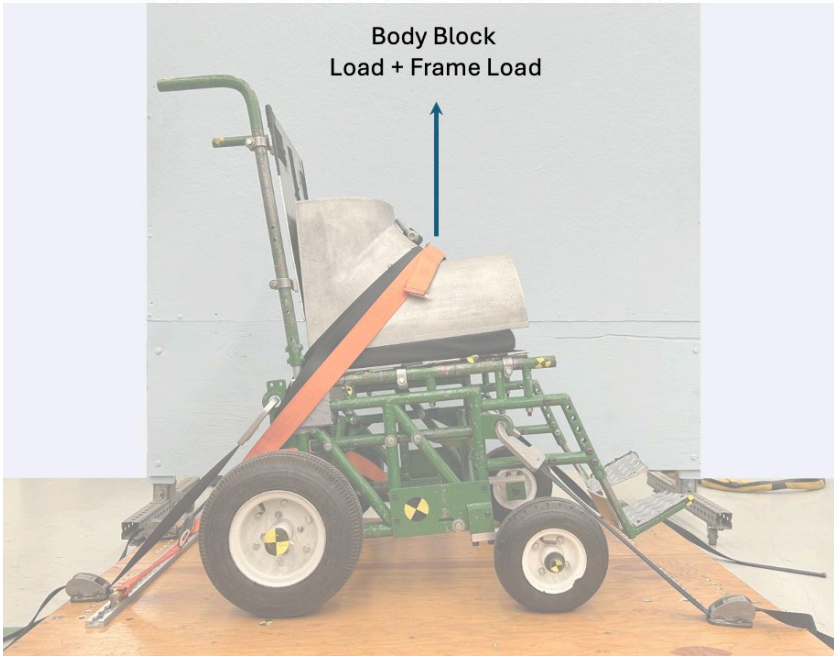

Figure 6. Upward Loading for Wheelchairs < 50 kg

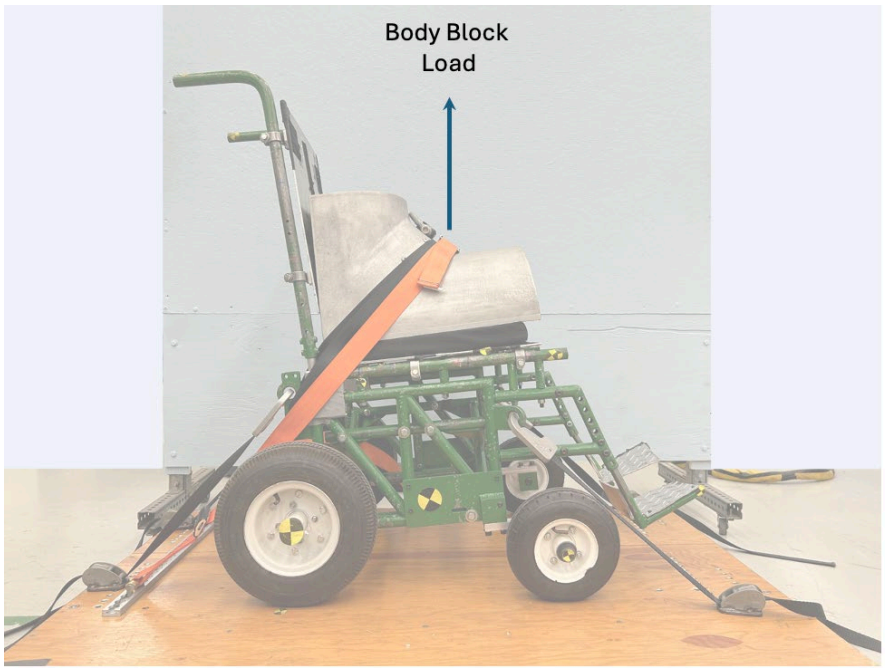

Figure 7a. Step One of Upward Loading for Wheelchairs > 50 kg

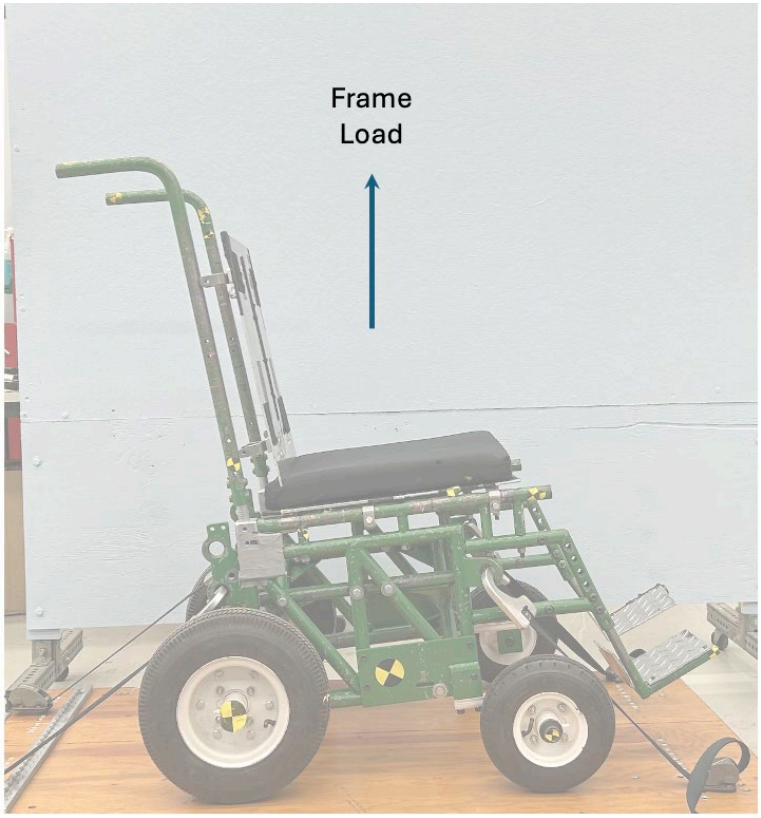

Figure 7b. Step Two of Upward Loading for Wheelchairs > 50 kg

Post-test Measurement

After the load is released:

1. Take post-test photos from the front, side, and rear of the wheelchair.
2. Inspect the wheelchair to determine if any parts failed or fully detached.
3. Document any deformation or breakage with photos.
4. Document the shape and quantify the level of deformation of the wheelchair after loading (i.e., use 3D scanner).

Wheelchair Performance Criteria

When tested according to the procedures in this document, the wheelchair should meet the following requirements:

1. The wheelchair shall not deform in a way that impedes evacuation of the wheelchair occupant or other passengers after an emergency landing.
2. The seat bottom rotational permanent deformation shall not result in an angle that exceeds 20 degrees pitch down or 35 degrees pitch up from the horizontal plane. This rotational deformation shall be measured between the fore and aft extremities of the seat pan at the centerline of each seat bottom (Figure 1A). Rotation of the seat pan shall not cause entrapment of the occupant.
3. The wheelchair securement point structural components shall not fail completely.
4. The wheelchair securement points shall not deform such that the hooks of the four-point, strap-type surrogate tiedown system cannot be disengaged and removed.
5. The wheelchair should be in an upright position at the end of the test with the body block on the seating system.
5. No rigid components, parts, equipment, or accessories with a mass greater than 150 grams (5.3 oz) should completely detach from the wheelchair during the test.
6. Wheelchair components that could contact the occupant seated in a wheelchair or nearby occupants should not break or separate in a manner that produces sharp edges with a radius of less than 2 mm (0.08 in.).
7. Seats and back supports shall not separate or detach from the wheelchair or wheelchair frame unless there is a backup at the same point that remains functional.
8. No webbing of the surrogate wheelchair tiedown and occupant restraint system (SWTORS) shall completely fail due to interaction with the wheelchair or its components during a test.
9. All securement hooks of the SWTORS or commercial tiedown shall remain attached to the wheelchair securement points throughout the test.
10. Wheelchair-anchored belt restraints shall not become detached at anchorages, disconnected at buckles, or show complete webbing failure.
11. Batteries of power wheelchairs or their surrogate replacement parts shall:
    a. not move completely outside the wheelchair footprint, and
    b. remain attached or tethered to the battery compartment throughout the test.

Appendix D. Detailed Static Testing Results

Appendix Key

Previous tests indicated in parentheses with these abbreviations

- V vertical
- R rear
- D down
- u upward through body block
- U upward through frame
- L lateral
- F frontal

Frontal Static Pull

AS13: Rovi X3 (V)

WC Mass (kg)	Target Load Frame (N)	Target Load Body Block (N)
160	14126	9076

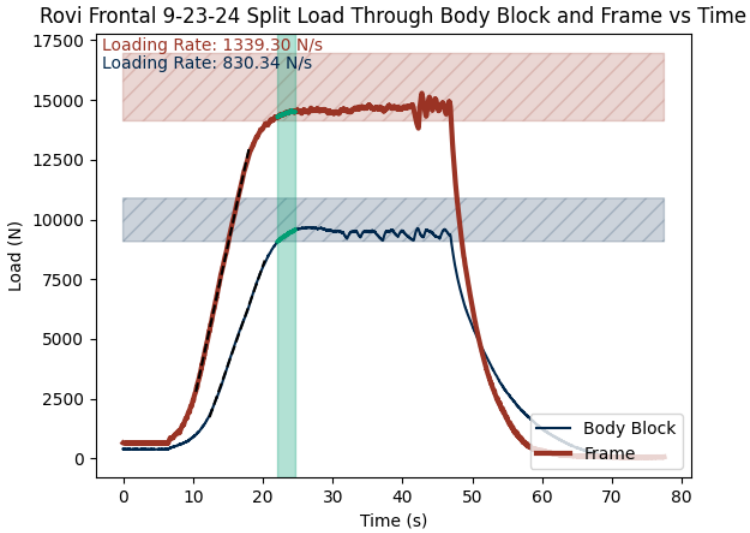

Figure 41. Loading history for Rovi frontal static test.

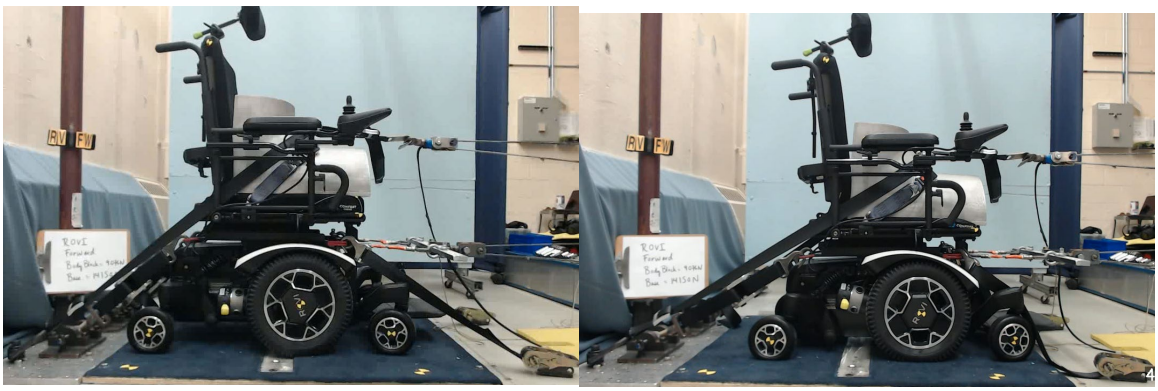

Figure 42. Rovi X3 frontal static test: initial test setup vs. peak from video

Table 7. Rovi X3 deformation analysis from frontal pre- and post-test scan data.

Landmarks	Pre X	Pre Y	Pre Z	Post X	Post Y	Post Z	Delta X	Delta Y	Delta Z	Resultant
SeatPanFR	452	1126	-76	444	1131	-69	-8	5	7	12
SeatPanFL	212	1404	58	214	1403	65	2	-1	7	7
SeatPanRL	-30	1257	-11	-26	1260	-10	4	3	1	5
SeatPanRR	255	965	-159	238	959	-164	-17	-5	-5	18
SeatBackTR	3	676	287	-20	693	296	-23	17	9	30
SeatBackTL	-104	808	359	-93	793	347	11	-15	-12	22
SeatBackBL	-169	1180	-102	-176	1182	-102	-7	3	0	8
SeatBackBR	83	873	-243	66	869	-255	-17	-5	-12	22
RDrTireTop	352	1057	-337	347	1058	-341	-4	1	-4	6
RDrTireBtm	372	1184	-613	368	1184	-615	-5	0	-2	5
RDrTireF	481	1208	-434	477	1227	-427	-4	19	7	21
RDrTireB	220	1041	-529	198	1040	-526	-22	-1	3	22
LDrTireTop	8	1441	-143	15	1442	-143	7	1	1	7
LDrTireBtm	0	1601	-410	9	1601	-406	9	1	4	10
LDrTireF	141	1609	-235	146	1610	-235	6	0	0	6
LDrTireB	-119	1438	-330	-115	1431	-335	4	-7	-6	10
FrTireR	585	1316	-468	630	1319	-470	46	3	-1	46
FrTireL	239	1726	-266	261	1701	-277	22	-25	-11	35
SecPtFR	420	1200	-202	416	1214	-200	-4	14	2	15
SecPtFL	221	1427	-87	215	1430	-83	-6	3	4	8
SecPtBL	-242	1115	-262	-213	1113	-267	29	-2	-5	29
SecPtBR	-59	902	-369	-50	963	-357	10	61	11	63

AS18: Edge 2 (V D D R L u U)

WC Mass (kg)	Target Load Frame (N)	Target Load Body Block (N)
163	14391	9076

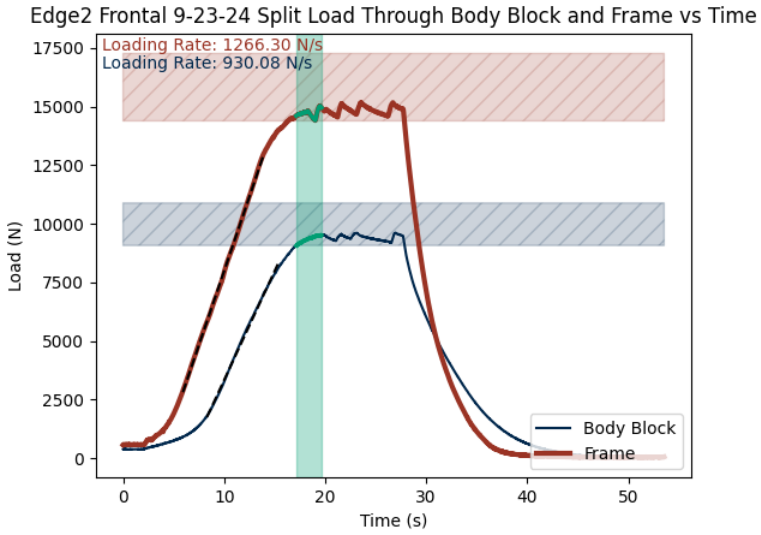

Figure 43. Loading history for Edge2 frontal static test.

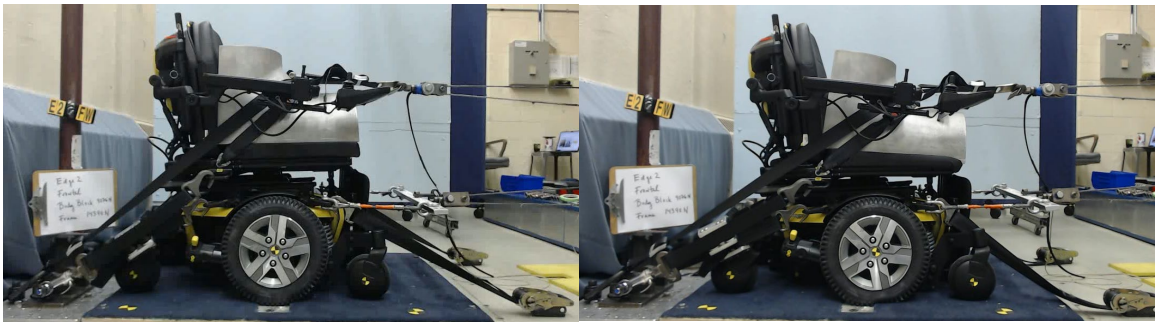

Figure 44. Edge2 frontal static test: initial test setup vs. peak from video

AS19: 4Front (V R L)

WC Mass (kg)	Target Load Frame (N)	Target Load Body Block (N)
176	15539	9076

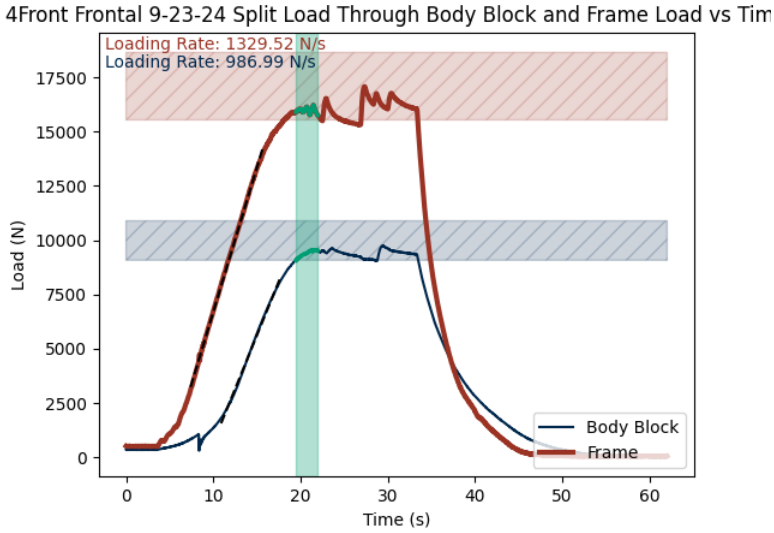

Figure 45. Loading history for 4Front frontal static test.



Figure 46. 4Front frontal static test: initial test setup vs. peak from video

Rearward Static Pull

AS29: Rovi X3 (V F u U L)

WC Mass (kg)	Target Load Frame (N)	Target Load Body Block (N)
160	2354	1513



Figure 47. Loading history for Rovi rear static test.



Figure 48. Rovi X3 rear static test: initial test setup vs. peak from video

AS08: Edge 2 (V D D)

WC Mass (kg)	Target Load Frame (N)	Target Load Body Block (N)
163	2399	1513

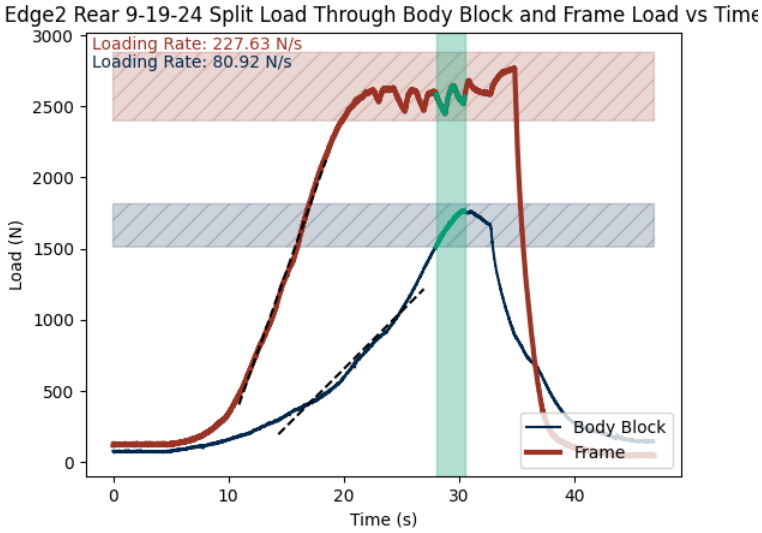

Figure 49. Loading history for Edge2 rear static test.

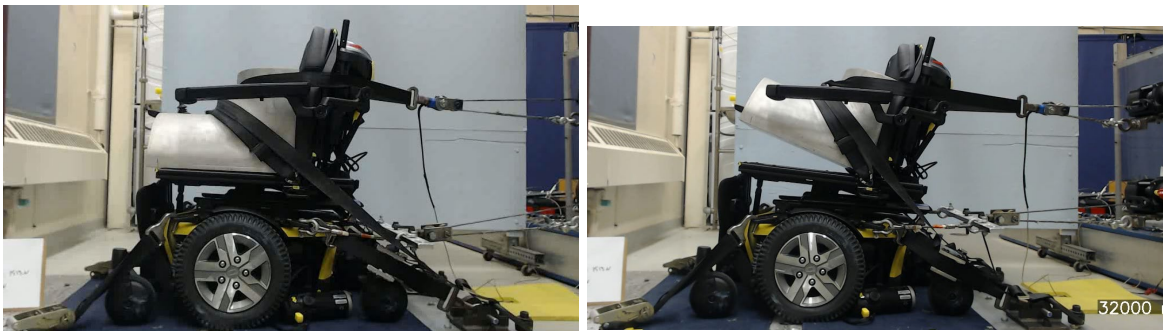

Figure 50. Edge2 rear static test: initial test setup vs. peak from video

S06: 4Front (V)

WC Mass (kg)	Target Load Frame (N)	Target Load Body Block (N)
176	2590	1513

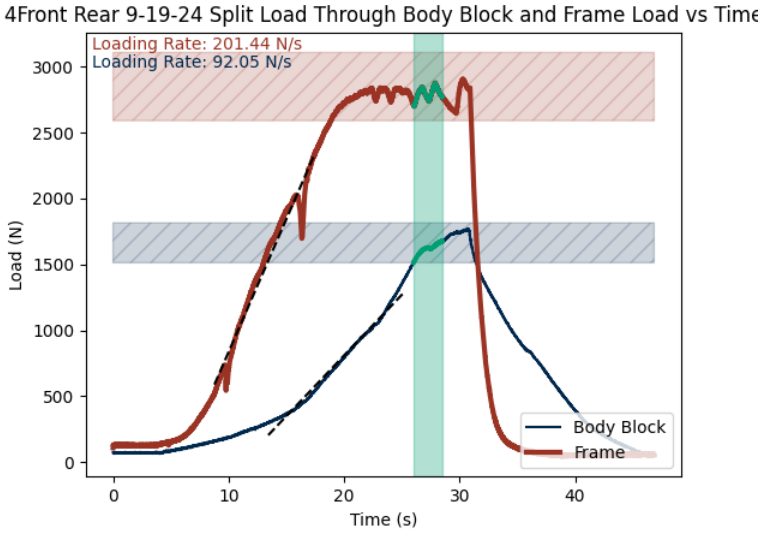

Figure 51. Loading history for 4Front rear static test.



Figure 52. 4Front rear static test: initial test setup vs. peak from video

Table 8. 4Front deformation analysis from rear static pre- and post-tests.

Landmarks	Pre X	Pre Y	Pre Z	Post X	Post Y	Post Z	Delta X	Delta Y	Delta Z	Resultant
SeatPanFR	453	925	-296	463	932	-292	10	7	5	13
SeatPanFL	540	1,300	-47	539	1,293	-59	-1	-7	-12	14
SeatPanRL	113	1,390	-43	123	1,390	-47	10	0	-4	10
SeatPanRR	59	1,006	-281	65	1,011	-281	6	5	0	8
SeatBackTR	-146	896	171	-148	897	167	-1	1	-4	4
SeatBackTL	-118	1,045	274	-114	1,057	280	4	12	6	14
SeatBackBL	-27	1,421	-71	-9	1,415	-75	18	-6	-4	19
SeatBackBR	-91	1,076	-313	-96	1,068	-311	-5	-8	1	9
RDrTireTop	305	993	-489	310	996	-486	5	3	3	6
RDrTireBtm	344	1,129	-762	344	1,139	-762	0	10	1	10
RDrTireF	468	1,038	-608	488	1,045	-615	20	8	-7	22
RDrTireB	170	1,111	-621	164	1,118	-628	-6	7	-7	12
LDrTireTop	402	1,495	-167	414	1,488	-173	12	-7	-6	15
LDrTireBtm	M	M	M	458	1,705	-390	M	M	M	M
LDrTireF	584	1,540	-290	592	1,527	-297	7	-13	-7	16
LDrTireB	257	1,601	-315	263	1,579	-314	7	-22	1	23
FrTireR	-248	1,283	-648	-258	1,281	-645	-10	-2	3	10
FrTireL	-155	1,705	-374	-155	1,709	-375	0	4	-1	4
SecPtFR	331	1,124	-448	335	1,112	-446	4	-12	2	13
SecPtFL	383	1,384	-271	390	1,366	-272	7	-18	-1	19
SecPtBL	-128	1,493	-297	-124	1,493	-299	3	0	-2	4
SecPtBR	-168	1,272	-448	-170	1,270	-443	-2	-3	5	6

AS05: Quickie2 (V u D)

WC Mass (kg)	Target Load Frame (N)	Target Load Body Block (N)
18	706	1513

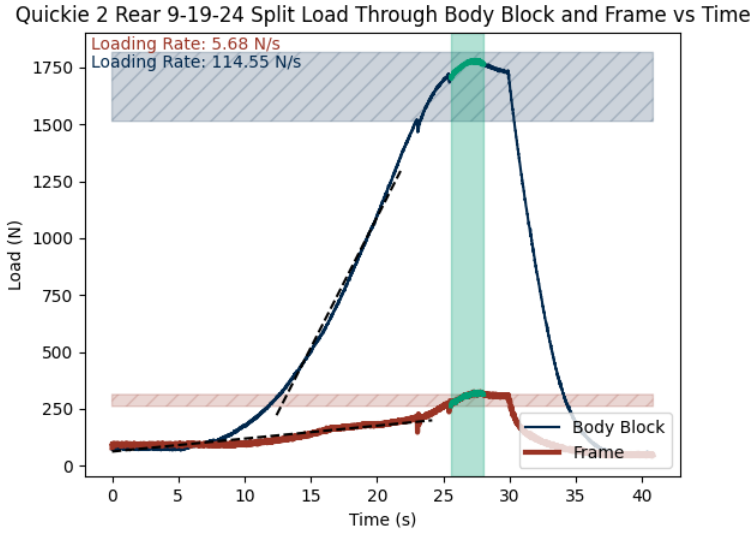

Figure 53. Loading history for Quickie 2 rear static test.

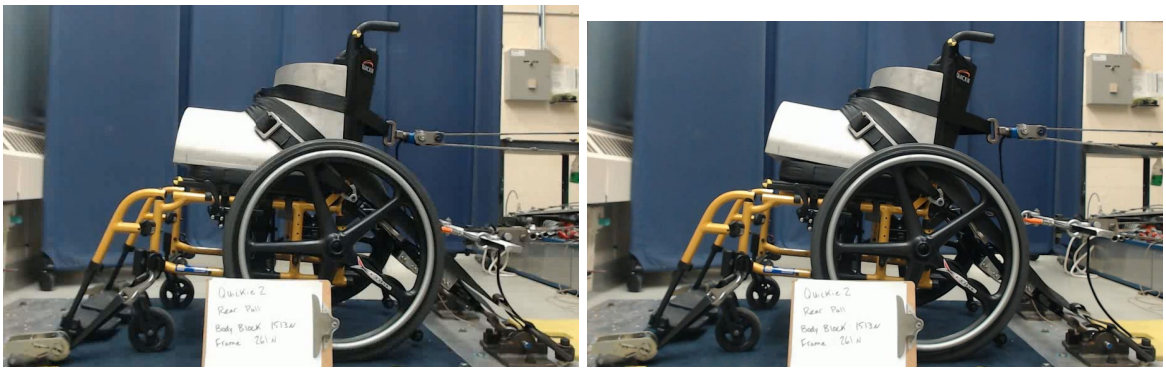

Figure 54. Quickie2 rear static test: initial test setup vs. peak from video

Table 9. Quickie 2 deformation analysis, pre and post rear static test

Landmarks	Pre X	Pre Y	Pre Z	Post X	Post Y	Post Z	Delta X	Delta Y	Delta Z	Resultant
SeatPanFR	243	1045	-3	232	1048	-1	-12	3	-2	12
SeatPanFL	239	1366	282	239	1366	282	0	0	0	0
SeatPanRL	9	1401	251	25	1418	239	15	17	-12	26
SeatPanRR	20	1058	-27	18	1060	-39	-2	2	12	12
SeatBackTR	-342	876	256	-335	879	252	7	3	-4	9
SeatBackTL	-332	1150	483	-322	1162	462	10	12	-22	27
SeatBackBL	-247	1358	263	-242	1359	254	5	2	-8	10
SeatBackBR	-257	1051	-2	-250	1051	-5	8	0	3	8
RDrTireTop	-210	999	-27	-205	1001	-29	5	2	2	6
RDrTireBtm	-112	1264	-520	-115	1265	-517	-3	2	-2	4
RDrTireF	128	1089	-226	123	1085	-218	-5	-4	-8	10
RDrTireB	-444	1187	-275	-435	1181	-290	8	-5	16	19
LDrTireTop	-212	1401	306	-193	1404	301	19	3	-5	20
LDrTireBtm	-101	1840	-40	-89	1831	-44	11	-10	3	15
LDrTireF	137	1579	177	137	1579	177	0	0	0	0
LDrTireB	-427	1626	100	-421	1630	87	6	5	-13	15
FrTireR	349	1230	-380	354	1229	-382	4	-1	3	5
FrTireL	358	1680	-5	361	1679	2	3	0	-3	4
SecPtFR	329	1125	-260	330	1129	-265	1	4	6	7
SecPtFL	358	1590	113	356	1587	119	-2	-4	5	7
SecPtBL	-257	1480	163	-266	1481	159	-9	2	-5	10
SecPtBR	-280	1128	-125	-287	1131	-132	-8	4	7	11

Lateral Static Pull

AS28: Rovi X3 (V F u U)

WC Mass (kg)	Target Load Frame (N)	Target Load Body Block (N)
160	6278	4042

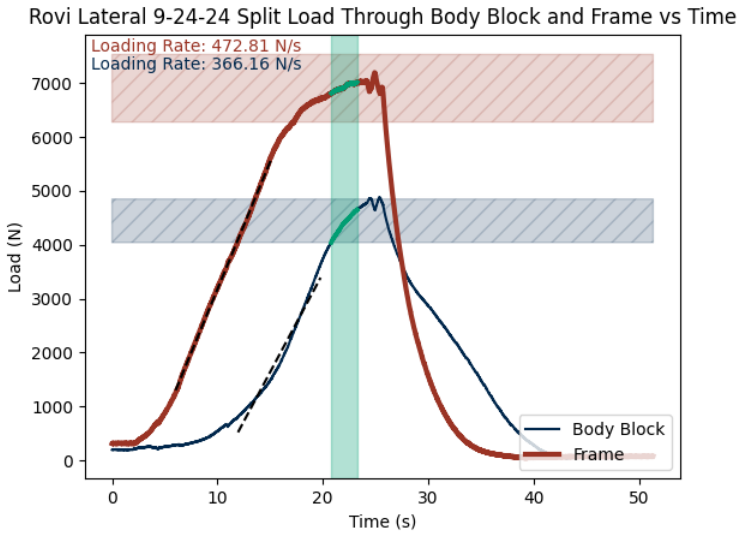

Figure 55. Loading history for Rovi lateral static test.



Figure 56. Rovi X3 lateral static test: initial test setup vs. peak from video

AS09: Edge2 (V D D R L)

Used 6 tiedowns.

WC Mass (kg)	Target Load Frame (N)	Target Load Body Block (N)	Level
163	9593	6051	Incorrect
163	6396	4034	Correct

Note: incorrect scaling (6 rather than 4) used for test.

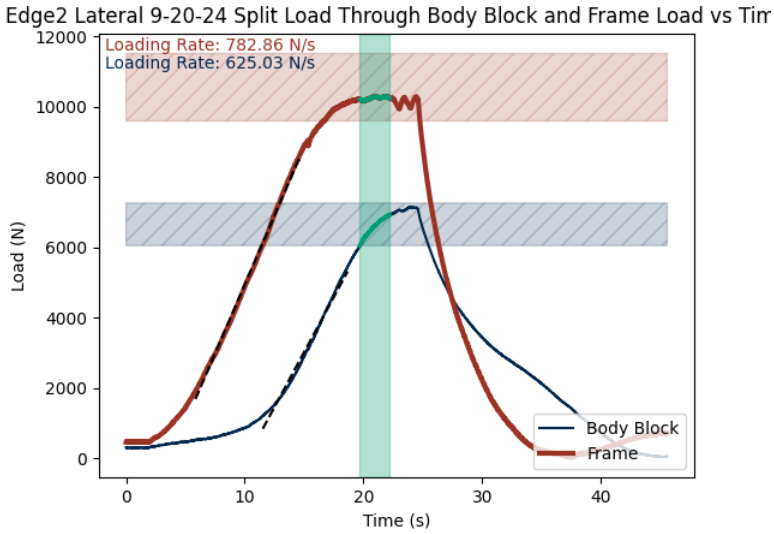

Figure 57. Loading history for Edge2 lateral static test.

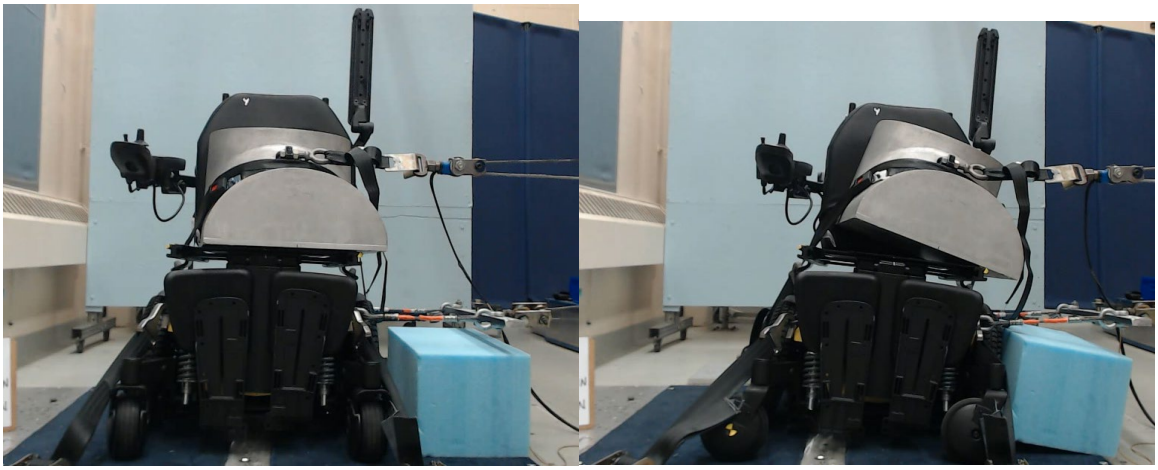

Figure 58. Edge2 lateral static test: initial test setup vs. peak from video

AS11: 4Front (V R)

For this test, a wheel blocked horizontal loading through the securement bracket. As shown in figure below, the cable routed over tire, with a smooth shim inserted on top.

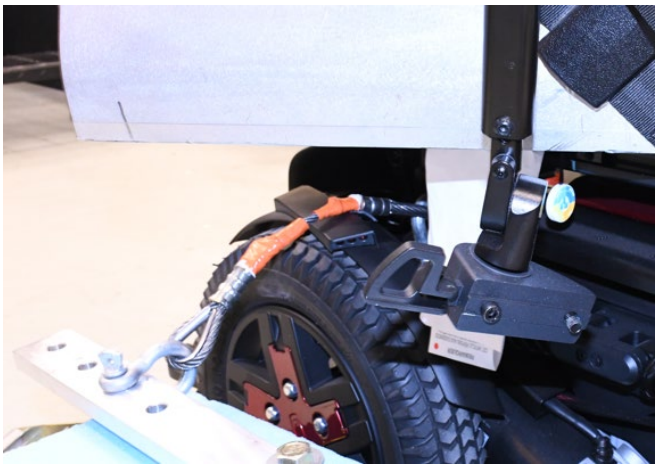

Routing cable over tile using shim for lateral 4Front static test.

WC Mass (kg)	Target Load Frame (N)	Target Load Body Block (N)	
176	10342	6051	Incorrect
176	6906	4034	Correct

Note: incorrect scaling (6 rather than 4) used for test

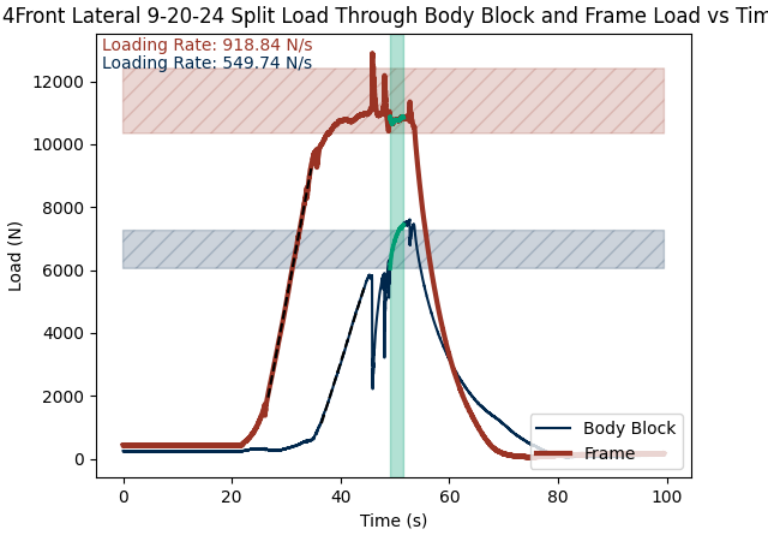

Figure 59. Loading history for 4Front lateral static test.



Figure 60. 4Front lateral static test: initial test setup vs. peak from video

AS10: Quickie2 (V u D R)

This test was not successful, but we include results because it led to changes in lateral test protocol. This test was conducted using our initial plan to split the load on all wheelchairs during lateral testing. We could not complete the test, because the bottom winch never tightened as the top winch dragged the chair sideways, causing it to lean sideways. This test also supported routing of the vehicle-anchored lap belt outside the rear propel wheels.

WC Mass (kg)	Target Load Frame (N)	Target Load Body Block (N)	
18	1042	6051	Incorrect
18	706	4034	Correct

Note: incorrect scaling (6 rather than 4) used for test.

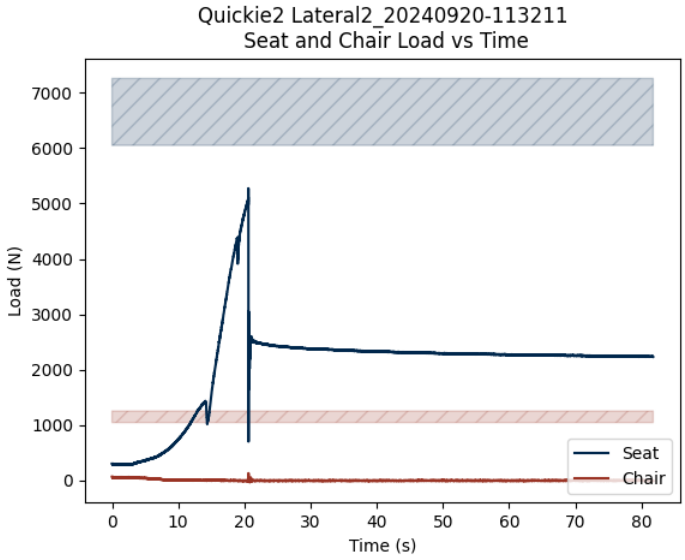

Figure 61. Loading history for Quickie 2 lateral static test.



Figure 62. Quickie2 lateral static test: initial test setup vs. peak from video

Upward Static Pull

AS21/AS22: Rovi (V F)

WC Mass (kg)	Target Load Frame (N)	Target Load Body Block (N)
160	4709	3025

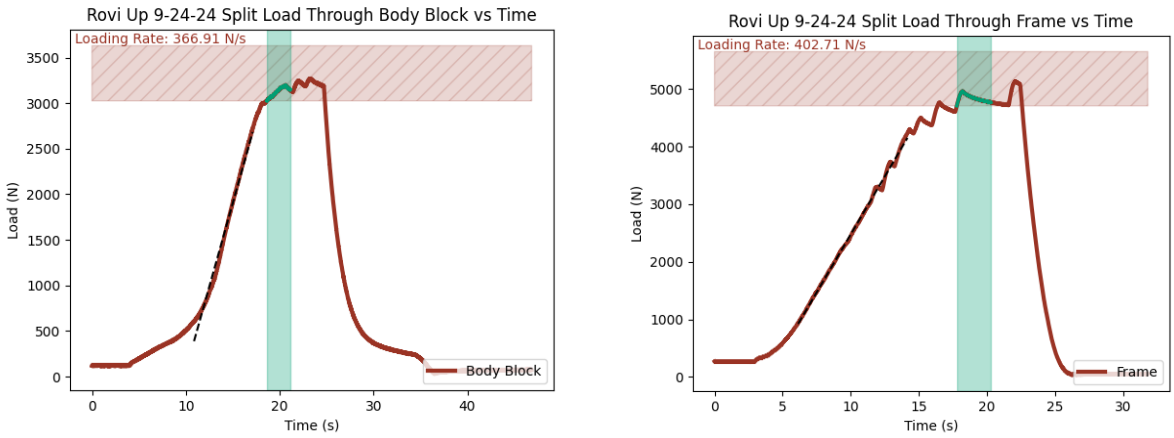

Figure 63. Loading history for Rovi upward static test.



Figure 64. Rovi X3 upward static tests: initial test setup vs. peak from video, with separate tests loading through body block (top) and frame (bottom).

AS16/AS17: Edge2 (V D D R L)

WC Mass (kg)	Target Load Frame (N)	Target Load Body Block (N)
163	4797	3025

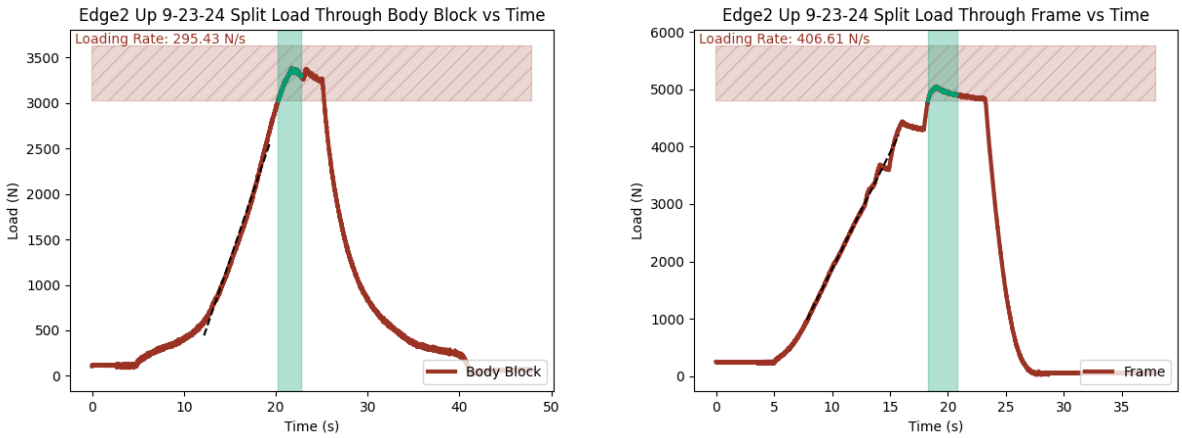

Figure 65. Loading history for Edge 2 upward static test.



Figure 66. Edge2 upward static test: initial test setup vs. peak from video, with separate tests loading through body block (top) and frame (bottom).

AS02: Quickie2 (V U)

WC Mass (kg)	Target Load Frame (N)	Target Load Body Block (N)
18	NA	3555

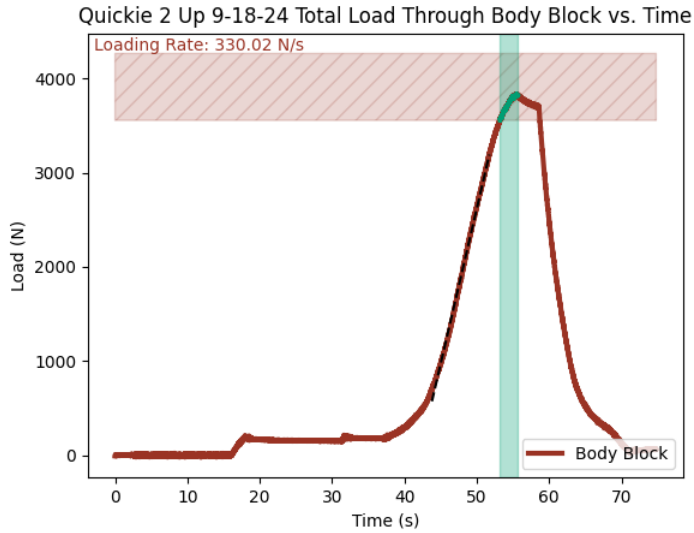

Figure 67. Loading history for Quickie 2 upward static test.



Figure 68. Quickie2 lateral upward test: initial test setup vs. peak from video

Table 10. Quickie2 deformation analysis from upwards pre- and post test measurements

Landmarks	Pre X	Pre Y	Pre Z	Post X	Post Y	Post Z	Delta X	Delta Y	Delta Z	Resultant
SeatPanFR	-369	1235	20	-374	1216	19	-5	-19	-2	20
SeatPanFL	-395	962	-218	-402	965	-211	-7	3	-7	11
SeatPanRL	-137	876	-190	-140	872	-179	-3	-4	-10	12
SeatPanRR	-130	1187	99	-133	1166	93	-3	-21	-5	22
SeatBackTR	8	890	382	12	890	376	4	0	-6	7
SeatBackTL	-19	607	109	-19	603	120	0	-4	11	12
SeatBackBL	11	827	-151	8	822	-146	-2	-5	-5	7
SeatBackBR	53	1123	149	53	1117	139	0	-6	-11	12
RDrTireTop	-3	1164	183	-3	1151	176	1	-13	-7	15
RDrTireBtm	141	1595	-129	135	1588	-146	-7	-7	17	19
RDrTireF	-213	1418	2	-218	1399	-4	-5	-19	2	20
RDrTireB	331	1295	62	328	1291	49	-2	-4	-13	14
LDrTireTop	-43	782	-172	-37	783	-164	6	1	-8	10
LDrTireBtm	82	1054	-637	74	1059	-638	-8	5	1	10
LDrTireF	-258	969	-403	-266	977	-400	-8	8	-3	12
LDrTireB	276	870	-363	280	872	-358	4	2	-5	7
FrTireR	354	1229	-382	354	1229	-382	0	0	0	0
FrTireL	361	1679	2	361	1679	2	0	0	0	0
SecPtFR	-397	1478	-96	-380	1464	-105	17	-15	9	24
SecPtFL	-445	1106	-482	-447	1102	-476	-3	-3	-5	7
SecPtBL	144	910	-289	160	918	-294	16	8	5	19
SecPtBR	225	1261	10	225	1255	9	0	-6	-1	6

Downward Static Compression

AS31: Rovi (V F u U L R)

WC Mass (kg)	Target Load Frame (N)	Target Load Body Block (N)
160	15468	

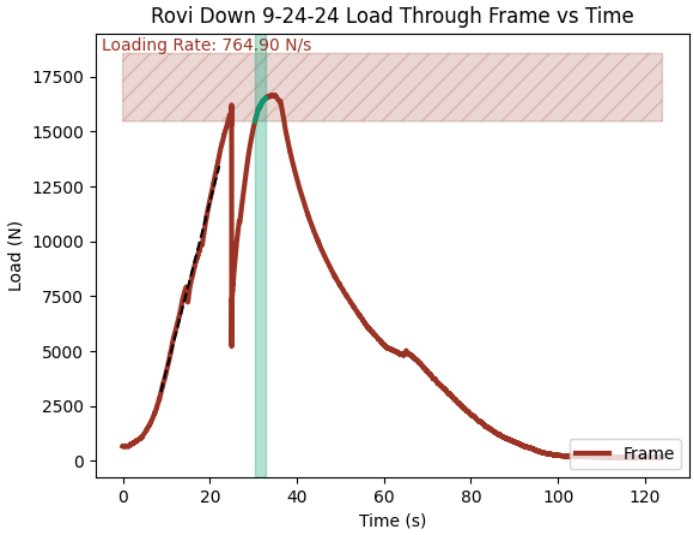

Figure 69. Loading history for Rovi downward static test.

Load discontinuity from wheelchair rotating forward, raising rear wheels off ground.

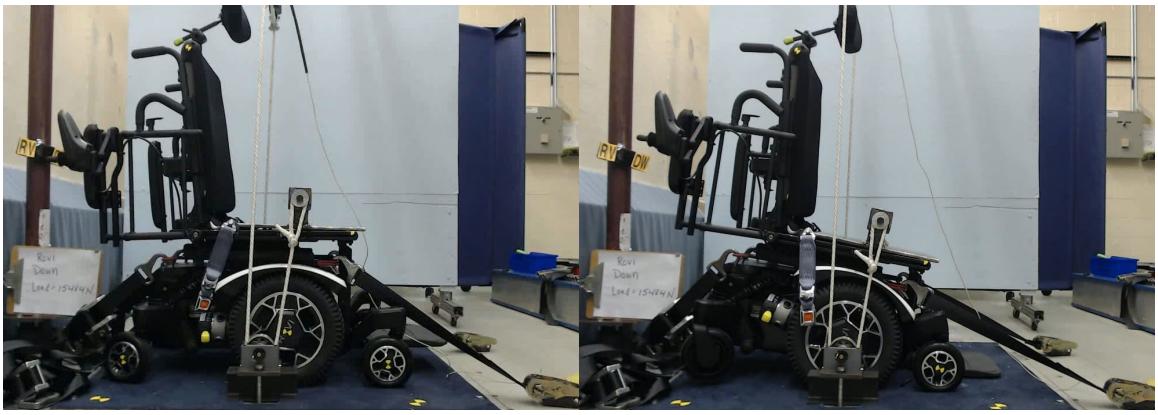

Figure 70. Rovi X3 Downward lateral static test: initial test setup vs. peak from video

Table 11. Rovi deformation analysis before and after downward static loading

Landmarks	Post X	Post Y	Post Z	Pre X	Pre Y	Pre Z	Delta X	Delta Y	Delta Z	Resultant
SeatPanFR	-301	1457	94	-309	1451	100	7	6	-6	11
SeatPanFL	-51	1144	-69	-70	1134	-58	20	10	11	25
SeatPanRL	248	1301	86	236	1294	94	12	7	-8	16
SeatPanRR	2	1620	253	-6	1609	246	8	11	7	15
SeatBackTR	94	1307	743	119	1307	752	-25	0	-9	27
SeatBackTL	226	1156	673	236	1172	692	-10	-16	-19	26
SeatBackBL	288	1307	157	278	1302	164	9	5	-6	12
SeatBackBR	32	1619	305	37	1606	316	-5	13	-11	18
RDrTireTop	-135	1677	82	-148	1667	78	13	10	5	17
RDrTireBtm	-115	1844	-159	-128	1837	-165	14	8	-7	17
RDrTireF	-250	1673	-108	-259	1660	-103	9	13	4	17
RDrTireB	15	1836	15	2	1819	13	14	17	2	22
LDrTireTop	183	1278	-111	159	1263	-110	25	15	0	29
LDrTireBtm	214	1407	-382	199	1401	-381	15	6	1	17
LDrTireF	63	1274	-297	41	1267	-303	22	7	-6	24
LDrTireB	328	1430	-187	305	1421	-180	22	9	7	25
FrTireR	-360	1669	-211	-364	1657	-213	3	13	-2	13
FrTireL	-31	1248	-423	-53	1240	-427	22	8	-4	24
SecPtFR	M	M	M	M	M	M	M	M	M	0
SecPtFL	-11	1272	-112	-27	1278	-109	16	-6	2	17
SecPtBL	436	1518	129	425	1511	126	11	7	2	13
SecPtBR	272	1735	243	259	1729	235	13	6	8	17

AS23: Edge2 (V D D R L u U F)

WC Mass (kg)	Target Load Frame (N)	Target Load Body Block (N)
163	16410	NA

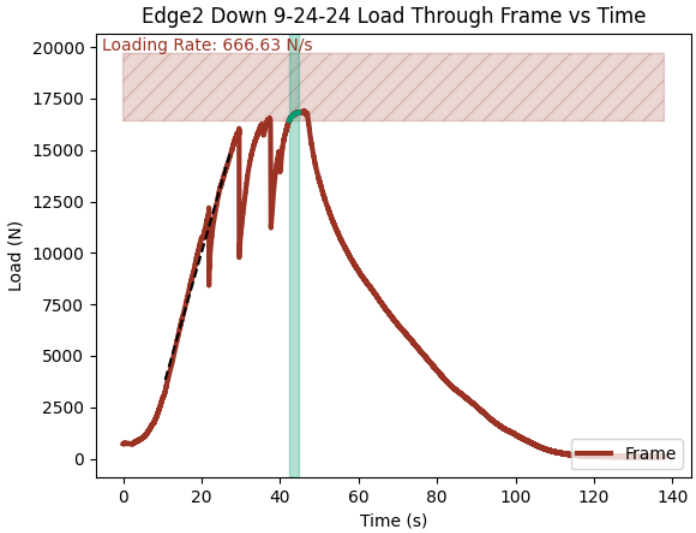

Figure 71. Loading history for Edge 2 downward static test.



Figure 72. Edge2 upward static test: initial test setup vs. peak from video

Table 12. Edge2 deformation from downward static testing

Landmarks	Pre X	Pre Y	Pre Z	Post X	Post Y	Post Z	Delta X	Delta Y	Delta Z	Resultant
SeatPanFR	-234	1446	-27	-240	1452	-35	-6	6	-7	11
SeatPanFL	-214	1081	-205	-219	1078	-215	-5	-3	-9	11
SeatPanRL	186	1089	-162	183	1082	-169	-3	-8	-6	11
SeatPanRR	157	1471	14	155	1476	16	-2	5	2	6
SeatBackTR	196	1153	374	199	1159	372	4	5	-1	7
SeatBackTL	225	958	274	222	952	278	-3	-7	4	9
SeatBackBL	182	1049	-143	186	1054	-157	4	5	-15	16
SeatBackBR	163	1436	22	155	1450	15	-8	14	-6	17
RDrTireTop	-11	1574	-99	-3	1578	-95	8	4	3	9
RDrTireBtm	6	1657	-222	5	1661	-220	-1	4	2	5
RDrTireF	-140	1654	-232	-147	1650	-238	-7	-4	-7	10
RDrTireB	162	1666	-210	166	1668	-206	4	3	4	6
LDrTireTop	30	1080	-342	22	1077	-342	-8	-3	0	9
LDrTireBtm	34	1143	-475	34	1143	-475	0	0	0	0
LDrTireF	-127	1143	-482	-131	1144	-479	-4	1	3	5
LDrTireB	187	1143	-468	200	1156	-464	14	13	4	19
FrTireR	-263	1705	-318	-265	1709	-322	-2	4	-4	6
FrTireL	-255	1167	-584	-245	1169	-588	10	2	-4	11
SecPtFR	-198	1521	-132	-194	1524	-132	4	3	0	5
SecPtFL	-187	1132	-320	-186	1129	-322	1	-3	-2	4
SecPtBL	275	1147	-291	274	1140	-294	0	-7	-3	8
SecPtBR	263	1532	-114	278	1545	-116	16	13	-2	21

AS24: 4Front (V R L F D)

WC Mass (kg)	Target Load Frame (N)	Target Load Body Block (N)
176	15645	

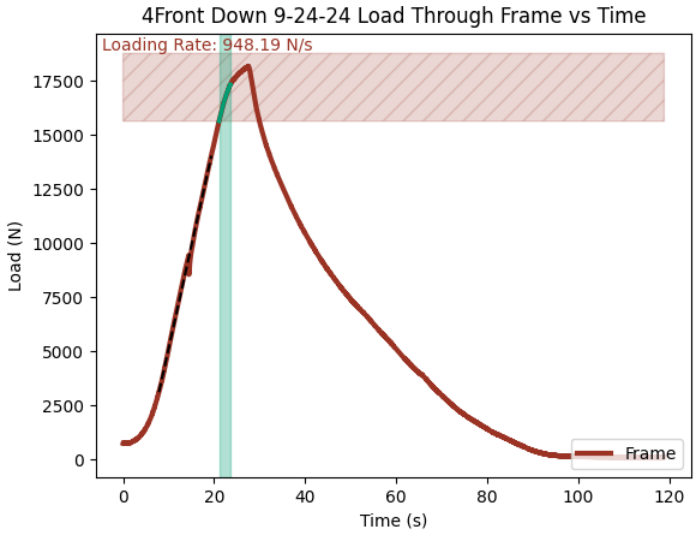

Figure 73. Loading history for 4Front downward static test.

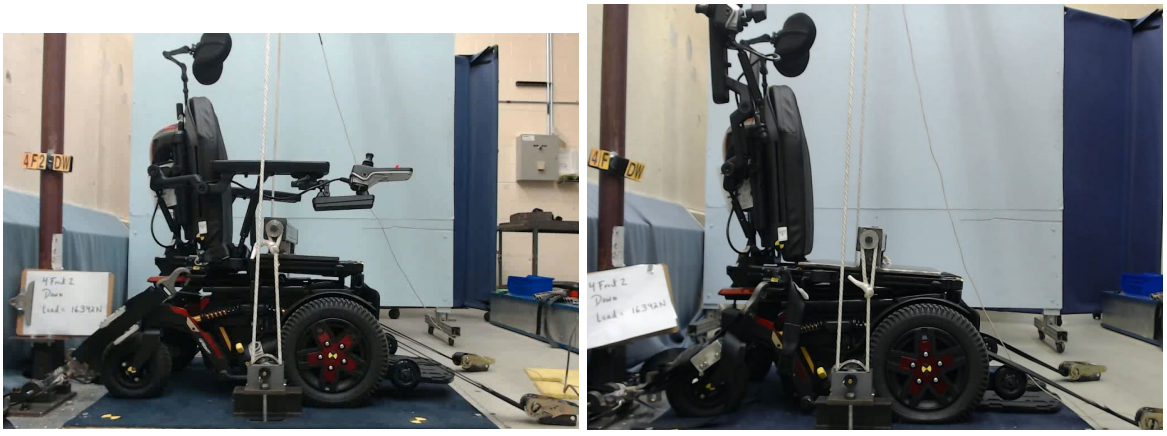

Figure 74. 4Front downward static test: initial test setup vs. peak from video

Table 13. 4Front deformation from downward static testing

Landmarks	Pre X	Pre Y	Pre Z	Post X	Post Y	Post Z	Delta X	Delta Y	Delta Z	Delta R
SeatPanFR	-235	1,472	32	-235	1,472	32	0	0	0	0
SeatPanFL	-180	1,094	-174	-187	1,095	-181	-7	1	7	10
SeatPanRL	244	1,124	-95	244	1,124	-95	0	0	0	0
SeatPanRR	180	1,483	108	186	1,491	108	6	9	-1	10
SeatBackTR	231	1,199	510	232	1,186	511	1	-12	1	12
SeatBackTL	288	984	430	290	974	411	2	-10	-19	21
SeatBackBL	293	1,120	-60	283	1,102	-74	-10	-18	14	25
SeatBackBR	191	1,461	117	193	1,473	111	2	12	-6	14
RDrTireTop	-155	1,601	-27	-155	1,601	-27	0	0	0	0
RDrTireBtm	-142	1,765	-280	-142	1,765	-280	0	0	0	0
RDrTireF	-298	1,656	-179	-302	1,649	-180	-4	-6	2	8
RDrTireB	18	1,696	-140	18	1,696	-140	0	0	0	0
LDrTireTop	-67	1,100	-288	-67	1,100	-288	0	0	0	0
LDrTireBtm	-47	1,220	-561	-47	1,220	-561	0	0	0	0
LDrTireF	-212	1,151	-438	-219	1,148	-436	-6	-3	-2	8
LDrTireB	98	1,180	-408	101	1,195	-412	3	15	5	16
FrTireR	436	1,753	-149	438	1,748	-153	3	-5	4	7
FrTireL	487	1,268	-408	485	1,269	-404	-2	1	-4	5
SecPtFR	-146	1,510	-121	-147	1,508	-127	-1	-3	6	6
SecPtFL	-94	1,239	-258	-109	1,240	-276	-15	1	18	23
SecPtBL	349	1,124	-143	349	1,124	-143	0	0	0	0
SecPtBR	293	1,563	93	293	1,563	93	0	0	0	0

AS03: Quickie (V U U)

WC Mass (kg)	Target Load Frame (N)	Target Load Body Block (N)
18	7110	NA

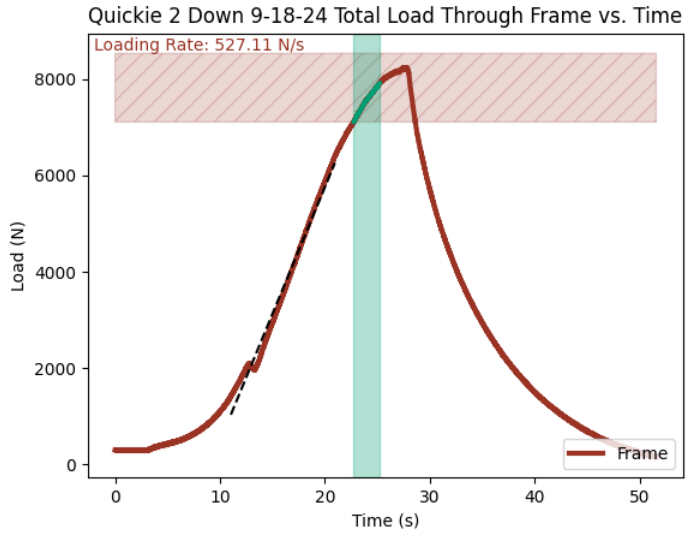

Figure 75. Loading history for Quickie 2 downward static test.

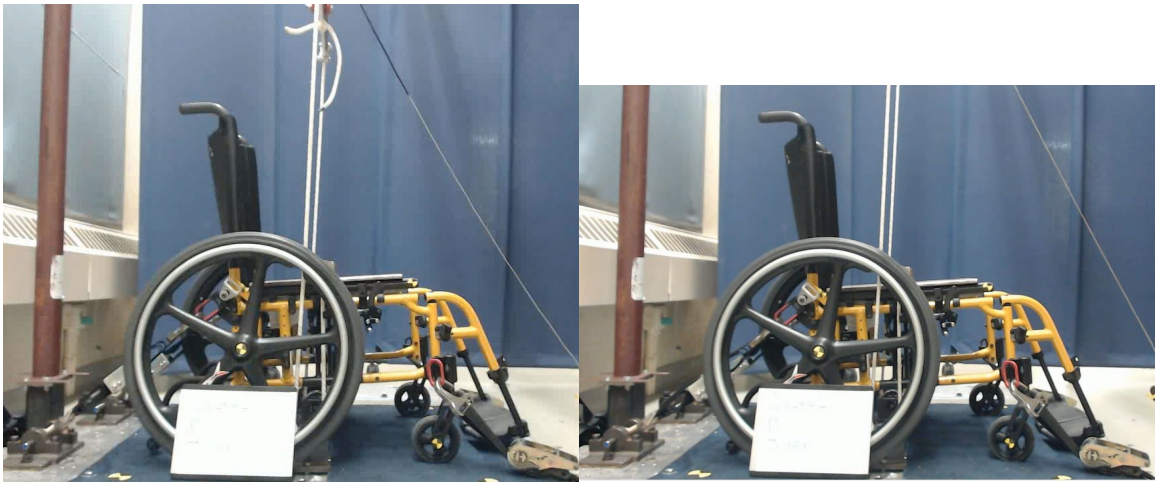

Figure 76. Quickie2 downward static test: initial test setup vs. peak from video